EUROPEAN SOUTHERN OBSERVATORY

VLT REPORT No. 49

INTERFEROMETRIC IMAGING WITH THE VERY LARGE TELESCOPE

FINAL REPORT

June 1986

Presented by the ESO/VLT Working Group on Interferometry

Very Large Telescope Project

INTERFEROMETRIC IMAGING

with the

VERY LARGE TELESCOPE

Final Report

June 1986

Presented by the ESO/VLT Working Group on Interferometry

FOREWORD

The aim of this Report is to discuss in detail the possibility of two- or more telescopes interferometry within the Very Large Telescope at optical, i.e. visible and infrared wavelengths, in order to achieve a gain in angular resolution of one to two orders of magnitude with respect to existing instruments.

Its volume is the result of a thorough analysis carried by an ad-hoc Working Group, which assembled experts from radio astronomy, optical and infrared astronomy and interferometry. The novelty of the field and the ambition of the objective deserves an in-depth approach which has been one of our aims, and is hopefully reflected in this Report.

Our conclusions try to reflect a difficult balance between two contradictory objectives : the VLT is not meant to be primarily an interferometer, and should not be. On the other hand, its initial concept, slightly amended, may offer a tremendous capability for high resolution work.

Planning a facility for a life-time of half a century should certainly be made in a broader frame of reference than planning a five-years space mission. In this respect, we have explored in detail this new field of optical interferometry. To our surprise, it appears that its implementation in the VLT project may not heavily bias it, neither in design nor in cost, providing that reasonable trade-offs be made.

While it is obvious that optical interferometry will require a strategy of its own, on the ground as well as in space, the VLT may be an important part of this strategy.

The Working Group

(June 1986)

Members of the ESO/VLT Working Group

O. CITTERIO, Université, Milano, Italia
D. DOWNES, IRAM, Grenoble, France
A. LABEYRIE, CERGA, Grasse, France
P. LENA, (Chairman), Université Paris VII et Observatoire de Paris, France
J.E. NOORDAM, Royal Greenwich Observatory, Great-Britain
F. RODDIER, Advanced Development Program, NOAO, Tucson, United States
J. WIJNBERGEN, Rijks Universiteit, Groningen, The Netherlands

Permanent consultants

G. WEIGELT, Universitat, Erlangen, FRG
L. WELIACHEW, IRAM, Grenoble, France +

ESO VLT project group

D. ENARD, ESO, Garching, FRG
F. MERKLE, ESO, Garching, FRG
M. SARAZIN, ESO, Garching, FRG
R. WILSON, ESO, Garching, FRG

Numerous colleagues have also contributed to various sections of this Report, either by providing written contributions, or by helpful comments or suggestions :
A. BOKSENBERG (Herstmonceux), M. DE JONGE (Grenoble), R. FOY (Grasse), S. GUILLOTEAU (Grenoble), C. KREYSA (Bonn), J. LEQUEUX (Marseille), A. MAEDER (Genève), J.M. MARIOTTI (Lyon), C. PERRIER (Lyon), J.P. SWINGS (Liège).

+ Leonid Weliachew died accidentally on July 23, 1986. This well-known radio astronomer contributed in a major way to our work and we shall treasure the memory of our friendly and enthusiastic colleague.

Note to the Reader

Chapter 1 is an introduction to the scientific perspectives offered by high angular resolution at optical wavelengths either with multi-telescope interferometry, or with a single large pupil. Chapter 2 offers a general introduction to the language and specifics of optical interferometry and ties it to the well known corresponding field in radio astronomy. Special attention may be brought to the sensitivity limits of optical interferometry. Chapter 3 and 4 are more directly related to the feasibility of interferometry with large telescopes (chap.3) and specifically with the VLT in its ESO-concept; detailed proposals and recommendations are made (chap.4). Most technical discussions are rejected in Appendices 1 to 6. Two separate bibliographies cover the specific interferometry aspects and the astrophysical references.

TABLE OF CONTENT

Chapter 1: HIGH ANGULAR RESOLUTION AT OPTICAL WAVELENGTHS

1.1 *High Angular Resolution in Astronomy*

The development of observing capabilities has always been oriented by a limited number of fundamental objectives : sensitivity, spectral and spatial resolution, wavelength coverage. Each progress in any of these fields has produced discoveries often unexpected. Each field is connected to the others : as soon as radio-astronomy (in the 1960's) or X-ray astronomy (in the 1970's) produced continuum maps with good sensitivity, the production of similar images with spectral resolution was required. Quite often a gain in sensitivity, such as the one to be offered by the Space Telescope, results from and benefits also to improved angular resolution.

When the atmospheric limitations were suppressed through observations carried in space, it became widely accepted that understanding an object and the physical phenomena within it required a reasonable matching of sensitivity over the whole electromagnetic spectrum (Fig. 1.1-1), and this requirement has, more or less, guided the priorities in missions or instruments selection. The result has been rewarding for the astrophysicist, who can build a fairly understanding picture of the object.

At almost any wavelengths except high energies (X and γ), spectral resolution already resolves the spectral lines at a width set by the physical condition in the source, and not by the instrument itself. The homogeneity criterion does not apply, here, and sensitivity is really the objective of spectrometers. The comparison of spectral data obtained in widely different spectral ranges is therefore easy.

Angular resolution is exceptional, by its extreme uneven character (Fig. 1.1-2) at various spectral ranges. Contrary to a simple minded diffraction analysis, the highest resolutions are currently obtained in radio-astronomy, at the longest wavelengths end of the spectrum.

If the criterion of more or less uniform angular resolution were adopted, certainly a major effort at optical (visible anf infrared) wavelengths should be undertaken, and extended to the ultraviolet at the earliest possible time.

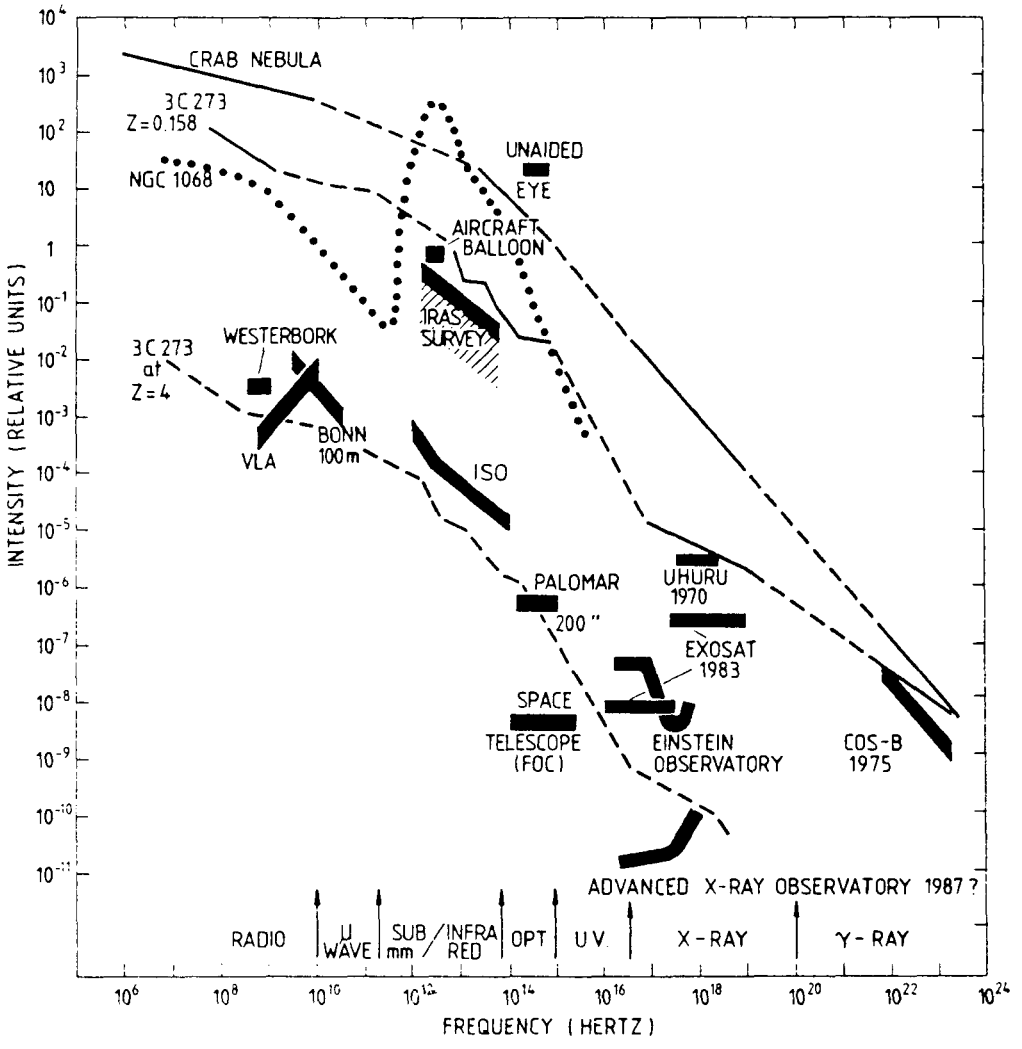

Figure 1.1–1 *: Overview of the relative sensitivity of existing or planned instruments at different wavelengths. The spectrum of a quasar (3C 273) and of an active galactic nucleus (NGC 1068) with thermal and non-thermal components are given for reference.*

Several space missions have adopted this guideline, at least for some of their instruments: the Space Telescope Faint Object Camera, the Infrared Space Observatory are providing one or two orders of magnitude gains in angular resolution over previous instruments.

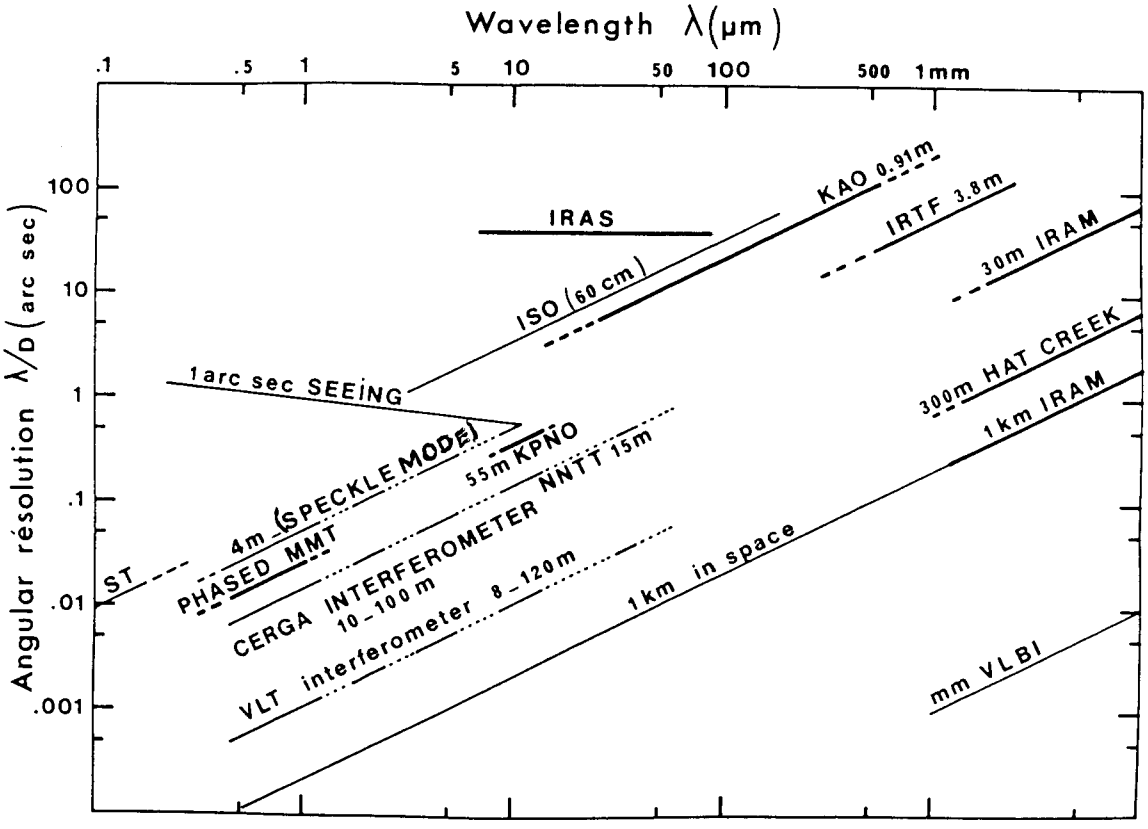

Fig. 1.1-2 *: Overview of angular resolution λ/D from UV (100nm) to radio wavelengths, obtained with existing (——) or planed (——) instruments. Diffraction limited resolution obtained with speckle techniques on large ground-based telescopes (4m class) is represented, as is the wavelength dependence of seeing (1 arc sec at 0.5 μm). Atmospheric absorption bands are shown (- - -) in the near IR, the atmosphere being fully opaque from the ground between 30 and 350 μm.*

ST= Space Telescope, MMT= Smithsonian Multi Mirror Telescope, CERGA= Grasse (France) 25 cm interferometer, KPNO= MacMath heterodyne interferometer operation, NNTT= National New Technology Telescope (US/NSF project), ISO= Infrared Space Observatory (ESA), IRAS= Infrared Astronomical Satellite (NASA), KAO= Kuiper Airborne Observatory, IRTF= Infrared Telescope Facility (UK), IRAM: Institut de Radio-Astronomie Millimétrique (F-RFA), Hat Creek= Berkeley interferometer, VLBI= Very Long Baseline Interferometry at millimeter wavelengths.

1.2 *Achievements at optical wavelengths*

Breaking the atmospheric seeing limit at optical wavelengths was first achieved over 60 years ago. After a long period of eclipse, optical interferometry, through various observationnal techniques, allows now to reach milliarc second resolution from ground observatories at visible and infrared wavelengths.

The first step was to overcome the ca. 1" limit imposed by atmospheric seeing, and to reach the diffraction limited λ/D (i.e. 10 to 100 m") capability of a telescope of diameter D, through speckle interferometry in the visible (Labeyrie 1970), then in the infrared (Léna 1977, Selby et al. 1979). Most 4 m-class telescopes can nowadays be operated in a speckle-mode at all optical wavelengths.

Since the original observations by Michelson and Pease (1921), optical interferometry was extended to longer baselines by Hanbury Brown et al. (1974) by the method of intensity interferometry. This technique is however limited by low sensitivity. In 1975 Labeyrie succeeded in observing interference fringes produced by two independent small telescopes, showing that long baseline inteferometry is feasible at optical wavelengths in a Michelson mode. The instrument now at CERGA consists of two 26 cm telescopes on a steady concrete alt-alt mount. It is now currently operated in the visible with variable baselines up to 67 m long (Koechlin and Rabbia 1985) and in the near infrared (di Benedetto and Conti 1983, di Benedetto 1985). This experiment has brought considerable impetus to optical interferometry all over the world. Similar instruments have been built in several places such as the University of Sydney (Davis 1979, 1981), the University of Maryland (Currie 1977, 1979), and Mount Wilson Observatory (Shao and Staelin 1977, 1980).

Meanwhile the multiple mirror telescope technology was developed in the U.S. as a possible solution for future giant telescopes. Although the resulting MMT was not intended initially to work in an interferometric mode, its cophasing was successfully achieved by Beckers, Hege and coworkers (Beckers and Hege 1984, Hebden et al. 1986), proving that interferometry can be done by coupling large telescopes together. A long baseline interferometer with two 1.5 m telescopes in a concrete mount is now completed at CERGA (Labeyrie et al. 1984) and is intended to work in the infrared as well as in the visible (Fig. 1.2-1). Heterodyne interferometry at 11 microns has been demonstrated

by Townes and coworkers (Townes 1984) and by Gay and coworkers (Assus et al. 1979), but Michelson interferometry is clearly superior at shorter wavelengths or for objects emitting only continuum radiation.

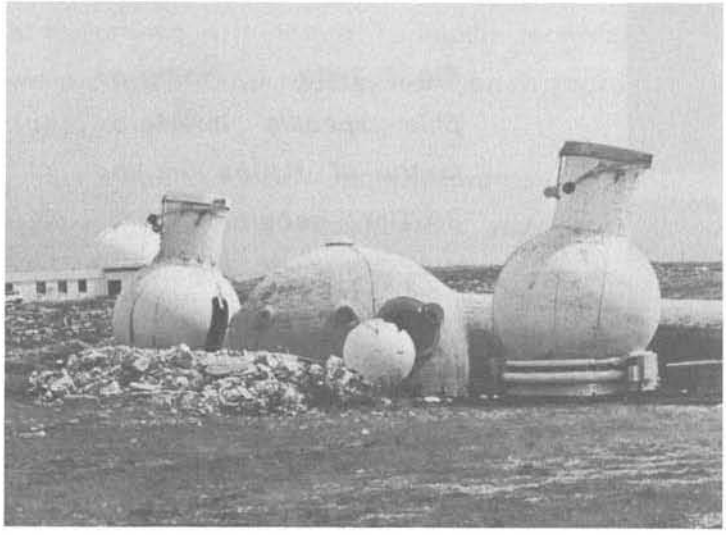

Figure 1.2–1 *: The 1.5 m-two telescopes interferometer at Cerga (Grasse, France), and the central laboratory for beam recombination.*

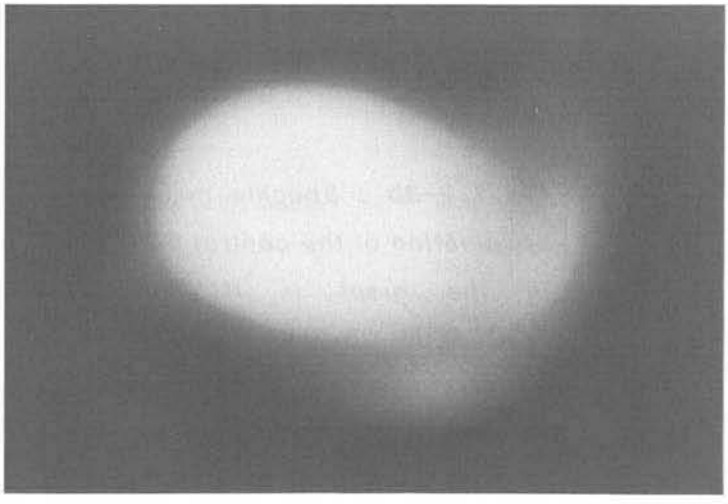

Fig. 1.2–2 *: Image of αOri at 535 nm (Δλ ~ 1 nm). The image was reconstructed from interferometric observations made at the 3.6 m CFH Telescope in Hawaii, using the Gull and Daniel algorithm. Circumstellar shell is obvious (Roddier and Roddier 1985).*

5 mm = 10 milliarcsec.

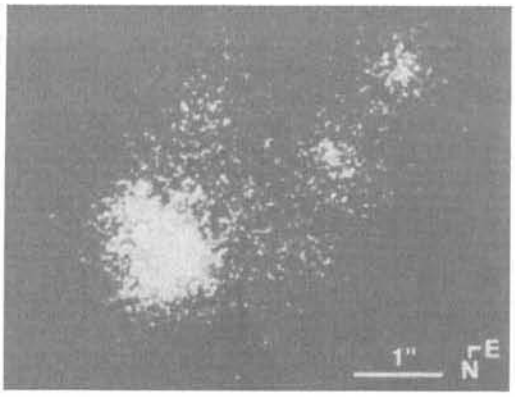

a

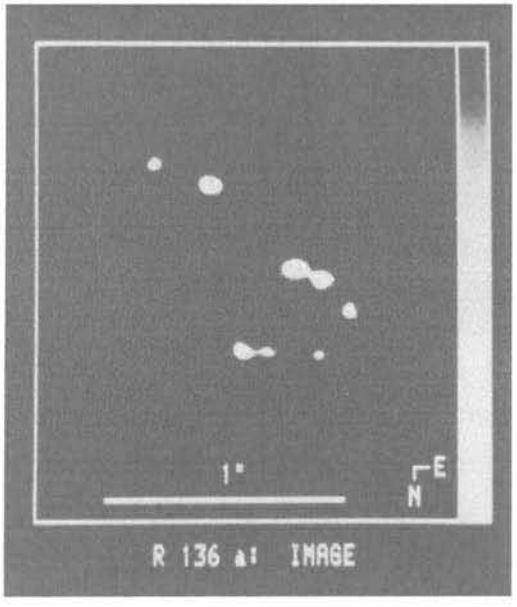

b

Fig. 1.2–3a *: Holographic speckle interferometry of R136a in the 30 Dor nebula.*
a : One of the 8000 reduced speckle interferograms.
b : Reconstructed diffraction–limited image.
(See The Messenger No. 40 for more details.)

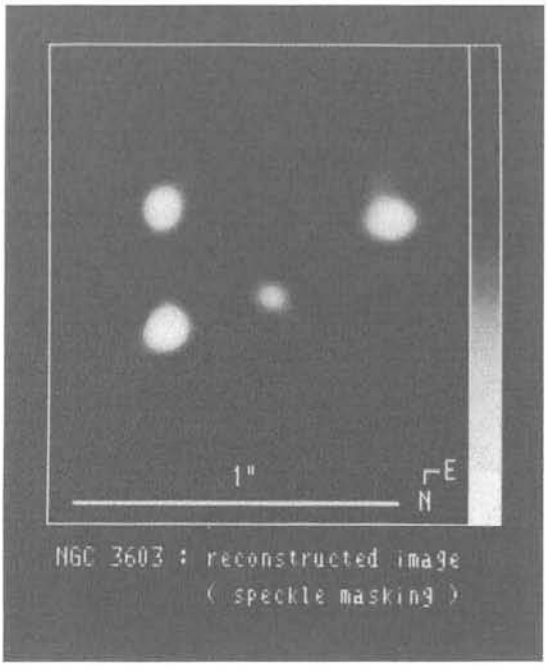

Fig. 1.2–3b *: Speckle masking observation of the central object in the giant H II region NGC 3603 (2.2m telescope). Speckle masking has the advantage that it can reconstruct diffraction–limited images of general objects. The magnitudes of the 4 resolved stars are 11^m, 12^m, 13^m and 14^m (Hofman and Weigelt 1986).*

Obtaining images or spectra at the diffraction limit either with a single large pupil or with two pupils from the ground basically suffers from the same limitation: the fluctuation of the index of refraction of the Earth's atmosphere at optical wavelengths. A great deal of knowledge has been accumulated during the last ten years in the acquisition and treatment of images distorted by the atmospheric turbulence (speckle techniques), both at visible and infrared wavelengths. The results have been thoroughly reviewed (Chelli 1984, Woolf 1982).

Among main achievements of speckle interferometry at visible wavelengths, one may retain measurements of numerous spectroscopic binaries, the orientation of asteroids rotation axis, the determination of Charon's orbit around the planet Pluto. Algorithms have been developped to restore the image, through measurements of both amplitude and phase of its Fourier transform: the enveloppe of gaz around α Ori (Fig. 1.2-2) and the discovery of a triple system in this star (Karovska et al. 1986), the multiplicity of stars such as R136a in the Large Magellanic Cloud (Baier et al. 1985) or as the central object in NGC 3603 (Hofman and Weigelt 1986 - Fig. 1.2-3). The limiting magnitudes given in Table 1.2-1 are now routinely reached by speckle cameras.

Table 1.2-1

Speckle sensitivity reached in the visible

	m_v
Asteroids	8-11
Pluto/Charon	15 17
Double stars	1-13
Star surfaces	1-5
Central objects in HII regions	10-16
Galactic nuclei	12
Quasars	13-17

Sensitivity of speckle measurements in the infrared(*)

λ (μm)	Band	Magnitude	Flux (Jy)
2.2	K	7.7	0.76
3.5	L	5.8-8.4	-0.14
4.8	M	4.5	2.1

(*) Values are strongly r_o-dependent and are given for 1.3" seeing.

A new technique called differential speckle interferometry (Beckers 1982) allows to go beyond the diffraction-limit λ/D by evaluating differential position at two adjacent wavelengths (Hebden et al. 1986) and has already produced good Hα images of αOri envelope.

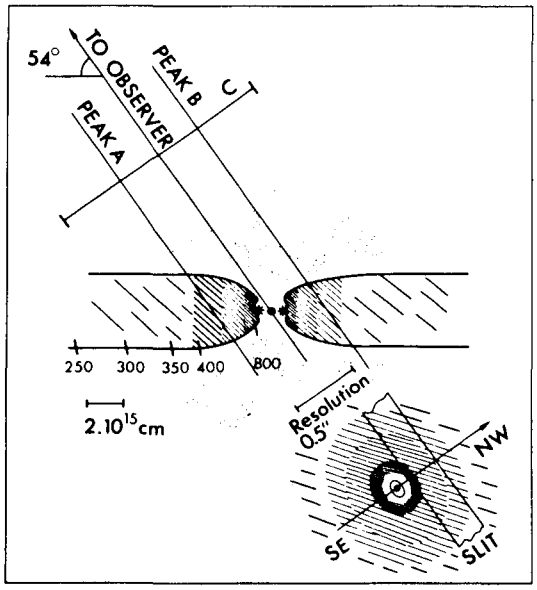

Fig. 1.2–4 *: A model of the source IRc2 in Orion, powering the Kleinmann–Low nebula. The model is partly deduced from speckle work at 4.64 μm at the ESO 3.6 m telescope (Chelli et al. 1984).*

In the infrared, most large telescopes in the world (4–5 m class) are now equiped with a dedicated specklegraph. Outstanding results have been obtained, such as the discovery of T Tauri binary structure (Schwartz et al. 1984), the unambigous resolution (Chelli et al. 1984) of the heating source (IRc2) of the Kleinman–Low nebula in Orion with 0.1 arc sec resolution or slightly better, or the discovery of solar–system size halos around young stars (Beckwith et al. 1985). The requirements of the diffraction limited imaging with single large pupils are discussed in Appendix A6.

Two–telescopes interferometry is only at its beginning stage of development, but its potential is already demonstrated by the measurements of over 15 stellar diameters at 600 nm from 2 to 15 milliarc sec, the determination of limb darkening coefficients and orbital elements, as shown by Fig. 1.2–5 and Table 1.2–2 (Koechlin et al. 1979, Faucherre et al. 1983), or the measurements of γ Cass envelope in the Hα line, 5.2 milli arc sec in diameter (Thom et al. 1986). Although very promising (§ 1.3) in the infrared, direct interferometry has not yet produced its first results, except in heterodyne mode (Sutton et al. 1977) where a few visibility determinations over a 5.5 m baseline have constrained the envelope diameter of the star NML Cyg.

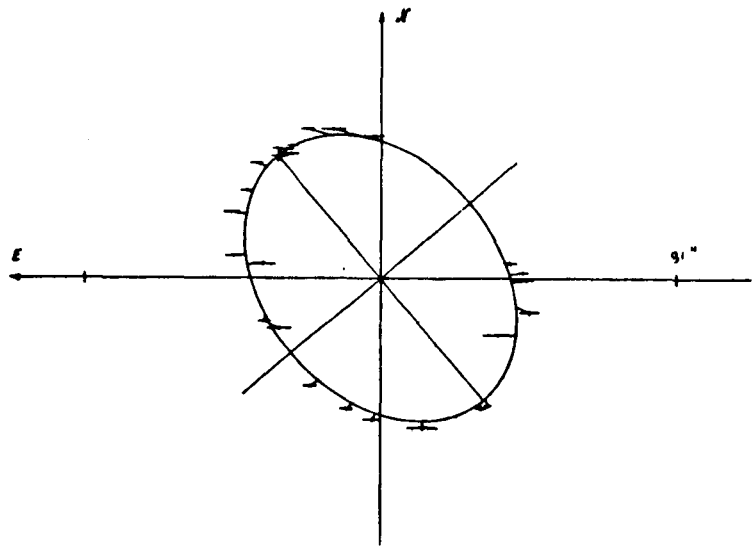

Figure 1.2–5 *: Orbit of αAurigae B as determined with the 26 cm two–telescopes interferometer at Cerga (Koechlin et al. 1979).*

Table 1.2–2

Giant stars resolved with the small interferometer

(67 m baseline at CERGA)

name	measured angular diameter (millisecond of arc)		$R/R_\odot$	effective temp. (Kelvin)	
	.55 μm	2.2 μm		.55 μm	2.2 μm
α Cas	5.4+0.6		26∓8	4700+300	
β And	13.2+1.7	14.4+0.5	33∓9	3800+250	3711+64
γ And	6.8+0.6		50∓14	4600+250	
α Per	2.9+0.4		55∓9	7000+600	
α Cyg	2.7+0.3		145∓45	8200+600	
α Ari	7.6+1		15∓5	4300+350	
β Gem	7.8+0.6		8+2	4900+220	
β UMi	8.9+1		30+9	4220+300	
γ Dra	8.7+0.8	10.2+1.4	45+10	4300+230	3960+270
δ Dra	3.8+0.3		15+5	4530+220	
μ Gem		14.6+0.8			3860+95
α Tau		20.7+0.4			3904+34
α Boo		21.5+1.2			4240+120
α Aur A	8.0+1.2		12+2	5400+200	
α Aur B	4.8+1.5		7+2	5950+200	
α Lyr	3.0+0.2		2.6+0.2		

Recent results with on-line fringe reduction (after Koechlin 1984):

α Cyg	3.2∓0.3	A2Ia
β And	14.0∓1.3	MOIII
α Per	3.8∓0.4	FSIb
ε Cyg	4.8∓0.5	KOV

1.3 *Scientific perspectives of an interferometric VLT*

The long history of interferometry at radiowavelengths gives the frame into which optical interferometry may shape its future. Yet, in order to make reasonable forecasting, a few assumptions should be stated; they will be detailed later in this report.

When a gain of two to four orders of magnitude in spatial resolution is within reach, it is difficult to make detailed predictions about its scientific potential. Yet, preliminary results obtained with modest size telescopes and extrapolation of observation made to date establish at a reasonable degree of confidence, on the conservative side, what a Very Large Telescope could achieve in an interferometric mode.

With a few hundred meters baseline, its angular resolution would span from 0.5 marc sec in the blue to 33 marc sec at 20 μm. Its capability to produce good images with a clean beam would, on the long term, be comparable to the one of the VLA or of the Quasat project (Fig. 1.3–1). Hundreds or possibly thousands of spectral channels could be simultaneously explored.

Its sensitivity is critically dependent on the development of adaptive optics. Relatively easy in the infrared, such a development is less obvious at visible wavelengths, unless new methods, using artificial reference sources, are implemented. Only such developments would fully exploit the capability offered by the interferometric use of large mirrors 8 to 10 meters in size.

The critical issues are image reconstruction capability, and sensitivity or limiting fluxes. The former will be assumed as a ten–years goal, which will be reached by steps, while the latter will be consistent with values discussed in § 2.5.

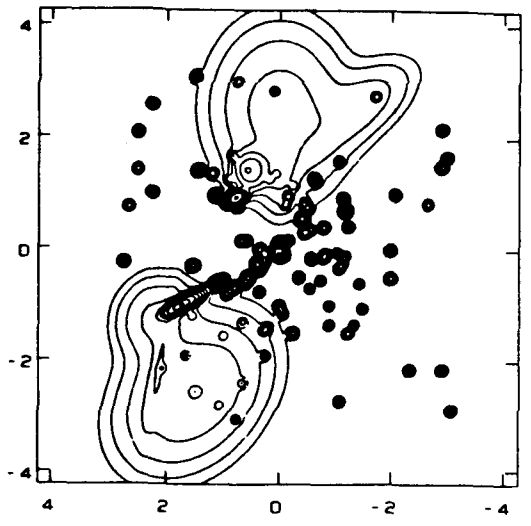

The original model of the source. Note that the source extends over 8 milliarcseconds, i.e. roughly 80x80 beam areas, and that the source contains compact and extended features as well as some well separated compact features. This model was chosen to provide a stringent test of Quasat.

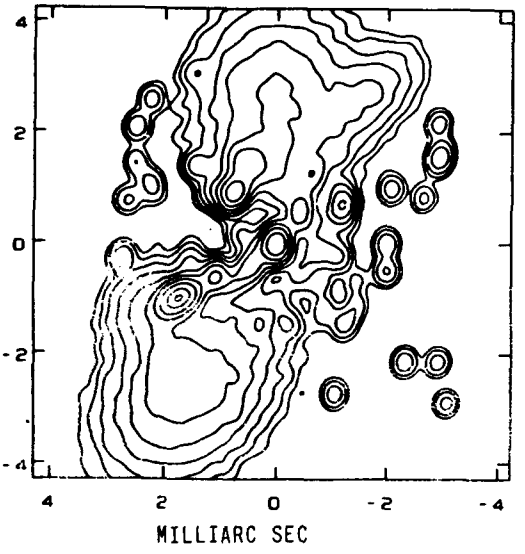

The VLBA map of the source (declination 45°, flux density 5.6 Jy). Note that much of the fine detail is lost. Contours: +/-1.1, 2.2, 4.4, etc. mJy/beam.

Figure 1.3-1: *Source restitution by the QUASAT array (orbiting VLBI observatory). Scaling these maps to VLT resolution needs to degrade the angular scale by a factor 4 at 0.5 μm, or 40 at 5 μm [Readhead et al. 1984, ESA SP-213].*

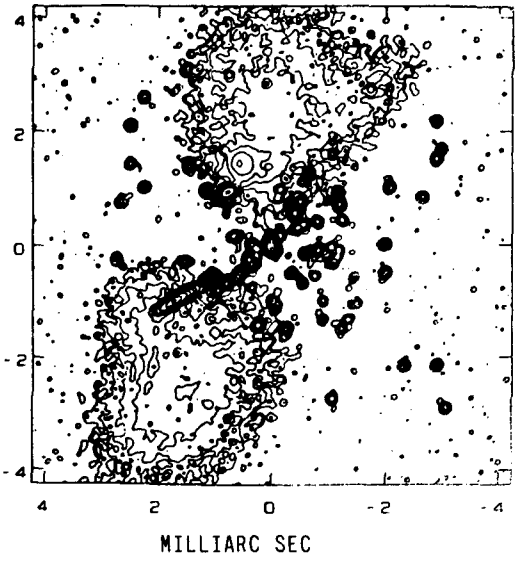

The Quasat plus VLBA map of the source (declination 45°). This map reproduces the essential features of the source down to a few times the thermal noise level for regions outside the source. It can be seen that the combination of Quasat plus VLBA does a reasonable job on both extended and compact regions of emission. However, the extended regions show variations significantly above the noise level. This can be substantially improved by adding more ground stations. Contours : +/-0.3, 0.65,1.3, etc. mJy/beam.

1.3.1. Infrared wavelengths

Infrared speckle interferometry with 4 m class telescopes has already provided very useful diffraction-limited observations on all the topics discussed below, and will continue to do with the factor of two in resolution brought by the VLT individual telescopes. It will also appear that real advances need a factor of ten in resolution gain, i.e. two telescopes interferometry.

We assume that the VLT interferometer works at $1.5 \leqslant \lambda \leqslant 25$ μm, in the atmospheric windows, with a maximum baseline length of 150 m, a resolution λ/D which will vary between 2 and 33 milli arc second and a sensitivity which is discussed in detail in Appendix A3 and summarized in Fig. 1.3.1-1.

The obtention of a detailed image, at milliarc second resolution, is certainly the final objective for most of the sources. But the availability of a more limited information, a 5 x 5 pixels image for instance, due to the limited number of baselines, is already a powerful tool for improving our understanding, as shown by the history of radio interferometry : it started with 3 to 5 antennas systems (Cambridge 1 mile, 0.5 mile, NRAO, Caltech) at centimetric wavelengths, as the present generation of millimetric interferometers has 3 to 5 elements (Hat Creek, Caltech, Nobeyama, IRAM).

a) Circumstellar shells and envelopes

Evolved stars are believed to be the major source of *interstellar dust*. (Holzer and McGregor 1985), but the actual production-mechanism, which occurs in the star envelope, is not fully deciphered. Recent observations of dust ejection around Betelgeuse (Roddier and Roddier 1984) and possible variations of its emission at 10 μm (Bloemhof et al. 1985) may indicate that dust properties vary on a year time scale.

Understanding the dust formation may progress by measuring the envelope size vs. wavelength, especially in specific spectral bands of NH_3 and H_2O ices or of silicates (Mira or OH/IR stars), since the condensation temperature of these species are very different. In carbon stars, the study of polyaromatic hydrocarbures (PAH) at 3.28 μm may decide if these "molecules" are precursors of interstellar graphite or, conversely, formed by collisional breaking of larger grains. In Wolf-Rayet stars, of high luminosity, the dust condensation zone is located further away from the star, and easier to analyse spatially.

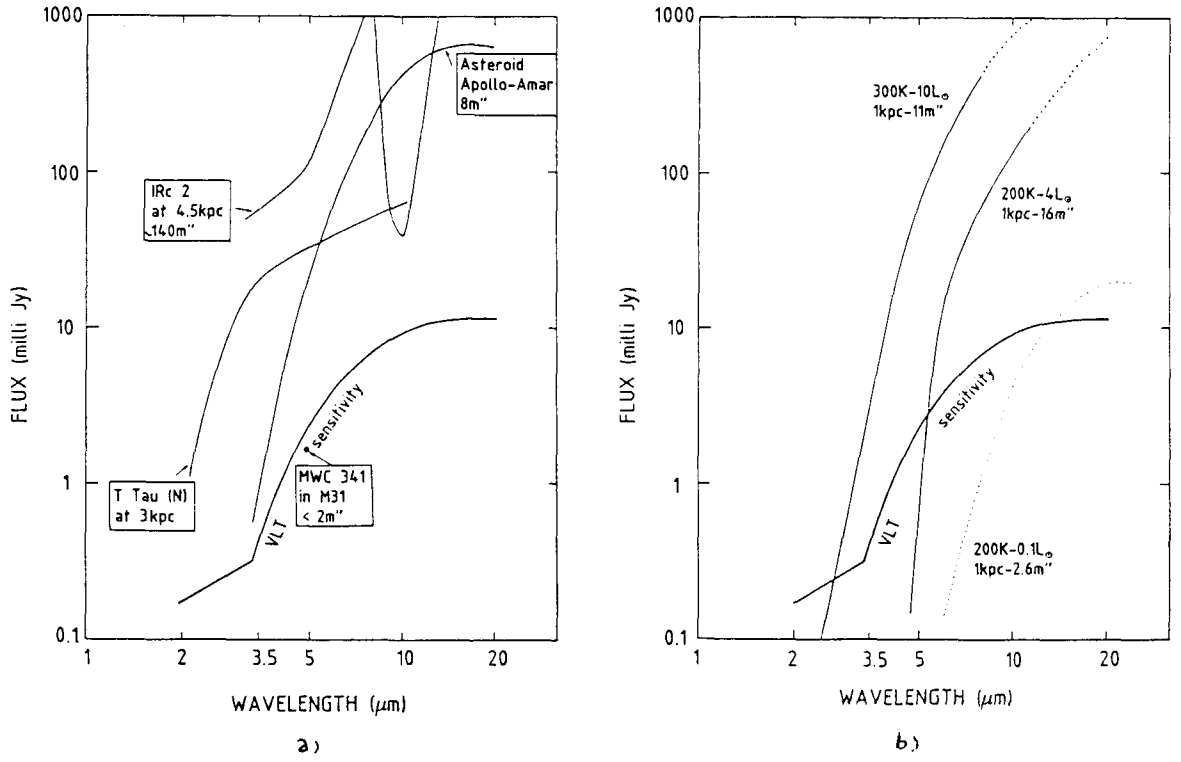

Figure 1.3.1-1

Scientific potential of the interferometer in the infrared. The VLT sensitivity is from Appendix A3 (Fig.A3-1) and corresponds to the fully phased pupil, 8 m in diameter, with 1 second integration, S/N = 1.

a) The infrared spectrum of a few important types objects is reported. Objects have been placed at various distances. T Tau (N) is the cold companion in the T Tau star; IRc2 is a typical bipolar flow source; MWC 341 is possibly a galactic accretion disc. An asteroid (Apollo-Amar) is also shown at its actual distance. Sizes, in milliarc second, are derived from measured sizes of the actual objects. Nuclei of Seyfert galaxies lie above the 100 mJy flux level. The galactic nucleus NGC 1068 is out of scale (2 Jy at 3.5 μm).

b) Thermal emission of blackbodies of various luminosity, size and distance. Their diameter is given in milliarc sec. The spectrum curve is dotted at wavelengths where the source would no longer be fully resolved on the maximum 150 m baseline.

SiO maser models propose to associate these masers to giant convection cells in the stellar photosphere, while, in χ Cyg, CO observations at high spectral resolution trace SiO in a specific layer at 800 K, 10 stellar radii from the surface (Hinkle et al. 1982). The study of the spatial extension of silicates emission is another critical observation : since measuring the effective size of SiO masers will soon be done by millimetric interferometry, the comparison of the two zones provide clues on the pumping mechanism.

The acceleration mechanism of the layers is unclear. Observation of IR molecular lines in several types of stars (H_2O in R Leo : Hinkle and Barnes 1979; CO in IRC 10216 : Sahai and Wooten 1986) indicate concentric layers which could be spatially resolved to track the acceleration.

While the outer part of the envelopes appear spherical, the cores of IRC + 10216 and VYCMa depart from this symetry (Dyck et al. 1984); other objects are highly bipolar (GL 2688). These bright objects will easily be resolved by interferometry and the role of binary structure in the ejection mechanism could be studied.

Diameter mesurements of Mira or OH/IR stars are related to stellar structure (§ 1.3.2) and will be of direct access to infrared interferometry. Measurements of CO vibration rotation lines at 2 and 4.6 μm of χ Cyg envelope (Hinkle et al. 1982) suggests a pulsating photosphere associated to the envelope.

b) Star formation

This capital problem of contemporary astrophysics progresses only through specific observations, because of the high dust opacity in star forming regions. Infrared photometry and spectroscopy, millimetric interferometric spectroscopy are limited to ca. 1 arc sec resolution, although IR diffraction limited imaging with large telescopes may gain one order of magnitude (§ 1.2). Only VLA observations at centimetric wavelengths of a limited number of molecules (SiO, NH_3) give access to the innermost part of the core in an object such as L 1551 (Snell et al. 1985; Rodriguez et al. 1986 - Fig. 1.3.1-2). Infrared interferometry is likely to be one of the most powerful tools to investigate the environment of proto- and young stars.

The IR emission of this environment is comparable to the emission of evolved stars, although the geometry, the dust origin and kinematics are completly different. IR speckle interferometry has already detected disc-like structure (protoplanetary ?) around HL Tau (Beckwith et al. 1984) or

Orion IRc2 (Chelli et al. 1984). The detection of dust rings around slightly more evolved stars such as β Pic or Vega (Aumann 1984, Aumann 1985) may be a related problem: the nature and size of these dust particles is a debated question (Anandarao and Vaidya 1986).

Presently, the sample of very young objects embedded in dense molecular clouds is limited to about thirty. The analysis of new infrared sources discovered by IRAS survey will undoubtly increase this number to one hundred or beyond, improving the statistics, providing objects of lower luminosity and/or mass. None of the known objects yet appears as an accreting proto star *stricto sensu*. Fluxes and color temperatures give sizes of 10 to 30 milliarc sec (Fig. 1.3.1-1b), which have been verified on a few objects : Orion BN (Foy et al. 1979) is surrounded by an H II region 80 m" in diameter (Moran et al. 1983), while far IR spectroscopic indication would indicate regions of accretion/ejection ten times smaller, accessible to interferometry only.

The generation and focusing mechanism of highly collimated mass outflows and *bipolar flows* is unknown, while this structure appears to be an extremely general, i.e. fundamental, phenomenon. Radio observation of the best studied object (L1551 IRS 5) could be interpretated as the internal edge of a shock-ionized accretion-disk, but such a disk has not yet been resolved, nor *a fortiori* mapped by infrared interferometry. About five disks are reasonably identified today, over ten are suspected in nearby associations, all are a few hundred a.u. in size. The relation between disks and large scale mass-outflows, local magnetic fields, locally collimated flow and rotation axis all need to be investigated at the sub arc second scale. Again, sensitivity and resolution capabilities of an infrared interferometer would allow to study any of the sample objects known today, even remotely located as is W3 IRS 5; in such highly contrasted objects, where temperature gradients are high over a 100 milliarcsec scale or less, sensitivity and dynamic range are essential.

The discovery of an infrared companion to T Tauri (Dyck et al. 1982) and of a faint optical companion (Nisenson et al. 1985) interrogate on the frequency of *binary systems in early-type stellar objects*, and on their relation to bipolar flows formation (Abt 1985). Systematic search in a nearby cloud such as ρ Ophiuchi has begun and shown interesting correlations (Zinneker and Perrier 1986), but the resolution obtained by speckle interferometry may not be sufficient. The range of 0.1-1 $L_{\odot}$ of these objects requires the sensitivity of a large interferometer.

***Figure 1.3.1–2** : The region of L1551 IRS 5.*

This composite figure shows the position and size of the CO emission from the ambient molecular cloud (upper left; Frame 1), the high-velocity molecular gas (upper right; Frame 2), the extended radio continuum source (middle right; Frane 3), the central part of the same radio source (lower right; Frame 4), and the expected circumstellar disk (lower left; Frame 5) (from Snell et al. 1985). Observation from the VLA (Rodriguez et al. 1986) at 0.3" resolution indicate a slight rotation of the axis at this scale.

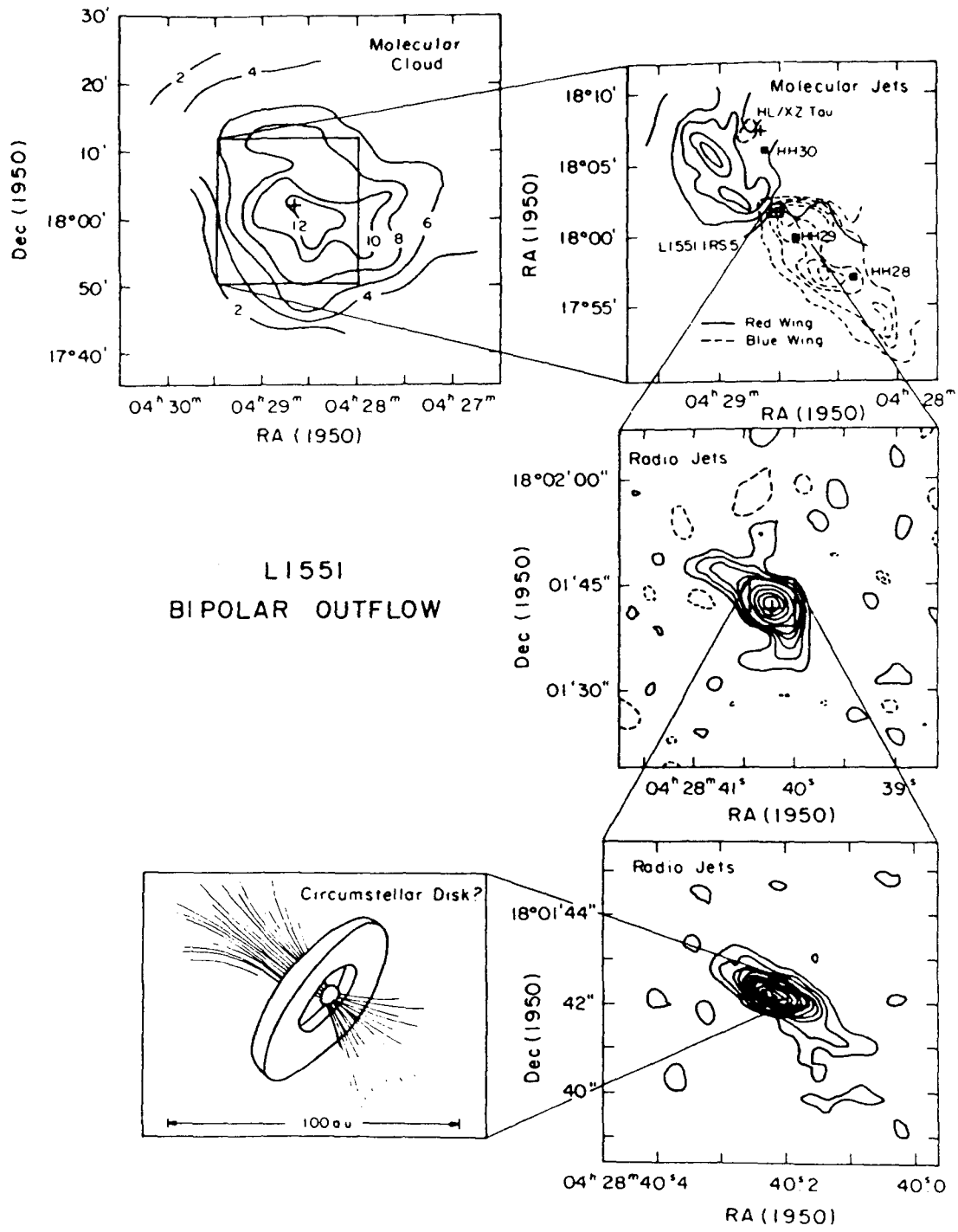

c) Formation of solar-systems and planets

This field is highly speculative, and will probably remain so as long as observations are so badly lacking. The above-mentioned discoveries of orbiting material around stars are far from being conclusive. The discovery of a brown dwarf companion in the Sun's neighbourhood (McCarthy et al. 1985) is controversial (Perrier and Mariotti 1986). On the other hand, simple sensitivity and angular sizes estimates (Léna 1983, Dyck and Kibblewhite 1986) indicate that infrared interferometry is one of the most powerful tools to observe solid fragments as cold as 250 K at distances of 0.1 to 1 Kpc from Earth. Moreover, the presence of a quasi-point like star in the field of view will allow phase reference (§ 2.5), therefore long time integration with the associated sensitivity and dynamic range.

d) Galactic nuclei

Results to date are as follows :

• NGC 1068 (20 Mpc). The results of Mc Carthy et al. (1982) show that 76% of the 2 Jy flux at a wavelength of 2.2 μm originates in a core 200 milliarcsec in diameter. Perrier and Chelli (1984) show that the nucleus at 3.6 μm may have a core-halo structure with a halo of 0.3" and a core < 0.1".

Although these speckle interferometry results give upper limits on the nuclear dimension of the order of 0.1", the major part of the emission is expected to arise in the "broad line region", responsible for the line emission in the visible, and which, from physical arguments, is probably of the order of milliarcsec or less (see Reviews by Ulrich 1981 and Rees 1981).

• NGC 4151 : speckle interferometry at Mauna Kea at 2.2 μm shows that the majority of the flux comes from a component < 0.2" (Dyck and Kibblewhite 1986).

• Unresolved fluxes from the nuclei of NGC 4151, Mrk 231 and 3C273 are typically 400 mJy, corresponding to T = 1000 K blackbody of size 1.1 milliarcsec at 5 μm, fully resolved with a baseline of 1.0 Km at λ = 5 μm.

Seyfert and normal galaxies have flux densities in the range 2-10 μm of 10 to 200 mJy (Devereux et al. 1986). Although these fluxes are close to the limit of sensitivity at present, they should nevertheless be detectable (Fig. 1.3.1-1). In principle, the visible nuclei of these galaxies (m_V = 13-16) might be used as a reference source for adaptive optics (Appendix A1) and for the monitoring of the fringe phase (§ 2.5).

• The nucleus of the Galaxy is formed of a complex of infrared sources, bright enough to be studied with an interferometer, and not resolved yet (Allen and Sanders 1986). Its detailed study at milliarcsec resolution at infrared wavelengths, both in the continuum and in spectral lines (H_2, NeII) will provide important data on energy production and transfer, densities, gross expansion or contraction of cloudy aggregates.

• Gravitational lenses. The high IR emission of optical quasars increases the probability of using such objects for gravitational studies, not only for the phenomenon itself, but also for the mass distribution in the deflecting object. In a sense, lenses are telescopes provided by nature which allow to investigate in detail cosmological parameters such as H_0 or q_0, but also structure of the object, especially the presence of unseen matter or its distribution.

e) Supernovae in other galaxies

Should supernovae in other galaxies be bright enough to be detected in the infrared, it will be possible to directly measure the distances to the galaxies and thus contribute to a fundamental parameter in astronomy. An infrared interferometer with a resolution of 1 milliarcsec could measure the expansion of a supernova shell at the distance of Andromeda (expanding at 10^4 Km/s = 10^9 Km/day) on a time scale of days, and in galaxies at a distance of 10 Mpc on a time scale of weeks.

1.3.2. Visible wavelengths

We assume that the VLT interferometer works at λ = 550 nm with a maximum baseline length of 150 m, a maximum resolution of 0.9 milli arc sec, a limiting magnitude of 14.

1.3.2.1. Two telescopes interferometry

Stars

Diameters are thought to be measurable with a better accuracy at near infrared wavelengths than in the visible (Di Benedetto 1985); they will not be discussed in the following, but peculiar cases.

The observation of the second lobe of the visibility function provides an accurate determination of the center-to-limb darkening. At visible wavelengths,

this is possible for every type of stars in the HR diagram cooler than the type AO, for the luminosity classes from VI to I (Foy 1981). The determination of the center–to–limb darkening measured at different wavelengths in the visible, where it is rapidly varying with λ, will enable to build up a new generation of semi–empirical model atmospheres, particularly for giants and supergiants. Let us recall that, up to now, such a work has been possible for only one star: the Sun.

Mapping the stellar surfaces with full resolving power of the interferometer will help in clarifying numerous problems :

– Wolf–Rayet stars : the physical parameters characterizing these stars (e.g. mass and radius) are poorly known, so that even their evolutionary status is not yet understood; however they are a keystone in the models of galactic evolution since they are the most important regenerators of the interstellar medium. They are expected to be rather small, typically $2R_{\odot}$, so that only the closest one : η Car can be securely considered as resolvable (and may be γ^2Vel). Determining its diameter will considerably improve our understanding of this complex object; it will be highly interesting to determine the extension of the ejected component (s) and its structure by observing at the wavelengths of different emission lines.

– Be stars : Thom et al (1986) have first resolved the circumstellar matter emitting around γ Cas at Hα : this work opens a large program about the structure of the circumstellar component of Be and shell stars, the goal of which being to provide the necessary informations to disentangle between the various possible models for Be Stars (Poeckert 1982). The diameter of the central star should be resolved in a very few cases.

– Ap stars : mapping the surface of Ap stars is a direct probe of the oblique rotator model; observations will have to be carried out at the wavelengths of strongly enhanced absorption features.

– Cepheids : The period–luminosity relationship established for these stars is a basic tool in the determination of distances in the Universe. The zero point is known with an uncertainty of ± 0.2 magnitude. It can be significantly refined by combining the diameter variations directly measured with an interferometer, with the radial velocity variations, from which it comes the stellar distance. Thompson (1976) has discussed that an accuracy of ± 2% in the mean angular diameter of sample of 29 stars should result in a decrease by a factor of two in the uncertainty of the zero point.

Another problem can be solved about Cepheids with a long base interferometer : that of the discrepancy between the masses predicted from the stellar evolution theory and those predicted by pulsation theory (Cox 1980). Presumably, the best way to solve this problem is to measure spectroscopic binaries as interferometric binaries. A by-product will be another, independent, estimate of their distances.

- T Tauri stars : the energy balance of these pre-main sequence objects is still poorly understood, as illustrated by the drastic revision of the model of T Tau itself when Dyck et al. (1982) discovered its cool companion. The spatial energy distribution in emission lines should be determined to know the structure of the sub-circumstellar medium.

- G. K. M giants : most of the stellar energy is carried outwards through the mantle by convection. The convection theory is still quite uncertain; it is able to predict a reliable value of the typical scale of the convective eddies. Super granulation in these stars could be surprisingly large (Schwarzschild 1975) and then could be measured with the interferometer. The inhomogeneities of the chromosphere should be also measurable, mainly in the 1.083 μm HeI line.

- Red evolved variables : we do not know the conditions of the emergence of the shock wave(s) which propagates through the extended atmosphere of these stars during the (pseudo-)cycle (Wilson and Hill 1979). The full resolving power of the interferometer observing in emission lines will allow to determine the structure of the shock when it begins to reach the photospheric layers τ (continuum, λ) $\simeq$ 1. Also, from the measurement of the diameter of the emitting shockwave together with the radial velocities, one will determine the distance of remote cool variables. This will be particularly interesting : i) for long period variables in the direction of the galactic centre, and ii) for peculiar stars of which the absolute magnitude is poorly known (e.g.: irregular variables, N or R stars).

- Flare stars : Proxima Centauri is the only flare star close enough from the sun to be fully resolved with a reasonable baseline (expected diameter : 2 marsec), so that it is the only case where we will still be able to "see" what is a flare. A large aperture interferometer is required to get a significant signal to noise ratio, due to the brevity of flares (typically 20 minutes).

- Contact binaries : Imaging a contact binary would considerably enlighten on the stellar inner structure and on the physical mechanisms involved in mass exchanges and in the formation of accretion disks, i.e.: on the basic

processes occuring in a lot of exotic objects. Very few semi-detached or detached systems are resolvable : it is likely that the interferometric performances of the VLT should be extended down to λ 400 nm to be able to fully resolve such a kind of objects. A large aperture interferometer is required to get observations within a run short enough as compared with the period of these systems.

Magellanic Clouds, Novae

At least two important observations can be undertaken with an interferometer :

– The spatial resolution of spectroscopic binaries will provide both the masses of the components and their distance. This is highly interesting since most of the candidates are very luminous stars (e.g.: Wolf-Rayet stars, B to K type supergiants), of which the mass is badly known. Now this parameter is critical in the models of the chemical evolution of the Clouds and, broadly speaking, of galaxies. Furthermore the determination of the distance of stars in the SMC will largely help our understanding of its structure, which is at present much controversed: its depth along the line of sight would be ≃ 32 kpc. Fig. 1.3.2-1 shows the typical (shaded) area in the log (period) versus log (semi-major axis) diagram for which these parameters (mass and distance) could be derived within a reasonable time interval.

– The observation of the diameter of the shell of novae in the post-maximum phase will also lead to the determination of the distance of the Clouds, in a much shorter time, when combined with the radial velocity measurements. It is clear from Fig. 1.3.2-2 that the observation of novae in the Clouds needs an interferometer (whereas a single 8 meter telescope is well suited to study galactic novae).

Supernovae

Supernovae are likely bright enough to be observable in the very strong emission lines Hα and [OIII] one year after maximum. Since the typical velocity of the ejected material of supernovae is ≃ 6000 km/s, the diameter of these objects will be measurable up to 2.8 Mpc at Hα or to 3.7 Mpc at [OIII], i.e. as far as the close neighbouring out of the Local Group. The probability to observe such an event within this range of distance is quite weak : 1 every 20th year. But it is very exciting : if we combine the angular diameter to the radial velocity, again we derive the distance, a basic parameter both to estimate the energy output of the supernovae, and to study the cosmic distance scale.

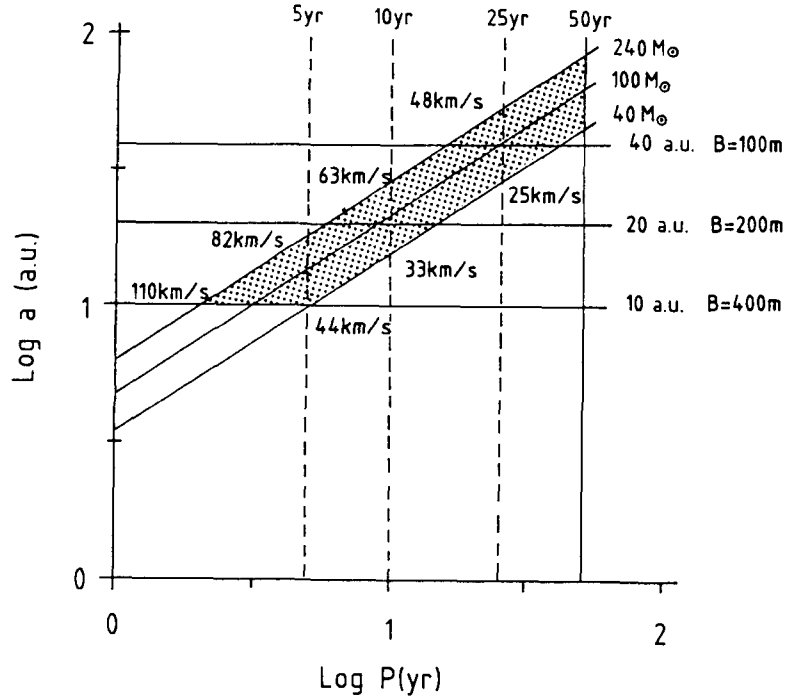

Figure 1.3.2–1 *: Binaries in the LMC.*
The distance is about 50 Kpc. Systems are made of two giants ($\Delta m \sim 0$) separated by the distance a (a.u.), of period P(yr).

$$Log\ a\ (a.u.) = \frac{1}{3}\ Log\ M(O) + \frac{2}{3}\ Log\ P\ (yr);$$

$$K(km/s) = 30\ \frac{sin\ i}{\sqrt{1-e^2}}\ \frac{a}{p};$$

$$i \sim 45^{o};\quad e \sim 0.3;\quad K \sim 22\ \frac{a}{p}.$$

B is the interferometer baseline.

Active galactic nuclei

The central zone of the active galactic nuclei (AGN) which emits the continuum radiation is expected to be highly confined: < 0.03 pc (Masegosa et al. 1986) or ≃ 0.03 pc (Ferland and Osterbrock 1986). The maximum baseline of the interferometer will allow to resolve 0.1 pc at the distance of NGC 4051, or 0.03 pc at the distance of Virgo, so that the size of the continuum region could be determined directly for the closest AGN: This will provide a very powerful information to the models, since the flux per unit surface radiated by the nucleus will then be severely constrained. The structure of the Broad Line

Region (BLR) is expected to be easier to determine since its diameter would be ≃ 1.5 pc at Hα (Kielkopf 1985; Whittle 1985) although it could be much smaller (Peterson, 1985).

The role of massive stars in nuclear regions of AGN may be understood (Terlevich and Melnick 1985), when the stellar population of AGN's will be resolved.

QSO's

The structure of the Narrow Line Region (NLR) in the closest QSO's would have about the same angular diameter as in the closest AGN so that the same goal could be carried on.

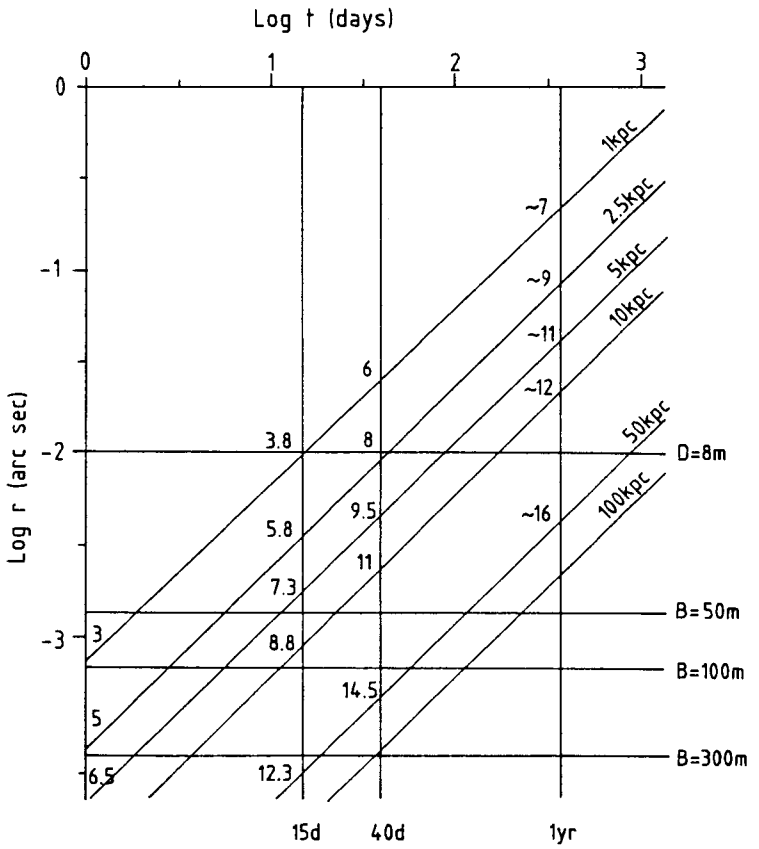

***Figure 1.3.2–2** : Novae in the Magellanic Clouds Radius of the envelope (Hα) versus the time t (days). The limit of various baselines B are indicated. Visual magnitude m_V of the central star is indicated. The resolution limit is given for the Hα envelope. Assumptions are :*
$M_V(max) \sim -7$;
$M_V(15d) \sim -6$;
$V_{exp} \sim 10^3 Km/s$;
$r(arc\ sec) = 0.58\ t(days)/d(pc)$.

1.3.2.2. Diffraction-limited imaging with a single telescope

Diffraction limited imaging with a single 8-10 m telescope provides 10 to 20 times less angular resolution, but is tightly complementary to fill the low frequency range in the (u,v) plane. Thus it is very appealing goal, which has little consequence on cost and on management of a VLT.

Speckle interferometry at visible wavelengths has proven its ability to achieve unique results in a wide range of astrophysical scopes. This enables to foresee the most outstanding observations expected from a single 8 meter telescope (Appendix A6).

Solar system

- Mapping the large scale structure of the remote bodies : Pluto-Charon and Triton (resolution: ≃ 210 km), face of Uranian satellites hidden during the Voyager 2 rendez-vous (resolution : ≃ 130 km).
- Determination of the size and shape of typical asteroids (down to 3.5-30 km depending on the minimum distance) (Encrenaz 1981) ; study of the duplicity (to date, no asteroid has yet been resolved into two components) and the question of the role of coalescence at the early beginning of the solar system.

Stars

The major breakthrough in the field of stellar physics will concern the atmosphere of cool evolved stars :

- Observations through narrow wavelength bandwidths provide a direct tool to take soundings into the hugely extended atmospheres of these stars, leading to an empirical determination of their structure. Indeed the optical depth in absorption lines or bands reaches unity at widely different levels in these atmospheres (Labeyrie et al. 1977; Bonneau and Foy 1983). The closest long period variable (LPV), Mira, is just resolved at blue wavelengths in the continuum with a 3.60 m telescope. About 40 stars (LPV's, semi regular variables, M, S and C, giants or supergiants) will be resolved, within a few hundreds with a Southern 8 m telescope. Together with the accurate trigonometric parallaxes which will be measured by the ESA satellite Hipparcos, these diameter measurements at several wavelengths will enable to compute reliable semi-empirical model atmospheres, which at present are lacking for these stars. Aspects concerning the dynamical properties and the shock-wave

propagation across the atmosphere will be able to be extensively investigated by observing in emission lines (Bonneau and Foy 1985).

– A few stars (Betelgeuse, Mira, Arcturus, and some more) are large enough so that the second zero of their visibility function should be observable even at continuum wavelengths with a 8 m telescope; then the centre–to–limb darkening can be measured accurately, leading again to semi–empirical model atmospheres. Also it will be highly interesting to search for surface inhomogeneities, presumably through TiO spectral features or through emission lines (Roddier and Roddier 1985). The stellar surface rotation and the typical size of supergranules (Schwarzschild 1975) will be derived: both are important parameters to model the stellar mantle and, consequently, to discover the mechanism responsible for the flux variability observed for most of the cool evolved stars.

These observations will make use of the full resolving power of a 8 m telescope; they are expected to markedly improve our knowledge of these stars, of the statistical properties and the dynamical mechanism in their atmosphere and therefore of the physical process of their large mass loss, and their evolutionary stages.

– Novae : The structure (i.e.: the linear and tangential distribution of the electronic temperature and density) of the shell ejected by a nova will be observable from as early as ≃ 10 days, assuming a typical distance of 2 kpc (Blazit et al. 1977). This will provide informations about the ejection mechanism and, together with the radial velocity curve, about the only available direct estimate of the distance, a basic parameter to derive the absolute energy outflow radiated during the explosion.

Magellanic Clouds

– Nature of the bright sources like R136a : supermassive single objects or very compact clusters (Meaburn et al. 1982; Baier et al. 1985).

– The trigonometric parallax and/or the proper motion of the Clouds can be determined using the motion of the Sun in the Galaxy and a few QSO's behind the Clouds. This galactic trigonometric parallax is expected to range from 0.6 milliarcsec/yr for the LMC to 0.8 milliarcsec/yr for the SMC. A very careful analysis of the data, using the full resolving power of a 8 m telescope should lead to significant results over a time interval of ≃ 5 years. Such unique determinations would markedly improve our understanding about the origin and

the dynamical evolution of the Clouds (Lynden-Bell 1975).

Active galactic nuclei

– Very little work has been done in this field with the 4 m class telescope (Meaburn et al. 1982). At the distance of NGC 4151, a single 8 m telescope resolves structures ≃ 1 pc wide at Hα. This is small compared with the expected size of the narrow line region (NLR): ≃ 300 pc (Heckman et al. 1984; Ferland and Osterbrock 1986). The direct measurement of the spatial energy distribution profile within 0.1" from the centre in different emission lines of the NLR for different Seyferts will bring severe constraints to the models within a wide variety of physical conditions (De Robertis and Osterbrock 1986).

Gravitational lenses

A survey of QSO's (at least those appearing intrinsically bright) in order to detect multiplied images will enable to reach basic results concerning :
- Cosmological probe, by sampling the mass distribution from $z \simeq 0.3$ up to $z \simeq 1.0$ from the count of lensed QSO's (Tyson 1983; Dyer 1984).
- Test of the interpretation of the missing mass problem with massive black holes in galactic holes. In the case of our Galaxy, these black holes would act as gravitational lenses with a mean separation of 7-10 marsec (Lacey and Ostriker 1985), ranging close to the maximum resolution of a single 8 m telescope.

Chapter 2 : OPTICAL INTERFEROMETRY : AN OVERVIEW

2.1 *Image formation in interferometry*

A single telescope provides a spatial frequency coverage which is the two-dimensionnal autocorrelation function of the pupil measured in units of wavelength. In other words, the diffraction-limited image contains all spatial frequencies from zero to the telescope cut off frequency λ/D (D=telescope diameter), weighted by a monotonously decreasing function (the Modulation Transfer Function or MTF). The spatial frequency domain is called the (u,v) plane, after its two coordinate axis u and v. The atmospheric turbulence introduces random wavefront phase errors over the pupil, which produce a speckled image (the "seeing" disc). The atmospheric MTF is now a random function, which highly attenuates the high spatial frequencies. Restoring this information is the goal of speckle techniques, and these technique have now succeeded in reconstructing with a good accuracy (a few percents) both amplitude and phase of the object complex spatial spectrum up to the frequency λ/D. This mode of operation is already a powerful prospect for the VLT, and described in detail in Appendix A6. (*)

Radio aperture synthesis has fully developed the original idea of Fizeau. The wave-front is sampled in two well separated points by two separate telescopes on a base $\vec{L}$. This samples the (u,v) plane at the frequency $\vec{L}/\lambda$, and measures one value of the object spectrum, called the complex visibility (amplitude and phase). The (u,v) coverage is obtained by varying the projected baseline $\vec{L}$ over the sky either by moving the telescopes or by letting the diurnal motion do it, or both. This coverage is usually incomplete, leaving

---

(*) Note: in all this chapter, and the following ones, the word "phase" will be used to designate different quantities. WAVE FRONT PHASE is the relative phase of the wavefront over the pupil, generally distorted in random fashion by the atmosphere. PHASE (visibility phase) of the object (or image) designates the argument of the co mplex Fourier transform of the object (or image) two-dimensionnal intensity distribution. Thcsc two quantities are indeed related, but not necessarily identical.

holes or empty stripes in the (u,v) plane. The treatment of radio signals is made easy by the existence of phase-stable amplifiers, that allow to split the broad-band input signal into many channels for separate analysis. The absence of such amplifiers for optical signals is one of the main differences between the two fields.

Radio aperture synthesis arrays of a few kilometer baseline can be made reasonably phase-stable. They can be calibrated by observing objects of known brightness, shape and position from time to time between the observation of unknown objects.

For longer baselines, especially VLBI, phase-stability is out of question. Even for smaller arrays, the phase-stability is not always considered sufficient. In these cases, the observed object itself must be used for calibration, in a process called SELFCAL, or phase closure, or hybrid mapping (Cornwell and Wilkinson 1983).

An absolute requirement for this technique is that most of the measurements errors can be traced back to the individual telescopes.

Fundamentally, trustable information is not obtained on the object itself but on its complex spatial spectrum, where real error bars can be given on amplitude and phase. Therefore, it is in the (u,v) plane that a confrontation should be achieved between models and observation. Fortunately or not, astronomer's eyes and minds are used to work with images. To reconstruct an image from a partially sampled (u,v) plane where visibilities are affected with errors introduces ambiguities and artefacts.

Image reconstruction

A first approximation of the image is obtained by Fourier inversion of the measured visibility data. Three factors already affect its quality :

-a) The u-v coverage: Since the (u-v) plane is incompletely sampled, the final image will contain the object convolved with some point-spread function (PSF). If the (u,v) coverage is very incomplete, this PSF has high sidelobes that may obscure faint objects in the vicinity of strong sources and provide unaestetic images of single objects.

-b) The amount of phase information: Visibility phases are believed to contain more information than amplitudes (Oppenheim and Lin 1981), but are unfortunately much harder to measure. Situation of increasing power are: no phases at all (amplitudes only), phase derivatives with respect to spatial frequency, phase closure and absolute phases. The latter is impossible with

non-phase-stable instruments.

-c) The noise in visibility data: One must distinguish between random noise and systematic errors. The latter can often be corrected, provided they are correlated over more than one (u,v) sample.

The next step to restore an image close to reality is to compensate for the incomplete coverage of the (u,v) plane, hence providing a full aperture synthesis. In radioastronomy the PSF of the instrument is estimated on a point-source or assuming that the object itself contains at least one source close to a point source. This process (CLEAN) allows also to estimate the phase errors due to individual telescopes. Other methods use the positivity of the source or the information present in the image (Maximum Entropy Method). The difficulty of such methods lies in the assessement of their dynamic range, i.e. the level of noise in the image due to the restoration process itself. These processes give a good convergence for arrays with a large number of telescopes (the VLA has 27 antennae). If the array has some redundant spacings, a model is not required to estimate telescope errors. One simply uses the fact that any differences between the output phases of identical interferometers must be caused entirely by measurements errors. This model-independence is very powerful, especially for extended objects that are difficult to model. The requirement that all errors must be telescope-based (which also implies a high S/N) remains the same however. It is important to realize that, as long as the PSF is accurately known and the object is relatively simple, excellent images can be produced with a very poor (u,v) coverage. The result gets worse only if high sidelobes coincide with other objects with a strength comparable to the sidelobes.

Radio aperture synthesis can now be called mature. It can produce maps with milliarc resolution (VLBI), a dynamic range of up to 10^4 (Westerbork), and truly breathtaking images of very complex and extended sources like the one of Cygnus A produced by the VLA (Fig. 2.1-1). This latter array was only designed originally to detect point-sources, but developed into a much more powerful instrument.

Current optical interferometers, such as the 0.26 or the 1.5 m CERGA systems, are only measuring amplitudes. The use of phase derivatives with respect to spatial frequency [(i.e. the quantity $\vec{\nabla}\phi(u,v)$] is now well developed in speckle interferometry (Knox-Thompson 1974). The use of other techniques such as phase-derivation with respect to the wave frequency (spectral phase derivatives), or as phase closure have not been developed yet in optical

interferometry partially because of the very small number of telescopes used in the interferometers existing to date.

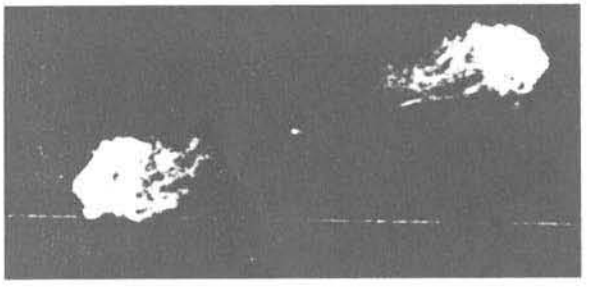

***Figure 2.1–1** : VLA image of Cygnus A at λ6cm. The dynamic range is about 10^4.*

2.2 *From radio to optical interferometry*

The quality of radio interferometry results from its ability to measure complex visibilities over a certain domain of the (u,v) spatial frequency plane. Then, various mapping techniques are used to improve the image quality.

At optical wavelengths, the added complexity comes from two facts, due to atmospheric effects:

-a) the phase of the wavefront issued from a point source is, in general, no longer uniform over the surface of each pupil;

-b) these phases are randomly varying with time, over short time scales (10 to 100 milliseconds).

Hence getting the amplitude of the complex visibility (or fringes contrast) is straightforward, but atmospheric phase disturbances do prevent a direct measurement of the phase of the wave-front. The most favourable situation is encountered when the size of the atmospheric coherence area (r_o, a wavelength dependent quantity) becomes comparable to the size of the pupil itself. At longer wavelengths, i.e. infrared, this condition allows the use of much larger telescopes (Table 2.2–1).

Table 2.2-1

Chromatic dependence of coherence area
(1 arc sec seeing)

λ (μm)	0.5	2.5	5	10	20
r_o (m)	0.1	0.59	1.58	3.64	8.36

At shorter wavelengths, or when the condition

atmospheric coherence area > *telescope diameter*

is not fullfilled, adaptive optics, operated in the focal plane is, in principle, able to restore in real time full coherence over the whole pupil. Whenever the full coherence of the wave front can not be achieved over each pupil, one must break the pupil into sub-areas, each one beeing coherent; the final result is much less favorable in terms of signal-to-noise ratio.

Comparing with radio wavelengths, where phase errors are constant with time and uniform over individual telescopes, it indeed appears that phase retrieval at optical wavelengths shall be more difficult.

Radio interferometry uses a single detector with possibly multiple spectral channels. Optical interferometry needs at least as many pixels, on each spectral channel, as there are coherent areas over the pupil. Since (u,v) coordinates are measured in wavelengths, different spectral frequencies represent different (u,v) points when they are measured with the same interferometer. As long as the object appearance remains approximatively the same at different frequencies, this spectral information may help to determine the phase, or rather the phase derivative $\vec{\nabla}\phi(\partial\phi/\partial u, \partial\phi/\partial v)$ with respect to spatial frequency.

Simultaneous measurements

The techniques that are used with such notable success in radio aperture synthesis have the following requirement: the number of independent measurement errors must be smaller than the number of visibilities measured. This gives the constraints that allow us to generate a model of the observed object iteratively. In the presence of rapidly varying atmospheric phase errors, consecutive measurements will have different errors (unless some method of phase-tracking is possible). The only way to reduce the number of independent phase errors in this case is to measure a number of visibilities simultaneously. There are several ways to do this:

a) With a single interferometer (2 telescopes), one can measure the phase-difference between two (u,v) points located at less than $\Delta\vec{w} = \vec{D}/\lambda$ apart, i.e. within the interfering pupils. In practice this provide the phase-derivative $\vec{\nabla}\phi$.

b) With only 2 telescopes it is also possible to measure the visibility at multiple frequencies by dispersing the light. Since (u,v) coordinates are

measured in wavelengths, each frequency corresponds to a different (u,v) point.

c) An array of N telescopes can provide N(N-1)/2 different interferometers. If all mesurements errors can be assigned to individual telescopes, the number of independent errors is N, which is smaller than N(N-1)/2 if N ≥ 3. The measured phases can be combined to build error-free quantities called "closure phases".

Of these three, the array is the most powerful, but requires simultaneous use of all telescopes. Feasible in principle, these methods remain to be tested in optical interferometry but have already been experimentally studied with success over a single telescope at visible wavelengths (Baldwin et al. 1986 - Fig. 2.2-1).

Speckle work with large telescopes has already provided a large amount of information on the wavefront phase perturbations and their remedies through image reconstruction methods. Specific methods, such as speckle masking (Lohmann et al. 1983, Weigelt and Wirnitzer 1983), a triple correlation method (§2.4), have already succeeded in image reconstruction at optical wavelengths.

The goal of an interferometer is to measure the complex visibility (amplitude and phase) of the object Fourier transform in the frequency (u,v) plane. The largest extension of the baseline sets the ultimate resolution, while the density of the (u,v) coverage and the signal-to-noise ratio sets the image quality. Once the complex visibility is obtained, conventional techniques well known to radioastronomers may be applied to restore the image.

An optical interferometer must be carefully investigated wherever it differs from a radio interferometer: beam combination, access to the complex visibility, nature of detectors, ultimate sensitivity.

Theoretical and experimental approaches to optical interferometry [Labeyrie et al. 1984, Roddier and Léna 1984, Woolf 1984] provide today a firm ground to establish the configuration in which telescopes of 8-10 m size could be used efficiently and to derive conservative performances. In the next section, we shall discuss in detail what an ideal interferometer would be, in terms of working condition, image production, and ultimate sensitivity. We defer to the next chapter the specific discussion on the VLT, where indeed many compromises would have to be done.

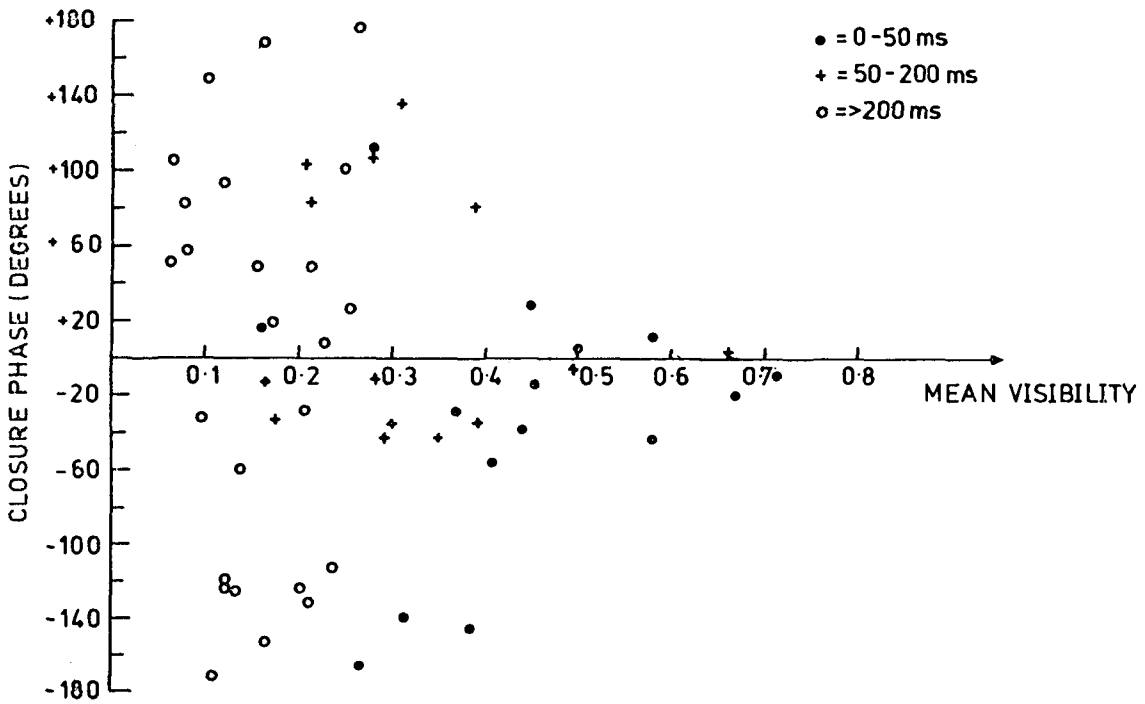

***Figure 2.2–1** : Phase closure at optical wavelengths. Several apertures (3 to 6) of a size comparable to r_0 (13–45 cm) isolate wave front elements over the single pupil of the 2.2 m University of Hawaï telescope at 677 nm. The focal plane image of an unresolved star is analysed and complex visibilities are deduced. Their mean amplitudes are measured and should ideally be unity for instantaneous exposures and uniform phase over the apertures. Closure phase is computed and should be zero. The observations show that it is indeed the case as soon as complex visibilities, even affected by atmospheric phases, are properly measured, and, in practice, $\phi \sim 0$ if $v > 0.7$ (After Baldwin et al. 1986).*

2.3 *Beam combination*

Each telescope provides an afocal beam, which is fed into a common "beam combination area". The different beams interfere over the detector, which measures the complex visibility.

When only two fixed telescopes are used, the "beam combination area" is mounted on sliding tracks, in order to keep constant the optical path from the source to the detector through either telescopes, correcting for the diurnal motion. When more than two fixed telescopes are used, optical delay lines

become necessary.

Optical delay lines are however not as easy to build as radio ones. Trombone-like arrangements of four mirrors are required, implying losses, polarisation problems, extra-maintenance costs, etc.

Delay lines are unnecessary if the telescopes are arrayed along an ellipse, intersection of the ground plane with a paraboloid aimed at the star. The central station where the beams are recombined is at the focus of this paraboloid.

The ellipse however keeps deforming itself during observation, since the axis of the paraboloid has to track the star motion. This implies that the telescopes must move during the observation if delay lines are to be avoided. The motion does not have to be accurate since small delay line elements, with travel in the 1-10 mm range, can easily be incorporated in the central table. Telescope positions (motion inaccuracies, vibrations...) can be monitored by laser beams and the compensation of errors be made by the small delay lines.

A system of radially arranged tracks can meet these requirements, but ideally superior flexibility would be obtained with a smooth platform of 300x300 metres carrying the four telescopes on air bearings.

Among the existing types of telescope mounts, those best adapted to such attractive designs are the alt-alt and the spherical. They indeed provide a horizontal coude output with only 3 mirrors (primary, Cass and Central flat). Instead, the alt-az mount requires seven mirrors and the vertical coude beam cannot be reflected horizontally in all directions. Alt-az mounts would be compatible with radial tracks, in which case the coude beam could propagate in a tunnel below the tracks. They do not seem adequate for the platform concept, where the coude beams would propagate in free air or tubes above the platform. The free-air propagation of coude beams is affected by seeing, but considerably less than the vertical propagation of the wide beam coming into the telescope.

The performances of Michelson interferometry with large ground-based telescopes operating at visible wavelengths have been discussed by Greenaway (1979a) and more recently by Roddier and Léna (1984). Expressions are given for the signal-to-noise ratio on the fringe visibilities. An important result is that it is more efficient to use the telescopes pairwise rather than to superimpose all the images unless the configuration is highly redundant (i.e. many telescope pairs contribute to the same spatial frequency) (Greenaway 1979b).

In a non-redundant configuration, the use of telescope by pairs has two disadvantages: first, it does not allow to apply phase-closure methods, classical at radiowavelengths and eliminating atmospheric phase errors. Second, it provides, at a given time, a (u,v) coverage limited to a single point per aperture pair or to a small neighbourhood of a single point for each aperture pair.

In the pair operation, two basic configurations are possible: either use a single pair at a time, or use all possible pairs.

Figure 2.3-1

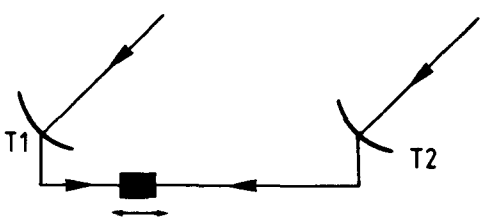

Pair combination: no optical delay line. Movable focal recombination area (■)

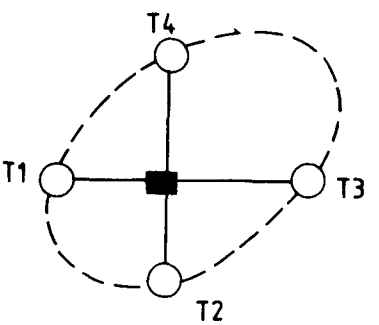

Pair combination, continuously movable telescopes, central beam combination area, no optical delay lines.
The telescopes move along radial tracks, at the intersection of a varying ellipse.

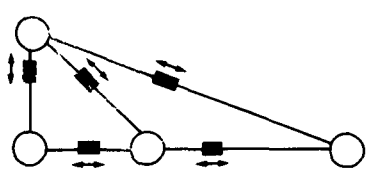

Simultaneous use of pairs: no central beam combination area, no optical delay lines

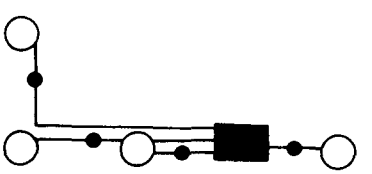

Simultaneous use of pairs: fixed central beam combination area, optical delay lines (●)

For simplicity, we restrict the discussion to single pair combination.

Beam superposition

Images from the several telescopes can be recombined in a variety of ways:

a- The beams can have different orientations, with no angular overlap at the point where they cross each other, either in the pupil or in the image plane.

This is achievable with any number of telescopes. The pattern of angles adopted between the beams may or not reproduce the pattern of apertures. In the former case, referred to as the Fizeau case, optical path differences are invariant in the field, at least to the first order. In the latter case, known as the Michelson case, a first-order dependence of path difference with respect to field position occurs and fringes are observed in the field. Fizeau arrangements have advantages for compact arrays, but require many pixels in the case of diluted arrays. Michelson arrangements are of interest for diluted apertures used in narrow fields. They also provide such possibilities as having a redundant entrance aperture with a non-redundant exit aperture (Noordam et al., in Olthof 1984).

b- Coaxial recombination with beam splitters. This is an extreme case of Michelson-type recombination. It can provide a flat interference field if the waves have uniform phase, which does not occur in the visible when dealing with large apertures, unless adaptive optical corrections are made.

Image plane and pupil plane interferometry have their advantages, but it is likely that the latter will ultimately be the most favorable for large telescopes interferometry (Chelli and Mariotti 1986, Roddier 1985).

Adaptive optics

Interferometric operation is optimized when a uniform phase is achieved over the individual pupils to be combined and a high gain in signal-to-noise ratio follows (§2.5). This can be achieved with adaptive optics. A closed-loop control system, that senses the actual phase errors, and an active optical element that reshapes the optical wavefront by adding a set of controlable optical path differences allow a real-time compensation of the wavefront. Adaptive optics is discussed in detail in Appendix A1; its feasibility at infrared wavelengths ($\lambda > 5$ μm), even on large telescopes, seems within reach, and may be assumed as a given fact for interferometer operation at these wavelengths. At shorter wavelengths, especially in the visible, interferometry will have to live with a distorted wavefront phase over the pupil.

Even with a corrected wavefront, residual phase errors left through or created by the adaptive system may affect the accuracy of the visibility measurement and may introduce extra noise on it. Only experimental work will allow to establish the practical limits.

Multiple spectral channels

Radio interferometers have multispectral capabilities: Westerbork has 32 000 channels, Nobeyama has 20 000, VLA has more than 10 000. The radio arrays choose to distribute these channels over different polarization (to improve signal–to–noise ratio) or over sine and cosine terms (to measure phase) or to measure many baselines simultaneously. They could also put all the channels on one or two baselines and immediatly reach 10^4 spectral channels.

At optical wavelengths, it may or not be of interest to display separately the interferometric information collected in different colors. Indeed, the color–dependent morphology of stars, galaxies, etc... has interesting variations associated to the various spectral lines. Like radio arrays, optical ones can observe 10 000 or more spectral channels simultaneously. A variety of spectrographic techniques can achieve the required separation of wavelengths, from prismatic dispersion to more elaborate Fabry–Perot and possibly Fourier transform spectrometer techniques using directly the fringe modulation (Mariotti and Ridgway 1986).

Differential interferometry may be conceived as an extrapolation of differential speckle interferometry.

Phase and amplitudes may be measured at a number of adjacent wavelengths. If the assumption is made that the object shape is wavelength independent over a certain spectral interval, it becomes possible to determine the amplitude and the phase gradient $\vec{\nabla}\phi(u,v)$ of the source (spectral phase–gradient estimate).

Detection requirements

Severe requirements on detectors in term of number of pixels are present, as soon as adaptive optics can not provide an uniform phase over the pupils. These requirements are evaluated in Table 2.3–1.

The need to freeze atmospheric phase drifts implies fast detection, faster in the visible (1 ms) than in the infrared (10 to 100 ms). Mosaics of image detectors are needed to record several spectral channels simultaneously.

Table 2.3-1

Number of pixels per spectral channel (*)

	visible			infrared		
Wavelength (μm)	0.4	0.8	2	5	10	20
Complete adaptive optics	1				1	
No adaptive optics (7m telescopes)	840x280	$\frac{420}{\lambda_{\mu m}} \times \frac{140}{\lambda_{\mu m}}$	210x70	42x14		21x7

(*) under typical (1 arc sec) seeing condition

Measuring $\vec{\nabla}\phi$

Atmospheric phase fluctuations between pupils prevent the direct determination of the phase of the complex visibility. But interferences between sub-areas of individual pupils provide again the phase derivative of the object in a given domain (spatial phase gradient estimate) as shown in Fig. 2.3-2.

Figure 2.3-2

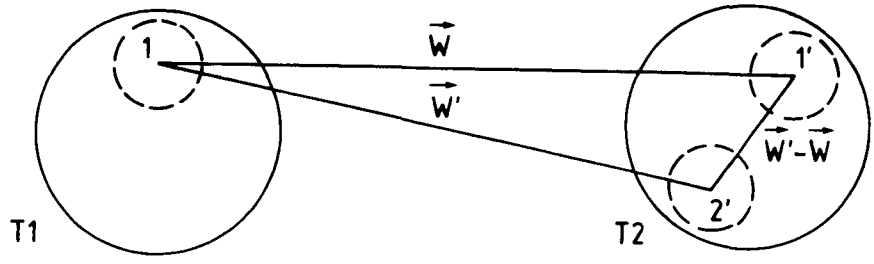

Forming pairs between sub-areas (r_o in size, or smaller) of the two interfering pupils, in order to obtain phase informaton.

$\delta\Phi_1 = \Phi_{1'} - \Phi_1 = \Phi_{source}(\vec{W}) - \Delta\Phi$

$\delta\Phi_2 = \Phi_{2'} - \Phi_1 = \Phi_{source}(\vec{W}') - \Delta\Phi$

$\Delta\Phi$ = atmospheric phase error

$\delta\Phi_2 - \delta\Phi_1 = \vec{\nabla}\Phi_{source} \cdot (\vec{W}' - \vec{W})$

There is no direct equivalent of this technique in radio interferometry, since the beam throughput always use the full pupil area. Speckle masking (see below) is another configuration to measure the relative phases.

It is interesting to consider the wavelength dependence of random atmospheric phase excursions between two pupils placed at a distance L apart. For stationary condition, the rms value σ_Φ is given by

$$\sigma_\Phi(rd) = \frac{2\pi}{\lambda}\sigma_z = 6.4 \left[\frac{L}{r_o(\lambda)}\right]^{5/6}$$

as long as L is smaller than the outer scale of turbulence (Venkatakrishnan and Chatterjee 1986) which is probably of the order of a few tenths of meter at an astronomical site. Since the rms optical path fluctuations σ_z is independent of λ, σ_Φ varies as λ^{-1} (Table 2.3-2).

Table 2.3-2

Rms phase excursion between two pupils, 50 m apart
[homogeneous turbulence, L(outer scale)>50m]

	λ (μm)	0.5	2	5	10	20
σ	2π units(*)	180	45	18	9	4.5

(*) under typical (1 arc sec) seeing condition

In practice, scarce data are currently available (Mariotti and di Benedetto 1984), but they show values significantly smaller (an order of magnitude) than the "worst case" given by the abova formula. In any case, the gain in phase stability is considerable at infrared wavelengths.

Field of view

An MMT offers a PSF which has very limited side lobes (typically those of an Airy function). Wide-field (arc sec) speckle interferometry is possible since

the exit pupil is always exactly homothetic to the entrance pupil. The situation is different in a thin array, where the PSF will present high side lobes. Objects which have a typical extension of the order of the resolution will not suffer from confusion or reduced photometry accuracy, as will larger objects, unless cleaning procedures are used a posteriori, as in radioastronomy.

The condition of path equalization for two telescope interferometry, when ever the object is on-axis or off-axis, is fullfilled with an MMT (similar in this respect to a standard telescope), while it varies with a multitelescope interferometer. The field-of-view of the interferometer will be limited to the size of the seeing disc (~1-2") [Waller 1980]. Corrective action may be taken at the cost of additionnal optics (Enard 1984), which may, on the other hand, introduce higher thermal loads for IR use.

Phase closure

This technique is of common use in radio arrays. In an array of N antennae, up to N(N-1)/2 simultaneous interferometers baselines can be used. If all the antenna pairs are combined, this factorization reduces the number of unknown complex gains that must be determined by calibration from N(N-1)/2 to N. When N < N(N-1)/2, it is thus possible, in principle, to determine both the unknown instrumental (and atmospheric) complex gains and some parameters of the source from the observation (self-calibration methods).

Speckle masking

In optical interferometry, N is no longer the number of telescopes, but the total number of coherent areas ($r_0(\lambda)$ in size) over all the pupils. With 4 telescopes, N may vary between several thousands (at 0.5 μm) to a few units (at 20 μm). Speckle masking (Weigelt and Wirnitzer 1983, Lohmann et al. 1983) can be used to measure phase information in this case of optical interferometry. In speckle masking the ensemble average triple correlation or bispectrum of all interferograms is calculated in the first processing step. It is not necessary to measure phase information in individual interferograms, which are usually very noisy. As illustrated by the experiment shown in Fig. 2.3-3 speckle masking can be applied in the case of strong photon noise (less than 1 count per pixel). Roddier (1986) has shown that triple correlation is a generalisation of phase closure in optics.

Figure 2.3–3 *: Image reconstruction from 4–telescope–interferograms by speckle masking. The figures show (1) the pupil function, (2) the laboratory object, (3) one of the 200 evaluated interferograms (with simulated photon noise corresponding to mean count number 0.3 photons per pixel), (4) theoretical and reconstructed Fourier phase, and (5) the reconstructed image (See Hofmann and Weigelt 1984 for more details).*

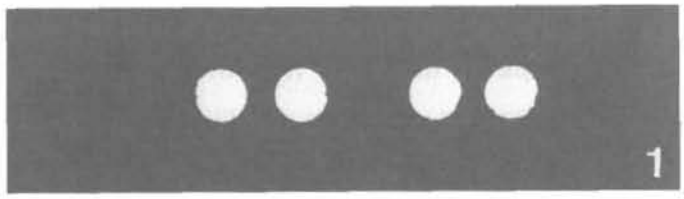

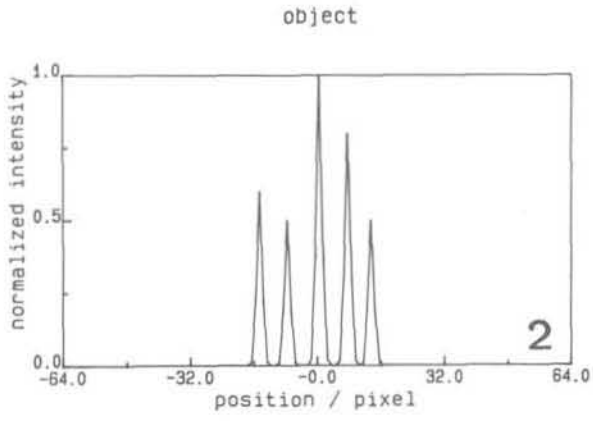

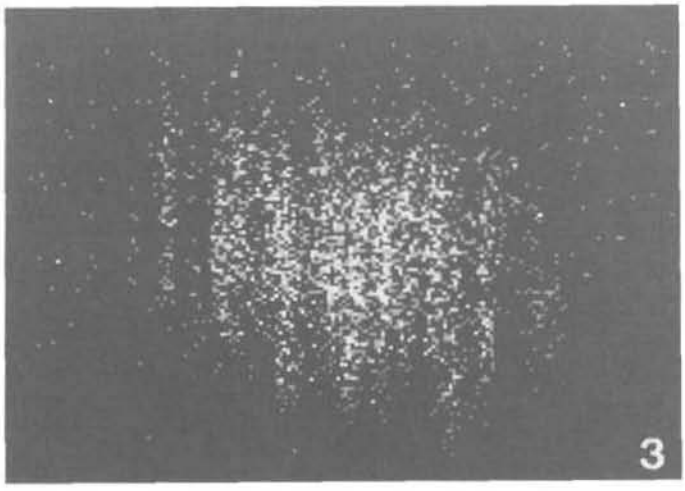

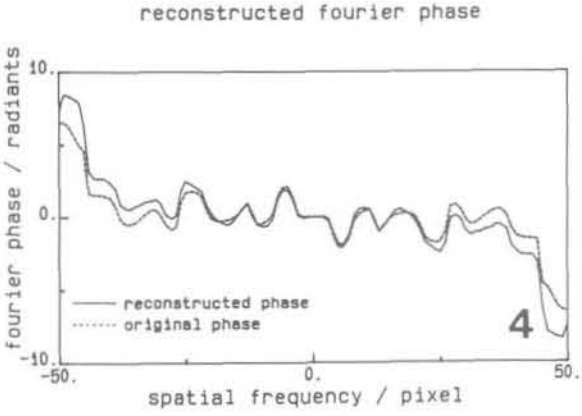

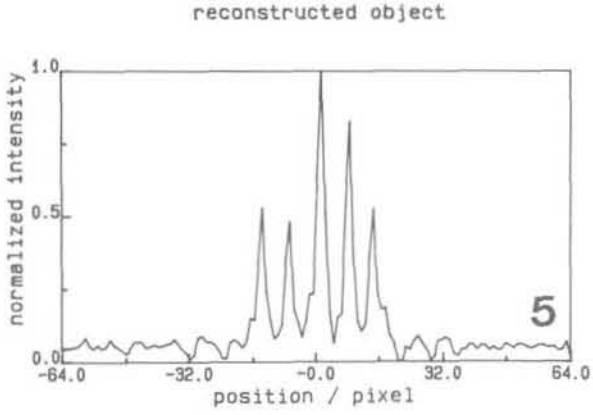

Compact pupils (non monolithic)

Beckers (1984) makes a distinction between monolithic arrays in which the internal pathlengths remain invariant while tracking the source, and non-monolithic arrays in which the internal pathlengths are continuously adjusted to compensate for external pathlengths variations. He also distinguishes between compact arrays providing full coverage of the frequency plane within an approximately circular outer bound, and thin arrays providing only partial coverage. He proposes a classification in three types of arrays. Type 0 are compact monolithic such as the MMT. Type 1 are thin monolithic such as the Michelson and Pease experiment or the University of Arizona proposed versatile array. Type 2 are thin non-monolithic. This distinction between thin and compact or rather continuously filled arrays is similar to the distinction made in early radioastronomy between "grating" synthesis and "aperture" synthesis.

Within Type 2 arrays, the diluted type gives a coverage which presents holes, while the continuous filled type gives a (u,v) coverage which presents a complete continuity (Fig. 2.3-4).

Figure 2.3-4

Compact array: the pupil autocorrelation function has no hole.

Diluted (thin) array: there are holes in the u-v coverage.

An interference pattern produced by a continuously filled array is basically similar to a speckle image given by the large pupil of a single telescope. In such a case, phase continuity is ensured over the whole covered area of the (u,v) plane, and the complex visibility of the source can be fully reconstructed. Various methods such as speckle masking (Fig. 2.3-5) achieve this goal.

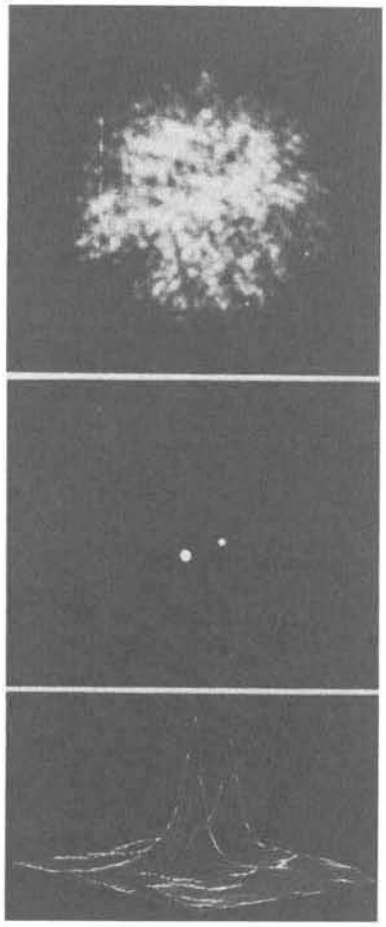

Figure 2.3–5 *: Speckle masking observation of the close spectroscopic double star Psi SGR (One of 100 evaluated speckle interferograms and reconstructed image, see Weigelt and Wirnitzer, Optics Lett. 8, 389, 1983). The advantage of speckle masking is the fact that no point source is required near the object for image reconstruction.*

Combining unequal pupils

It can be shown (Roddier and Léna 1984) that the combination of unequal pupils does not in general bring a significant advantage in term of signal-to-noise ratio. The signal-to-noise ratio given by a pair of telescopes of unequal size is, in the best case, only $\sqrt{2}$ times larger than the one given by a pair of telescopes of the smaller size. In the worst case (numerous speckles in the image), the largest telescope does not even bring this improvement. It is only at short infrared wavelengths (2–3 μm) that the classical situation, encountered in radioastronomy, may be obtained: the signal-to-noise ratio varies as the geometric mean $\sqrt{sS}$ of the two areas.

Combining a smaller telescope with one of the dishes of the VLT may therefore be useful in terms of improved (u,v) coverage, but it will not take benefit of the largest pupil in the pair in term of signal-to-noise ratio.

2.4 *Image reconstruction*

From the analysis of the combined beams, one may safely assume that either one of the following measurements may be achieved.

a) Amplitude $|V_\lambda(u,v)|$ of the complex visibility V_λ. No phase information is available. This is the most straight case. Noise will cause an rms error $\sigma_{\lambda,|v|}$.

b) Amplitude $|V_\lambda(u,v)|$ and phase gradient $\vec{\nabla}\phi_\lambda(u,v)$. The phase gradient may be determined either by the spatial or by the spectral method. Measurement errors are $\sigma_{\lambda,|v|}$ and $\sigma_{\lambda,|\phi|}$.

c) Amplitude $|V_\lambda(u,v)|$ and phase $\phi_\lambda(u,v)$. This optimum case could be obtained directly only in a favorable phase closure configuration, or in the speckle masking configuration discussed above.

(u,v) coverage

The autocorrelation of the pupil gives the instantaneous (u,v) coverage of the instrument. With a type 0 array (MMT), this coverage is independent of tracking and time. The power spectrum of this pupil function is the point-spread function (PSF) of the interferometer.

Any array of individual telescopes (non-monolithic arrays) provides a coverage of the (u,v) plane which is time-and declination-dependent. For a given source declination, fixed telescopes provide a fixed coverage. Movable telescopes obviously extend this coverage.

A goal of interferometer observations will be to make 2-dimensional images, with a roughly circular beam (point spread function). At centimeter wavelength, this can be done, for high-declination sources only, by east-west arrays, which synthetize the image as the earth rotates. At visible and IR wavelengths, however, the atmospheric absorption is large, preventing optical/IR arrays from tracking sources down to the horizon, as centimeter radio arrays do. A typical cutoff is 2 air masses, or elevation 30 deg. This means that a one-dimensional visible/IR array will always have large sectors missing from its (u,v) coverage, even for high-declination sources.

This major difference to radio synthesis telescopes, combined with the many important sources located near the celestial equator (Orion, 2C273, 3C279, the galactic center, etc...), where a linear array is anyway limited, makes it imperative for a useful optical interferometer to have two-dimensional

coverage.

In order to gain insight on the image quality provided by various interferometric configuration, computer simulations have been made and are described in Appendix A2 in great detail.

To simulate image reconstruction, five configurations were studied, all with 4 telescopes (Fig. 2.4–1):

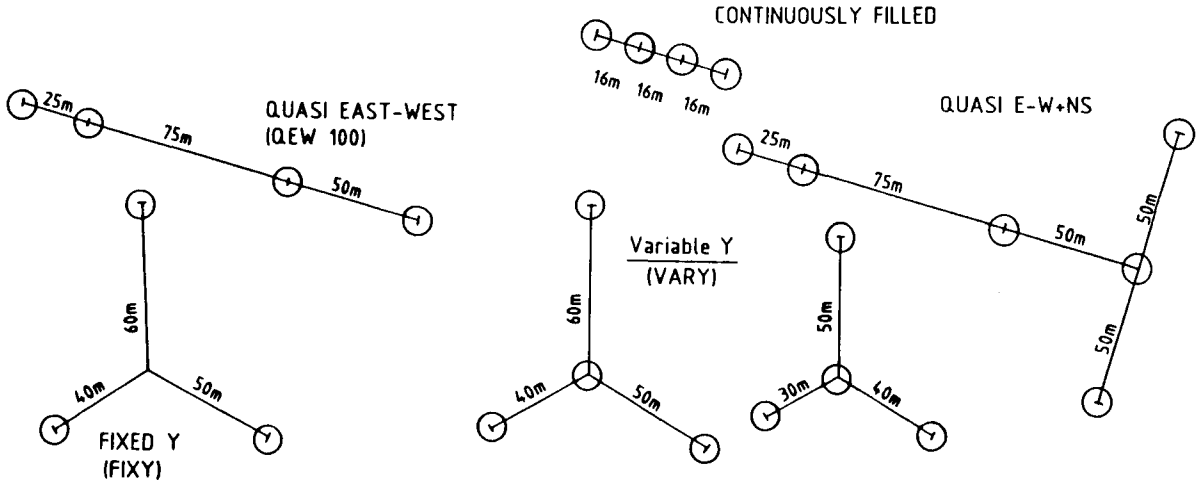

Figure 2.4–1 *: The five configurations used to test the VLT–PSF in the interferometric mode. The four telescopes (10m) are on scale with the selected baselines.*

a– Continuously filled array : In this configuration, the continuity in the (u,v) plane allows the use of phase restoration techniques, if all telescope are simultaneously used. If not, the continuity still provides a better (u,v) coverage, hence a better PSF.

b– Thin arrays. The (u,v) coverage is not continuous. Four different interferometer configurations were considered (Fig. 2.4–1):

- The first (QEW100) has four fixed telescopes on a line at azimuth 100 deg. The departure from a strictly east–west line leaves some north–south resolution even at the equator. The four telescopes are placed so as to provide the six space harmonics of 25 m up to 150 m.
- The second test configuration (FIXY) is a wye with four fixed telescopes at the crossing and at the tips of three arms placed at 120 deg from one another. One of the three arms is north–south.
- The third configuration (VARY) has one fixed telescope at the centre of the wye and three movable telescope, one on each arm of the wye. Vary has been tested in two different configurations thus providing twelve space harmonics against six for the first two interferometers under test.
- The fourth (QEW 100+NS) allows to move one of the four pupils along a line perpendicular, in order to improve the (u,v) coverage.

The u–v coverage of these configurations, placed at a latitude of -25°, has been computed for sources at various declination and the point spread function is directly deduced.

A model source, having four components of different intensities and sizes is then used for simulation. Observations of this source have been simulated with the five interferometers described above. Point spread functions have been used to restore the images through the CLEAN algorithm which is one of the methods to recover the missing space harmonics by interpolation in visibility space. This process does not extrapolate in visibility space that is to say it does not provide improved resolution relative to the actual observations.

The conclusions are the following : the restoration with QEW 100 is quite unacceptable at all declinations. The restoration is acceptable with Y–shaped configurations, and the same applies to the QEW+NS configurations.

It again appears that some two–dimensional coverage is essential for image quality. Moreover, if many (u,v) tracks cross one another, a common relative phase reference is easier to obtain and phase gradient information is sufficient to reconstruct the images.

Table 2.4–1 provides an overview of the various possibilities.

Table 2.4-1

Type of array	u-v coverage	PSF	maximum baseline	angular resolution at 5 μm(*) (milli arc sec)	Available information			image restoration
					Amplitude	Phase gradient	Phase	
MMT	continuous isotropic	excellent	25 m	40	yes	yes	yes	excellent
Continuously filled linear array	continuous anisotropic	highly anisotropic	50 m	20	yes	yes	yes	excellent
Compact 2D-array	continuous isotropic	excellent	40 m	25	yes	yes	yes	excellent
Thin linear array OEW (Fixed telescopes)	holes anisotropic	highly anisotropic	150 m	7	yes	yes	no	difficult
Thin linear OEW + NS	holes more isotropic	good	150 m	7	yes	yes	some	good
Fixed Y-array	holes isotropic	good	150 m	7	yes	yes	some	good
Movable Y-array	no holes isotropic	excellent	150 m	7	yes	yes	yes	excellent

(*) Inverse of cut-off frequency D/λ.

Higher resolution is obtained if some a priori information is available.

2.5 *Sensitivity performance and limiting magnitudes*

The limited amount of experience available in two telescopes optical interferometry leads here to a careful and conservative approach. Yet, it may be noted that speckle interferometry achievements in terms of sensitivity (Appendix A6) are extremely good and actually close to theoretical limits. Since the limiting factors namely the atmospheric phase perturbations are basically the same, there is no reason to doubt the ultimate performances of an interferometer.

It is necessary to treat separately infrared and visible wavelengths, because the limiting factors are different.

Infrared wavelengths ($1.6 \leq \lambda \leq 25$ μm)

Broadly speaking, interferometry in the infrared is characterized by two factors :

a) the atmospheric properties become more and more favorable with increasing wavelength. The r_o parameter increases, hence the number of coherence

areas over a given telescope pupil drastically decreases. Coherence times are increasingly longer, image stabilisation is easier.

b) detection of signal is generally dominated by thermal noise, especially with the use of high performance modern array detectors.

A detailed discussion of sensitivity at IR wavelength is given in Appendix A3. Its conclusions may be summarized as follows :

• the use of large telescopes, with size larger than the atmospheric parameter r_o, is of value *only if the pupil can be phased with adaptive optics*. A considerable gain in sensitivity over smaller pupils is then obtained (Fig. 2.5-1), which makes extremely interesting the use of the VLT in interferometry.

Figure 2.5-1

Sensitivity of an infrared interferometer
Curves a: $F_{0_A}(\lambda, D)$. Limiting flux, with fully phased pupils.
Curves b: $F_{0_T}(\lambda, D)$. Threshold flux, array detector of N_S elements.
Curves c: $F_{0_S}(\lambda)$. Sensitivity of a space interferometer, D = 1 m.
Conditions are :
(a) and (b) : $t = \eta = \epsilon = 1$, T_a = 280 K, n = 500 e^-rms, $r_o(v)$ = 10 cm,
(c) $t = \eta = \epsilon = 1$, detector noise given in A3.3.3, $\delta\sigma = 0.1\ \sigma$, T_s = 100 K
(a), (b) and (c) : T = 1 s

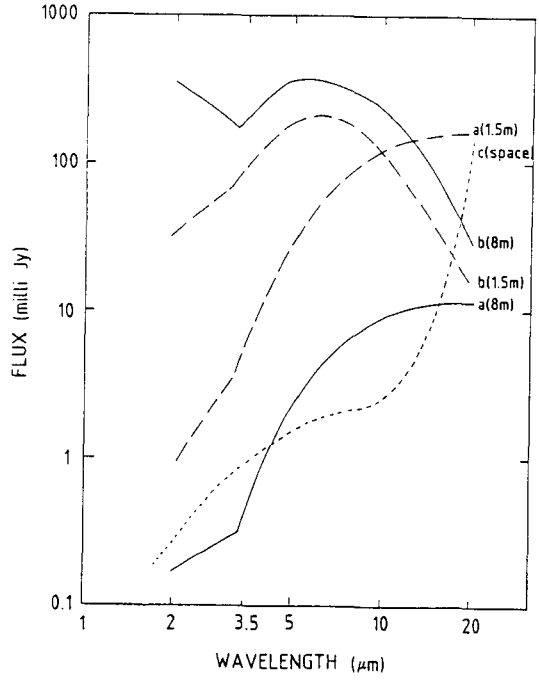

• random phase fluctuation with time between the two telescopes, several tenths of meters, constrain the time integration of the signals. For bright enough objects, time integration is possible, and longer exposures improve the S/N ratio, hence the accuracy on the visibility measurement (phase and

amplitude), hence the dynamics of the object restoration. For weak objects, time integration does not bring any improvement, unless an independent phase reference is found in the field of view from a brighter object. When such independent phase tracking can be achieved, extremely high sensitivities are obtained.

• when adaptive optics is used, the S/N ratio becomes independent of $r_0(\lambda)$. Nevertheless, the seeing quality remains mandatory for three reasons : (i) the better the seeing, the easier the adaptive correction; (ii) the better r_0, the smaller the rms phase differences between the two pupils (varies as $r_0^{5/6}$), making easier long time integration; (iii) at the shortest wavelengths ($\lambda < 3\ \mu m$), where only partial adaptive correction is possible, S/N ratio varies as r_0^4.

Visible wavelengths ($0.35 \leq \lambda \leq 1.0\ \mu m$)

At visible wavelengths, detector noise becomes completely negligible, but the atmospheric coherence area is small ($r_0 \sim 10$ cm) and the coherence time small (~1ms). Fast detectors, with a large number of pixels, are therefore necessary.

• Limiting magnitudes have been estimated for typical seeing conditions (1 arcsec seeing) assuming that fringes can be frozen on 0.02 second exposures. Several cases have been considered. The limiting magnitude is found to be of the order of $m_V = 4$ for visual fringe detection independently of the telescopes size. Photoelectric fringe tracking should allow to observe objects up to at least $m_V = 9$ (Tango and Twiss 1980; Shao and Staelin 1980), possibly $m_V = 14$ (Roddier and Léna 1984), with very little dependence on the telescope diameter. An increasing telescope diameter D does not improve the limiting magnitude beyond $m_V \sim 14$, but it reduces the observing time requested to reach, on objects brighter than m_V, a given S/N on the visibility measurement. This reduction is in D^{-2}.

• The limiting magnitude is extremely seeing-dependent, as r_0^3 or r_0^4 depending on the detail of observing condition (Roddier and Léna 1984).

• Adaptive optics would, as at IR wavelengths, drastically improve the situation. Yet its prospects at visible wavelengths, as discussed in Appendix A1, are dim in a near future.

If adaptive seeing correction proves feasible with artificial reference sources, a range in magnitude from 13 to 20 and possibly more would become

accessible. The feasibility of using laser pulse techniques to provide such references sources should be further investigated (Foy and Labeyrie 1985).

It may therefore be considered that "bright" objects (m_v < 9–14) would be of easy access with a VLT but "faint" objects definitely require significant developpements before they can be measured.

For "bright" objects, the use of a large telescope as compared with a smaller one brings a favorable gain in observing time: the time required to obtain a given signal-to-noise ratio on visibility varies as the reciprocal of telescope area.

Comparing with space platforms

The interferometric mode of the a VLT has the great advantage that it can yield higher angular resolution than the Hubble Space Telescope and other space telescopes and ground-based telescopes of the near future. Only a long-baseline interferometer in space, for example TRIO (Labeyrie et al. 1982), could yield higher resolution. Table 2.5-1 compares a VLT interferometer with 100 m baseline with the Hubble Space Telescope.

Table 2.5-1

Comparison of a VLT interferometer with the Hubble Telescope

telescope/method	resolution	limiting magnitude m_v
100m VLT interferometer	0.001" (at 500nm)	14 (very seeing-dependent)
Hubble Space Telescope: direct imaging	0.05"	28–30
Hubble Space Telescope: roll deconcolution (Walter and Weigelt, 1985)	0.015"	22

At visible wavelengths, an interferometer placed in space is only suffering from phase errors due to relative drifts of its individual telescopes. The sensitivity is greatly enhanced (Fig. 2.5-2; Roddier 1983).

In the infrared, the main factor which limits the sensitivity on the ground is the background noise due to the thermal emission of the telescope. A space instrument brings significant gain only when it is cooled. This is illustrated on Fig. 2.5-1. Because cooling the whole optics is a costly and difficult task in space, it appears that ground based interferometry with large telescopes has a wide field of possibilities.

Figure 2.5-2 : *Sensitivity of two telescopes interferometry in space at visible wavelength:*

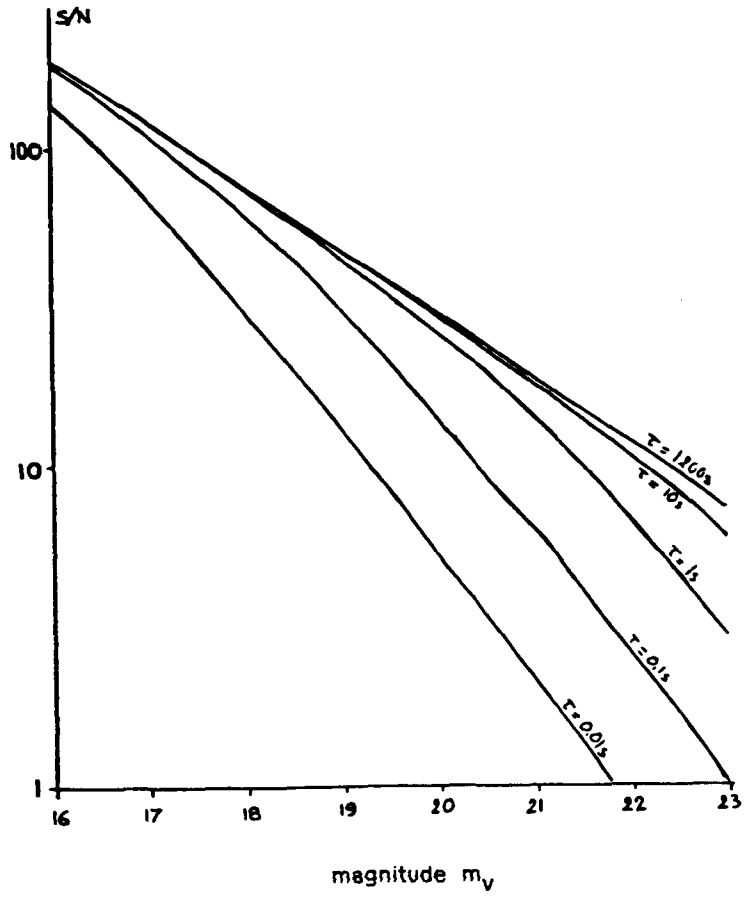

Expected signal-to-noise ratio for the object energy spatial spectrum, in a Michelson-type interferometric experiment, in the visible, as a function of the stellar magnitude. We assume a detector quantum efficiency of 0.2, an optical bandwidth of 60 nm, a fringe visibility of 0.5. We further assume that the telescope optics gives diffraction-limited images when the aperture is reduced to an area of $1m^2$ and that a total observing time of 20 mn is divided into subexposures of duration τ to allow for pointing errors (Roddier 1983).

Chapter 3 : THE VLT CONCEPT AND OPTICAL INTERFEROMETRY

The initial VLT concept of a fixed linear array provides indeed an interferometric capability, which has triggered the present study. In order to keep flexibility, this study has been placed in a broader frame of discussion : given 4 pupils, 8–10 m in diameter, what are the different configurations which provide high angular resolution ? It is fairly obvious that an MMT configuration is straightforward: most of the difficulties and challenges lie in the coupling of separate telescopes. Whether these telescopes should be close–packed or far apart, in line or in a Y–shape, fixed or movable is part of the flexibility which has to be kept at this stage of the analysis in order to search for the optimum configuration. The final compromises will be discussed in Chapter 4.

3.1 *Single telescope constraints*

3.1.1 Image formation

Interferometry first requires a high quality of the images given by the individual telescopes.

Although the optical specification of the VLT unit telescopes has not yet been formally fixed, it is expected it will be something like:
80% of the geometrical energy within 0.1 arcsec at visible wavelengths.

This specification is based on the New Technology Telescope specification which expects to reach diffraction limited performance for low spatial frequencies and 80% within 0.15 arcsec for high spatial frequencies (ripple).

Active optics

The active optics system envisaged is (following the NTT) a closed loop system for correction of low band pass errors with time frequencies lower than the time corresponding to integration of atmospheric seeing (Wilson 1982; Franza and Wilson 1982; Wilson 1983). The aim is to correct all low spatial frequency modes (those influencable by flexure of optics or tube) to the diffraction limit all the time. The limitation will then be non–correctable high

frequency (ripple) effects left by the optician, on which a severe specification will be set.

The NTT optics test set-up (1 m thin mirror) has now proven the practical functioning of this system, so that the development for the VLT of a system based on similar principles is seen as straightforward.

The possible extension of the same system to the correction of the effect of wind buffets is under study.

Guiding

In the NTT the active optics system works with an image analyser which uses the offset-guide star from time to time by mirror switching between the image and the auto-guider. In the larger sense, the auto-guider is simply part of the active optics, correcting tracking errors in real time and also any small wavefront tilts arising from the active optics corrections. The NTT auto-guider will be a well-tested TV system under developpement (Tarenghi and Ziebell 1982) using a window about 4 x 4 arcsec and an integration time (currently) of about 1-2 s. Higher frequency tracking errors must therefore be $\leq$ 0.1 arcsec.

Adaptive optics

A considerable gain in sensitivity of the interferometric mode is expected if atmospheric distorsion of the images may be partially or totally corrected.

"Adaptive" optics is used here (following Woolf 1984) as a term referring to the correction of high temporal band errors caused by atmospheric turbulence. A detailed discussion of adaptive optics is given in Appendix A1.

Because of the limitations of the isoplanatic angle, a general solution for visible wavelengths still seems quite utopic.

The infrared case is much more favorable longward of 3 μm given the properties of atmospheric turbulence. The large IR isoplanatic field (up to 2 arc min at 20 μm) would allow to use an offset visible star to correct the central faint IR image (Léna et al. 1986). The number of elements to correct on a pupil is also manageable (a few tenths).

In any event, progress in adaptive optics at infrared wavelengths will be essential for the VLT since, assuming the active optics achieves its aims, the atmospheric seeing will be the major limitation. The gain for the S/N in interferometry goes at least with the inverse cube of the PSF width (Roddier 1975; Dainty 1975; Roddier and Léna 1984) so no other parameter can bring such an advantage.

3.1.2 Mechanical stability

It is assumed that each telescope provides an afocal beam to a central "beam combination-area", where appropriate motion compensates for Earth rotation (§ 3.4). Optical path differences are introduced by the atmosphere on each beam. The temporal power spectrum of these fluctuations is seeing-dependant, and can be reasonnably estimated on the basis of turbulence models, now well confirmed by speckle work. Let $\tau(\nu)$ be the rms path fluctuation (in micrometer) at the frequency ν. At telescope exit, the afocal beam suffers from other perturbations: the wave front has additional path fluctuations with respect to the ground frame reference, induced by mirrors (primary, secondary or tertiary) vibration or by the mount motion, which have their own spectrum $\tau_T(\nu)$. The system is atmosphere limited if the condition

$$\tau_T(\nu) < \sup \left[\frac{\lambda}{20}, \tau(\nu)\right]$$

is fulfilled.

Figure 3.1.2-1 (Roddier 1985) is a graph of $\tau(\nu)$, from which one may derive the mechanical stability requirement.

The mechanical vibration constraints have been discussed in detail by Roddier (Roddier 1985), relative to the optical path fluctuations induced by the atmosphere. In general, the time spectrum of mechanically induced fluctuations must lie below the time spectrum of atmospherically induced fluctuations. This means that the rms values of the mechanical fluctuations of the optical path should lie below the lines of Fig. 3.1.2-1 [continuous line: "lucky observer" conditions according to Barletti (Barletti et al. 1976); dotted line: average conditions]. It is assumed that wind speed increases linearly from 0 at ground level up to 10 m s^{-1} in the tropopause and decreases afterward. At high frequencies, the limit is a horizontal line corresponding to fluctuations of ≤ 0.025 μm for visible wavelengths ($\lambda/20$). For IR observations at $\lambda = 2.2$ μm corresponding to a frequency of about 1 Hz, amplitudes of the order of 0.1 μm would be acceptable.

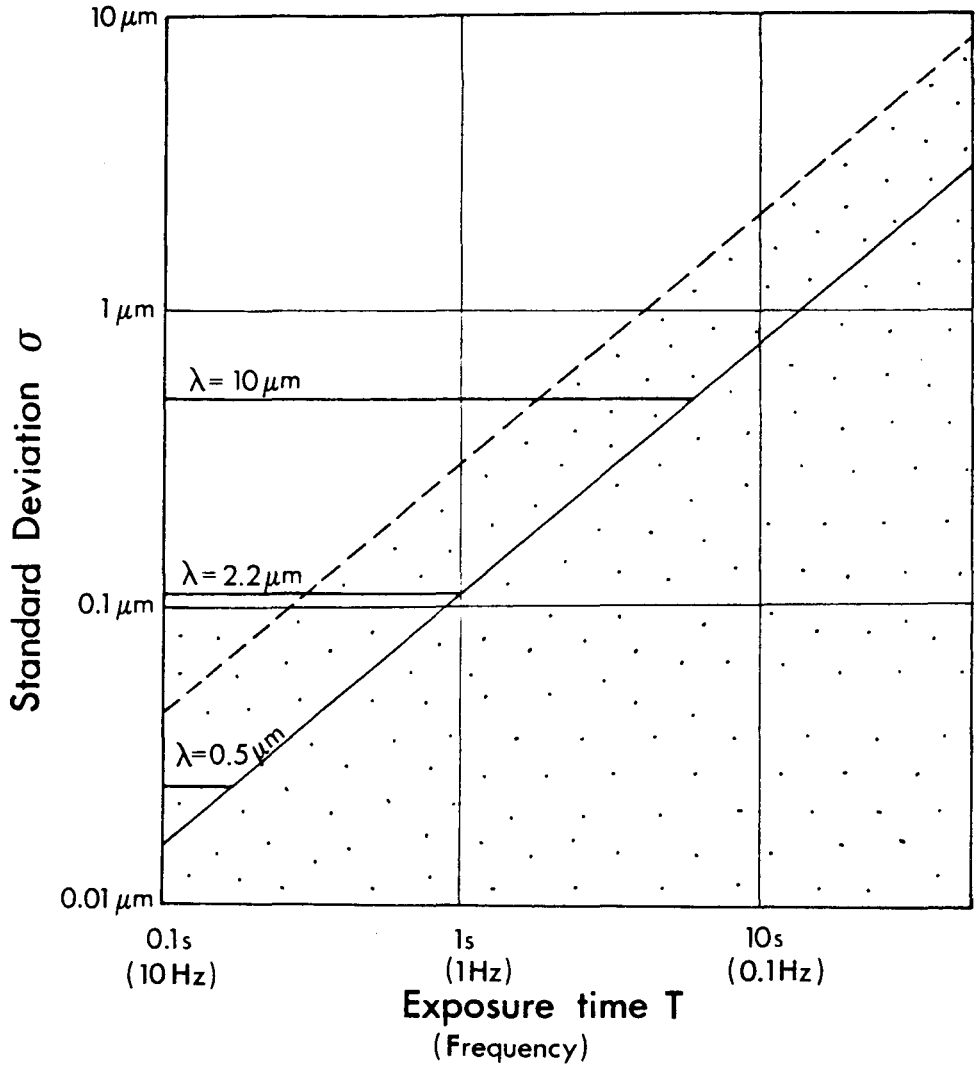

***Figure 3.1.2–1** : Expected standard deviation σ of the optical path fluctuations during an exposure time T. Full line: lucky observer model. Broken line: average model. The dotted domain boundary gives the stability requirement for a 2.2 μm operation with average seeing.*

Labeyrie (1985) has pointed out the increasing problem of mechanical vibrations with size of telescope. While the problem is simple with 25 cm telescopes, with 1.5 m apertures fluctuations of optical path of about 3 μm rms, with lifetimes over a few seconds, may result from the tracking and be a major problem in preventing fringe detection. Improvement of more than an order of magnitude would be necessary to meet the above tolerances in a passive system. The spider vibration in Cassegrain telescopes may also present a potential problem. This can be well illustrated by the case of the ESO NTT

where the lowest eigenfrequency of the top unit is about 70 Hz. It is far more difficult to calculate the amplitude since the existing signal and the damping conditions must both be defined. However, it is very unlikely to be below 1 μm and may well be several μm. Such amplitudes are completely insignificant for normal telescope use but would be fatal for interferometer in a passive system.

Clearly, therefore, the mechanical requirements, above all for vibration at high frequencies, are going to be far harder for telescopes intended for interferometry, even in the IR, than in the normal case. Indeed, they are so hard that it seems more reasonable to consider active compensation rather than the imposition of absolute tolerances. Labeyrie (1985) has considered possible systems for achieving this. Although difficult, this active control should anyway be easier than adaptive optics control of the atmosphere.

Labeyrie's "Boule" mounting may well offer advantages of mechanical stability if very smooth tracking can be achieved and the spider problem solved.

3.1.3 Thermal Background

The reduction of local emissivities to improve the sensitivity is not a specific requirement of interferometry. Therefore requirements established by the VLT infrared Working Group are fully applicable here.

Because of thermal radiation, detectors experience a photon noise in the infrared that degrades their performance if its value surpasses the intrinsic noise of the detector. For this reason detectors are operated in a low temperature environment that generates a number of photons negligible when compared to the number generated by the atmosphere.

A detailed discussion of thermal noise effects on interferometric sensitivity is given in Appendix A3.

Other noises due to thermal background may appear in the specific optical arrangement required by interferometry, namely the beam combination from the Nasmyth focus to the common interferometric focus, especially at 10 μm where minute temperature and emissivity differences in the system may produce appreciable offset signals and noises. Assuming the telescopes to be thermally clean from the primary to their Nasmyth foci, special care will have to be taken along the beam combining paths, such as oversized low emissivity mirrors, cooled somewhat below ambient temperature.

Adaptive optics, where a mirror at ambient temperatures is deformed, may also be the source of thermal noise. A preliminary study of this problem (Roddier 1985) has shown that it does not present any sensitivity degradation for detectors in the 10^{-17}–5 10^{-16}W–Hz$^{-1/2}$ NEP class.

3.2. *Movable telescopes*

The discussion on image reconstruction (§ 2) shows the unescapable conclusion that the (u,v) coverage has to be as dense as possible, and certainly two–dimensional. It is therefore worth investigating the possibility to move the telescopes.

Movable telescopes can have two significations:
- the telescopes could be brought to separate stations in order to vary the baselines. Once they are set, optical delays are compensated as discussed above, the telescopes remaining fixed during the time of the observation.
- the telescopes could be moved all the time during the observation, in order to avoid optical delay lines.

At first, the concept of moving 8–10 m telescopes may seem odd to optical astronomers, while radio astronomers, having gained a large amount of experience in such matters, would consider the concept worth of investigation (Citterio 1985). For example, the VLA telescope weights 170 tons each, have a pointing accuracy of $\leq$ 15" and a positionning accuracy of $\leq$ 1 cm. The IRAM–Bures telescopes weights 100 tons, are pointed within 1.2" and have a positionning accuracy of 1 mm.

Concerning the movement of the telescopes two possible configurations may be considered:
a–Point to point translation of the telescopes
b–Continuous movement of the telescopes following a predetermined law.

Conceptual solutions to these problems have been investigated following the approach to take hints from systems already working and proved on other field of applications and to extrapolate them to the interferometry case (Appendix A4).

3.3 *Array configuration*

Apart from operational aspect to be discussed below (§ 3.5), the optimum configuration of an interferometer has the following requirements, as imposed by image reconstruction procedures:

a) dense coverage of (u,v) plane, from zero frequency up;

b) two dimensional coverage

c) simultaneous use of telescopes for adequate phase reconstruction

d) maximum redundancy.

It is obvious that a 4-telescopes interferometer such as the VLT can not fulfill all these conditions in the optimal sense. Yet, some configuration are more adequate than others toward the goal of high angular imaging; some of these compromises are envisaged in this section, and the final choice will be deferred to Chap. 4. The discussion will refer to the results obtained in Appendix 2, which are summarized in Table 3.3-1 and in Fig. 3.3-1.

Table 3.3-1

Case	Configuration	Telescopes	Comments
a	QEW 100	4 fixed	Although 100° gives some 2D (u,v) coverage, images are poor
b	QEW + NS	3 fixed 1 movable	Considerable improvement over the previous case. Good images.
c	Compact	4 fixed	Poor images as in a/, but phase restoration is greatly improved by continuous (u,v) coverage from 0 up to maximum frequency.
d	FIXY	4 fixed	Reasonable (u,v) coverage, but holes in the (u,v) plane.
e	VARY	1 fixed 3 movables	Very good images and phase reconstruction.

As soon as at least one telescope is in a N-S direction, the capabilities of the interferometric mode are greatly enhanced. A full two-dimensionnal motion over a large platform would be even better.

A critical point is the coverage of low spatial frequencies. At first, it was estimated that each 8-10 m telescopes could not be brought at a distance closer than 25 m axis-to-axis in order to avoid mechanical interference. This distance criterium is somewhat dependent of the type of mount to be selected, as well as of the f/ratio of the primary: spherical mounts may allow to provide compact coverage of the (u,v) plane at low frequencies. Another attractive alternative is to place two mirrors on the same mount, the two other telescopes beeing movable independently and further apart. The configuration c/ shows that a one-dimension compact system presents severe defects for image reconstruction.

Figure 3.3.1

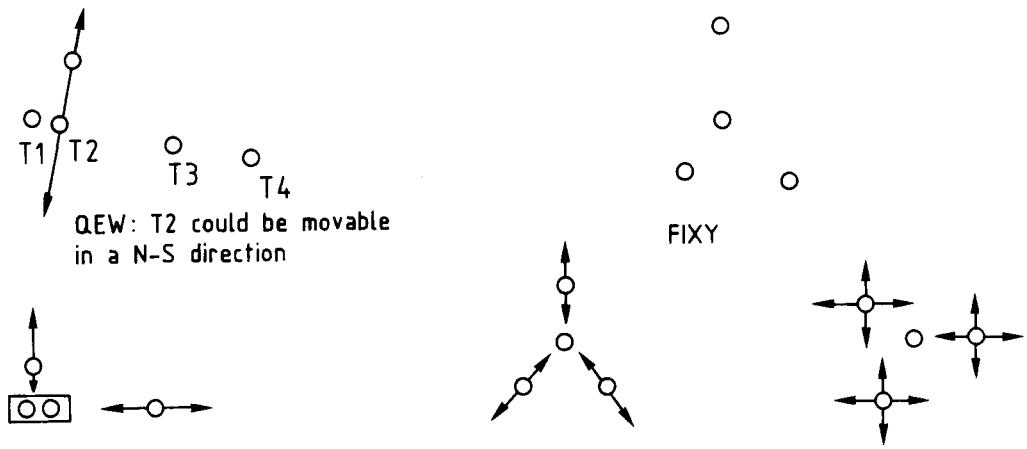

Combining unequal pupils

As shown above (§ 2.3), the use of a smaller pupil in a pair gives practically, at almost every optical or infrared wavelength, a signal-to-noise ratio which is quite identical to the one obtained with two telescopes of the smallest size. Yet, combining a large (8-10m) mirror with a small (2-3m)

mirror may be very efficient to explore the (u,v) plane and determine the phase (Fig. 3.3–2). The sensitivity will be set by the smaller telescope, but the image reconstruction procedure will be greatly accelerated and improved.

Baseline extension

This is a compromise between maximum resolution and good u–v coverage. In other words the array must not be too thin. Moreover, the site capability limits the array extension. It can be shown that the signal–to–noise ratio drops very rapidly when the object is fully resolved. The resolution of the array should therefore be adapted to the size of the objects to be studied.

At infrared wavelength (2–20 μm), the size of typical objects of interest is listed in Table 3.3–2 (cf. § 1.3).

A maximum baseline of 150 m seems therefore appropriate (6 marc sec at 5 μm), site compatible and providing not too thin an array. Whatever the bases, positionnal accuracy and good metrology are essential.

It should be noted that the telescopes do not need to be exactly within an horizontal plane.

***Figure 3.3–2** : Combining the small pupil S with the sub pupils L1 to L4 of the large pupil L will provide estimates of phase gradient $\vec{\nabla}\phi(\vec{f}_1)$, $\vec{\nabla}\phi(\vec{f}_2)\ldots$ $\vec{\nabla}\phi(\vec{f}_4)$.*

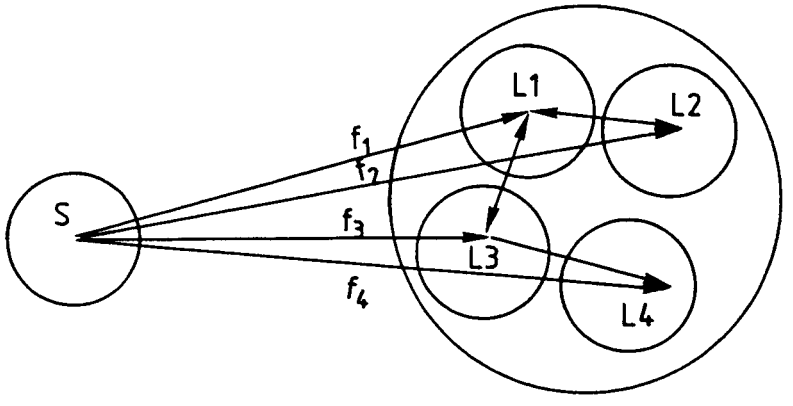

Table 3.3–2.

Resolutions required at infrared wavelengths

	resolution (milli arc sec) for an object at 1 Kpc
Accretions flows Bipolar flows	10.000 - 100
H_2O masers clumps Fragmentation, Discs, Multiple cold stars	10
Stellar winds Magnetic structure	1000 - 1
Protoplanetary evolution, discs, haloes	1000 - 1
Ultra compact HII regions	100
Dust condensation processes Maser pumping processes (OH, NH_3, Sio...)	10.000 - 10
Evolved stars: dust, chemistry, cycles (Miras)	1000 - 10
Galactic nuclei: dust, energy production, time evolution, jets	object at 10 - 10^3 Mpc 1000 - 1
Gravitational lenses	1000 - ?

MMT type

The relative merits of the "MMT" approach compared with the "Array" approach (limited number of individual telescopes in each case, about 4) have been much debated. The array has, in its very nature, more flexibility for which there are certain prices to be paid. For example, the field that can be transmitted between two telescopes will reduce with increasing separation and will tend to be less with an array than in an MMT. However, the use of the individual telescopes is free and their field unrestricted by the requirements of a single mount. Thus, even without interferometry (phasing of the telescopes), the choice of an array of a small number of telescopes can well be justified, either in the mode of incoherent optical combination or in that of electronic (post–detection) combination.

However, the coherent use of the array telescopes in interferometry undoubtedly adds substantially to the attraction of the array solution. Even with fixed telescopes in one line, the total baseline of the order of 150 m is about

8 x more than that available in the fixed, compact scheme of an MMT. Although the aperture is inevitably more dilute, adequate (u,v) plane coverage is possible with 4 telescopes. Step-wise movement over a line, or better a plane, seems technically feasible and adds greatly to the possibilities. Continuous movement would be technically much more ambitious but would produce the ultimate as an interferometer facility. Addition of smaller, movable telescopes to large fixed one will be discussed in Chapter 5.

Beckers (1984) stresses about the same conclusion about type O array (monolithic MMT): easy cophasing of telescopes at submicron precision by an internal metering system for sources of any brightness, compact PSF but more limited angular resolution.

3.4 *Beam combination*

Present experience in interferometry has been limited to the use of two telescopes. A non-redundant distribution of 4 telescopes simultaneously used offer six possible pairs and phase closure capability. This implies the optical capability to split each beam and to recombine the various pairs, after each beam has been properly compensated for phase delay.

The following steps are therefore required to achieve a proper interferometric combination. Most of them are discussed in detail in Appendix 5, some of them are common with the incoherent beam combination requirements.

3.4.1 Delay lines

By setting the VLT to the interferometric mode the beams from two telescopes can be combined with an equal path length in the interferometric laboratory. There are three options for the path length correction:
(a) use of a trombone as an optical delay line in the combining beams of the individual telescopes and a stationary combining systems,
(b) use a moving combining system to ensure equal path length,
(c) move the telescopes themselves.

3.4.2 Active control of the path correction

The operation of the VLT in the interferometric mode requires a continuous path correction. The required precision and stability is only achievable with closed loop active optical control systems.

In case of continuously movable telescopes the complexity of beam combination and the control of the path corrections would be increased drastically.

3.4.3. Image recombination

This implies to solve a number of problems : pupil foreshortening and rotation, polarization, beam splitting, field of view.

3.5 *Interferometer operation*

To form an acceptable image of an astronomical source, there should be at least 12 to 15 tracks in the (u,v) plane, each track lasting a full night per source, including calibrations. For comparison, the VLA, with 27 dishes, gets 351 tracks in 8 h; Westerbork, with 14 dishes, gets 91 tracks (some redundant) in 12 h; the Cambridge 5-km telescope, with 8 dishes, made many maps with 16 tracks, obtained in 12 h. The final image has roughly as many pixels as the square of the number of tracks. A map with only 3 or 4 tracks will be poor, firstly because there are not enough points to do a Fourier transform, with proper weighting to suppress sidelobes, and secondly because the final image will have dimensions of only 3x3 or 4x4 pixels.

This simple fact means that an array of 4 fixed telescopes has inherent limitation right from the start, so all efforts should be made to design array telescopes which can be displaced on rails, or to include more telescopes in the array.

However, the need to collect at least 12 to 15 baselines for interesting images, also illustrates another possible difficulty with the VLT interferometric mode. If the interferometry uses only two telescopes per night, while the other telescopes are scheduled for non-interferometric projects, then 12 to 15 nights will be needed to make a map of just one object. As the good season for

interferometry may be only three months per year, in which excellent seeing, clear sky, low turbulence and low winds occur 50% of the time, then such a mode of operation allows complete imaging only 3 sources per year, or possibly up to 6-8 if an outstanding site is selected. Moreover, since telescopes are used by pairs, phase closure, or equivalent speckle masking, is not available for phase determination.

Greater productivity is obtained if information is collected on all baselines simultaneously (6 tracks per source per night, for a 4-telescope array). If the array is dedicated to interferometry, none of the telescopes being used for single telescope projects, about 3 months per year, 50% of the time, then 20 sources per year could be mapped.

Another operational consequence of the interferometry is that to collect the 12 to 15 tracks required, the telescopes would probably not make major moves every day. As with radio arrays with a small number of elements, the array would be left in the same configuration for a period or two or three weeks, during which time it would observe many sources, proposed by many different observing groups. After several weeks, the configuration would be changed, and the same sources would be observed again. After several configuration changes, typically lasting a few months, the observers could start to put their maps together. Since it would take a few months to do an observing program, it is most unlikely that observers would come to Chile or even to ESO headquarters during their programs. Instead, the use of an array will force ESO to provide standard instrumentation for interferometry, and to have observatory personnel carry out the programs, as with most radio interferometers.

The only way to avoid this, and to give astronomers a "hand-on" feeling of participation in the observing, is to have a dedicated array with enough telescopes to synthesize a map in one night -six to eight telescopes for example. In this case, it would be possible for astronomers to travel to the observatory, as for normal observing.

3.6 *Site constraints*

In additions to the qualities expected from a good astronomical site, interferometry has specific requirements.

Seeing quality

High angular resolution interferometric or adaptive techniques put more stringent conditions on seeing quality than other astronomical observations. These conditions are discussed in an ESO workshop (Roddier 1983). We summarize them here.

First of all the S/N ratio for interferometric observations varies as the inverse second to fourth power of the seeing disk size giving high weight to sites which, at least occasionally, provide exceptional seeing conditions. Stability of seeing conditions is important for accurate calibration of the atmospheric transfer function.

The S/N ratio depends also upon the so-called wavefront boiling time which is related to wind velocities in the atmosphere. Sites with low wind speed should be preferred. Turbulence near the tropopause can be detrimental because it is often associated with high wind velocities. High altitude turbulence also reduces the size of the isoplanatic patch within which high angular information can be restored. A good site for interferometry should have little high altitude turbulence.

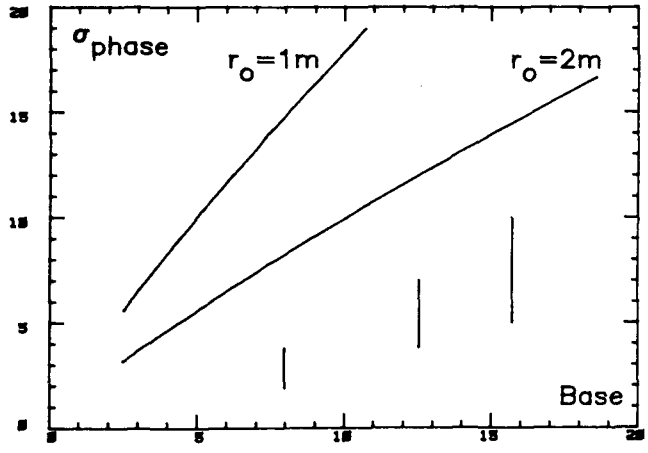

Figure 3.6-1

Vertical bars are the estimations of phase dispersion, in radian, measured at the three baselines (in meters). Observations were carried at λ = 2.2 μm where $r_0 \sim 0.6$ m for 1" seeing. Continuous curves show the expected values for r_0=1 and 2 meters (Mariotti, J.M., di Benedetto, G.P., 1984)

Stellar scintillation is directly related to high altitude turbulence (Loos and Hogge 1979, Roddier 1983) and its measurements is highly recommended in the site testing campaign. Sites showing little stellar scintillation should be preferred.

The outer scale of turbulence specifies the rms phase excursion between telescopes, and should be as small as possible. Very few measurements (Fig. 3.6-1) are yet available (Mariotti and di Benedetto 1984).

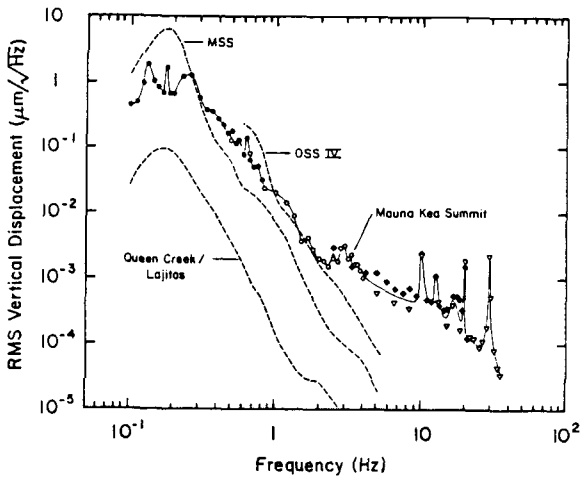

***Figure 3.6-2** : Spectrum of seismic disturbances measured at Mauna Kea. The location of the site is 40m SW of the Air Force 24 inch telescope. Shown for comparison are data from three other sites described in the literature (Dyck et al. 1985).*

Seismicity

The origin of the seismic background noise is to be related to different kinds of sources (Citterio 1984).

At long periods (T>20 sec) the earth noise is mostly related to atmospheric and oceanic sources, with the addition of the noise caused by the free oscillation of the earth excited by deep energetic earthquakes.

At short periods more sources must be added to the atmospheric and oceanic one: mostly anthropic sources (such as highways, railways, factories and human activities in general) and, in same areas, endogeneous sources (permanent volcanic noise). The intensity spectrum of the seismic background noise is strongly dependent on the specific sites.

As an example the high frequency activity recorded at some italian sites shows the following values:

Periods: 1 to 2 sec; 0.06 to 0.08 sec.

Amplitude: 0.02 to 2 micron

Max tilt: 0.006 arcsec.

From these data one can say that in particular conditions the microseismic activity could affect the stability of the phase of the fringes in the visible and in the near infrared. Specific considerations can only be made after direct measurements of the microseismic activity at the candidate sites. The measurements shoud be distributed through the year in order to monitor the most significant seasonal conditions. Such measurements have been carried at Mauna Kea (Dyck et al. 1985) and show that the most unfavorable effects come

from man made activity (Fig. 3.6–2).

Available area

A surface of 150 x 150 m seems the minimum requirement. If a LINEAR array is selected, with the addition of a single, movable N–S telescope, the N–S baseline could be compromised on a moderate slope (< 20°).

Chapter 4 : THE INTERFEROMETRY MODE : ITS IMPLICATIONS ON THE VLT PROJECT

The analysis carried in the previous chapters shows the high scientific interest of providing an interferometric capability within the VLT project. It also shows that the initial design: 4 fixed telescopes in a line, is far from optimal to achieve it. Yet, given the expected life time of the VLT –probably over 40 years– it would not be wise to exclude from it all interferometric capability. This chapter will examine :

a) how to compromise the design in an acceptable way.
b) how to insert the VLT interferometric use in a broader high angular resolution strategy
c) which parts of the VLT design are critical for interferometry and should be investigated in detail.

4.1 *A compromise design*

The configuration

The large telescopes can be combined by pairs in order to obtain the high sensitivity (in the infrared) or the short integration time (in the visible). All pairs combination should be available to get the frequency coverage.

The large telescopes may be used all together to use phase–closure and/or speckle masking image reconstruction techniques. Such a combination will be extremely efficient from the imaging point of view, but will represent an heavy operationnal load on the instrument. Moreover, techniques of beam splitting and beam combination will have to be developped. Therefore, this can only be envisaged several years after full completion of the array.

A two dimensional coverage is essential. This may be obtained either by having

- 3 movable telescopes and 1 fixed (VARY type)
- or 1 movable telescope and 3 fixed (QEW+NS)
- or 4 fixed telescopes plus smaller auxiliary telescopes

If the arguments of mutual seeing influences, hydrodynamics of the wind flow

and site constraints favor heavily a line configuration for the VLT array, the perpendicular coverage can be achieved with two smaller telescopes (Tel. 5 and 6), 2 to 3 m in diameter.

Figure 4.1-1

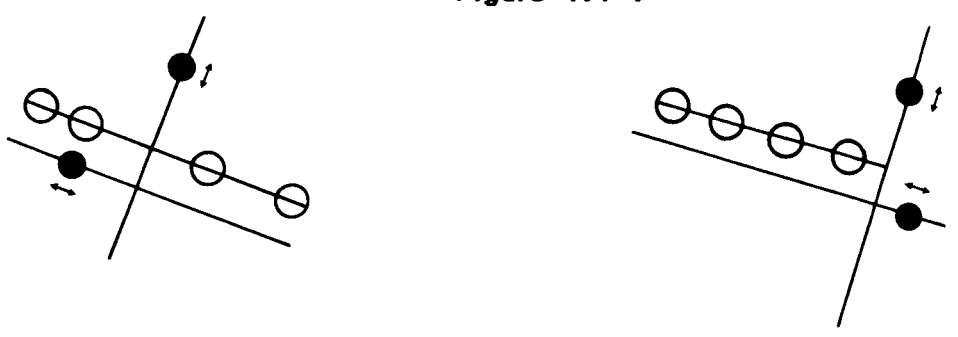

OPTION A

4 fixed telescopes, non redundant
+ 2 movable 2-3 m telescopes.

OPTION B

4 fixed telescopes, compact
+ 2 movable 2-3 m telescopes

The non-redundant configuration of the large pupils is preferred over ca. 150 m baseline, while the more compact, redundant configuration over 100 m baseline may be acceptable. The quasi N-S excursion should be comparable in amplitude to the QEW baseline extension. Site constraints will ultimately influence the choice.

As an option, Tel. 4 could be kept movable by steps in a QNS direction, providing high sensitivity coverage in this direction.

The operationnal aspects of such a concept are favorable since:

- continuous (100% of time) interferometric operation is possible with Tel. 5 and Tel. 6, providing good (u,v) coverage, extensive training and full use of the expensive interferometric focal plane instrumentation.

- combination of any of Tel. 1, 2, 3 or 4 with Tel. 5 and/or 6 allows to practice interferometry with a large pupil, use adaptive optics, prepare the combination of two large pupils, develop phase reconstruction, exploit the large telescopes as soon as one is built.

- combination of any of Tel. 1, 2, 3, 4 in pairs or all together is completely feasible at a later stage, using only a fraction (10 to 25%) of the VLT observing time in a stationnary regime, not to be reached before the years 2005 or 2010. At this stage full exploitation of the VLT sensitivity would become possible.

Figure 4.1-2 outlines possible implementations of options A and B on various sites.

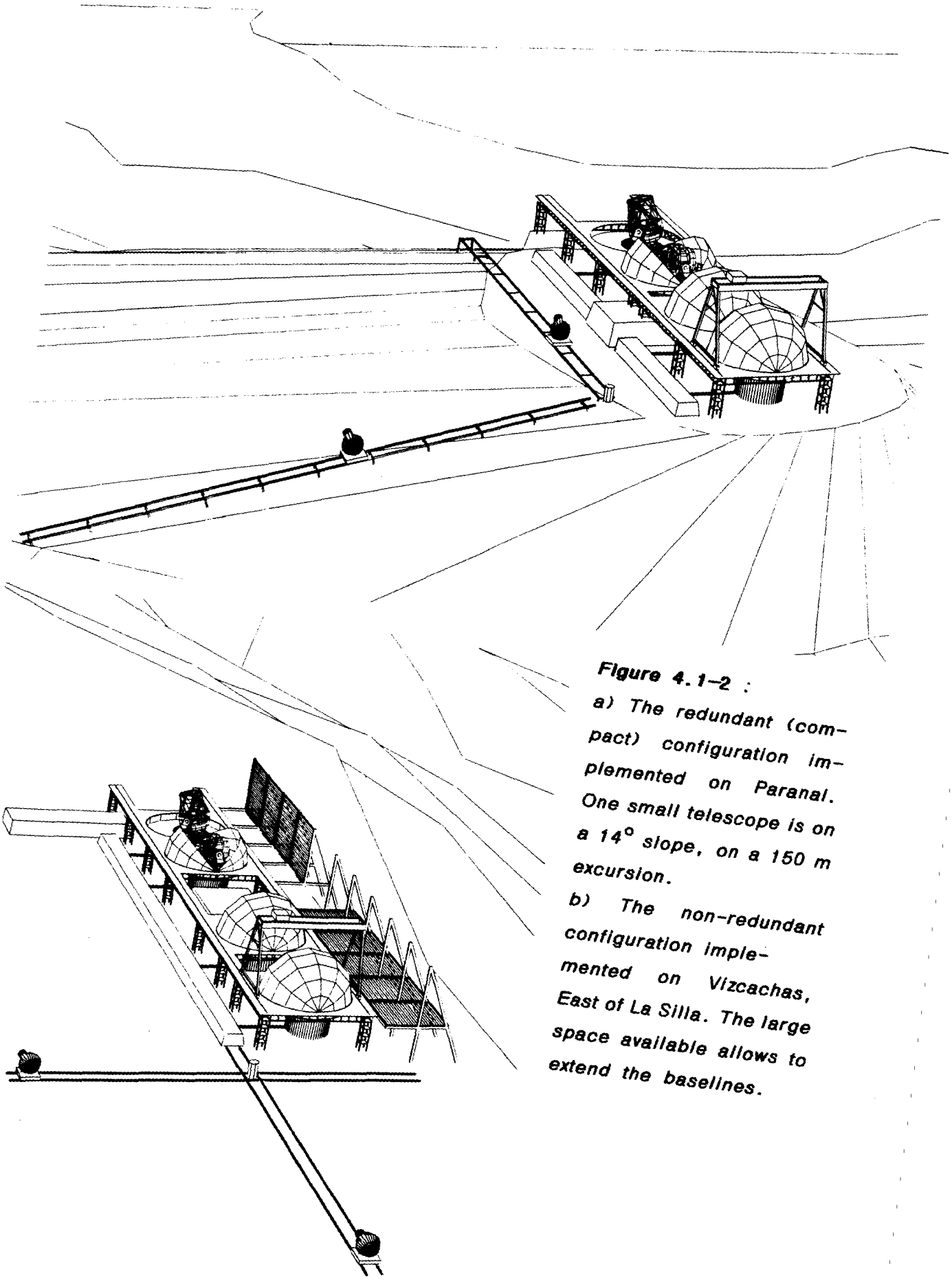

Figure 4.1-2 :
a) The redundant (compact) configuration implemented on Paranal. One small telescope is on a 14° slope, on a 150 m excursion.
b) The non-redundant configuration implemented on Vizcachas, East of La Silla. The large space available allows to extend the baselines.

The wavelength coverage

The wavelength range of operation has to be kept as broad as possible, in order to preserve the long term. It is quite obvious that atmospheric properties, adaptive optics, sensitivity gains, ease of stability control all favor the infrared at 3.5, 5, 10, 20 microns.

On the other hand, many of the problems to be solved are common to all wavelengths: beam combination, data processing, seeing control. A dual approach should therefore be kept as far as possible; it is likely that the performances of mechanical errors active control system (§ 3.1.2) and the detector requirements (§ 2.3) may be decisive to make the early steps of the interferometer at infrared wavelengths.

The critical points

The study in this report is not a feasibility nor a detailed design study. But it has shown that the interferometric mode of the VLT puts a very limited number of additional constraints on a non-interferometric VLT. These constraints are :

- site selection to allow non-redundant baseline, baseline orientation, N-S coverage.
- microseismic quality, small outer scale of local turbulence (§ 3.6)
- construction of 2 extra telescopes with associated tracks; beam combination tunnel and feed from all 6 telescopes.
- mechanical stability of the telescopes, to be kept as low as possible (§ 3.1.2) and followed by an active control of internal path differences. This is the only specific constraint which may influence the detailed design of the large telescopes and should be considered accordingly.

Other requirements are more or less common to the general VLT design, such as :

- excellent seeing
- excellent infrared transmission
- thermal cleanliness of the telescopes
- coupling of Nasmyth foci to ground
- adaptive optics for $\lambda > 3.5$ μm

Preliminary cost analysis

A preliminary analysis has been carried at ESO to examine the costs of options A and B described above. This cost estimate is provided by the ESO-VLT Study Group (Cf "Very Large Telescope - Interim Report", January 1986 - VLT Report N°44) :

- The cost estimates for all building and ground work are based on feasibility studies.
- The costs of the auxiliary telescopes are estimated with the D 2.7 scaling law and have the ESO NTT and the Boule Telescopes as references.
- The estimates for the optics, interferometric table, active control etc. are very delicate and based on provisional ESO estimates by comparing this interferometric with technical systems of similar complexity.

The following tables give the additional costs on top of the so-called "baseline version", which is the linear array in its most compact version with a length of approx. 100 m and fixed telescopes. For interferometry a minimum configuration is necessary which in both options would consist of items I and II. In case of option A this includes the additional cost to increase the length of the building, windscreen, incoherent beam combination, etc. All other suboptions increase the cost by the amounts given in the tables.

The amount of 18 MDM which was given in the VLT report 44 refers to Option B. It includes items II and III. Item 1 was already included in the total building and laboratory costs.

Option A

Non-redundant configuration (150 m)

(Minimum for interferometric work : I and II)

I.	Interferometric lab.	1938 KDM
	incl. all building and ground work	+ 6042*KDM
	Total	7980 KDM
II.	Optics for combining 2 of the 4 VLT telescopes at a time (incl. interferometric table and active interferometer control)	11710 KDM
III.	2 additional small movable telescopes (1.4 m in simple (200 m) tracks)	+ 7500 KDM
IV.	Suboptions (this amount has to be added to i. and II.) :	
	– one large movable telescope	+ 26012 KDM
	– 2 small 2 m telescopes with stepwise motion (200 m)	+ 15000 KDM
	– continuous motion (200 m)	+ 22000 KDM
	– 2 small 3 m telescopes with stepwise motion (200 m)	+ 28000 KDM
	continuous motion (200 m)	+ 39000 KDM
	– optics for combining all 4 telescopes at a time (incl. necessary delay lines)	+ 6500 KDM

** All necessary extensions of building, windscreen, etc. caused by the increase length 150 m.*

Option B

Compact redundant configuration

(Minimum for interferometric work : I and II).

I.	Interferometric lab incl. all building and ground work	1938 KDM
II.	Optics for combining 2 of the 4 VLT telescopes at a time (incl. interferometric table and active interferometer control)	10510 KDM 1)
III.	2 small movable telescopes (1.4 m on simple 200 m tracks)	+ 7500 KDM 1)
IV.	Suboptions (this amount has to be added to I. and II.) :	
	- one large movable telescope	+ 26012 KDM
	- 2 small 2 m telescopes with	
	stepwise motion (200 m)	+ 15000 KDM
	continuous motion (200 m)	+ 22000 KDM
	- 2 small 3 m telescopes with	
	stepwise motion (200 m)	+ 28000 KDM
	continuous motion (200 m)	+ 39000 KDM
	- optics for combining all 4 telescopes at a time (incl. necessary delay lines)	+ 6000 KDM

1) *Total of 18 MDM was given in the VLT Report 44. The additional cost for the interferometric buildings have been included in the overall building costs.*

This cost analysis does not include the focal plane interferometric instrumentation (detection...etc).

It may appear desirable that the beam-recombining "focal package" be interchangeable, as are spectrographs and photometers on conventional telescopes. Following the construction of a "number-one" focal package by

institutes, more sophisticated instruments will probably be developped and made available to the community.

On the other hand, the complexity of this package and the relatively small number of European experts for such instrumentation shoud probably lead to the formation of a consortium of laboratories, well integrated and in close connection with the VLT project group itself.

The design study would lead to an estimate of the technical staff requested to run the interferometric mode of the VLT. Beside the normal telescope staff, experience with radio arrays indicates that 10 to 15 fulltime people could be necessary in the final (2005-2010) stationary regime to maintain the specific adaptive optics and active loop systems, the metrology, the beam-combining instrumentation and the associated software. This technical group, in close connection with the interferometry consortium, could provide a centralized service to the European community of astronomers.

The supporting consortium of European scientists may take the shape of a centralized laboratory, at least for the initial phase of developpement. A preliminary survey made in the European countries member of ESO indicates that about 80 scientists (at 50% of their time) could be directly involved in the first phase of the VLT interferometric mode (1990-2000).

Development of the project

Within the existing VLT plans, the following interferometry schedule may be envisaged :

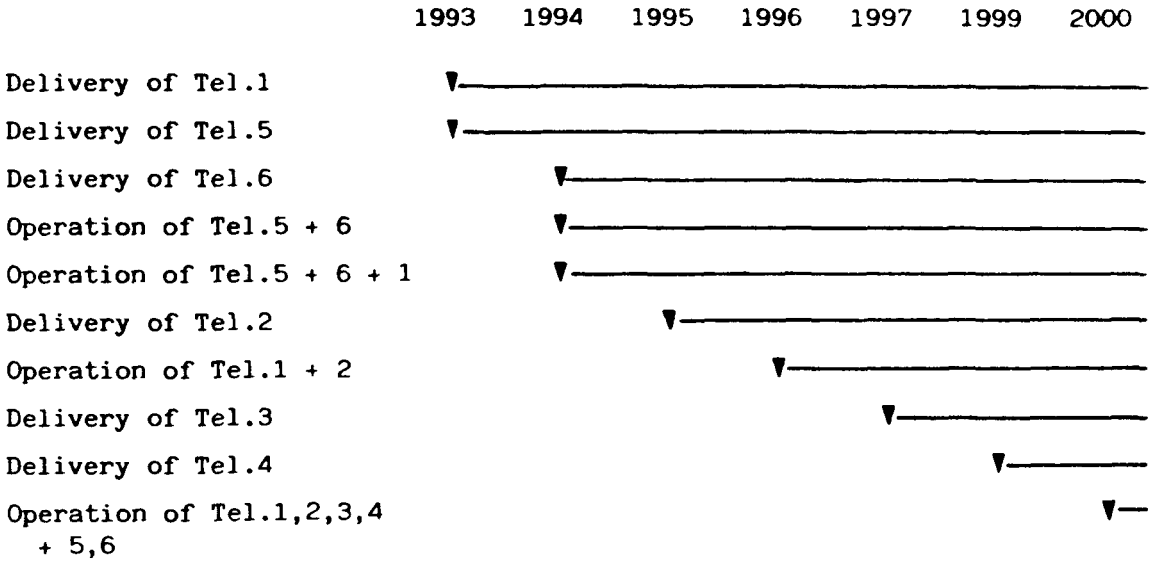

4.2 *A long term view on spatial interferometry*

It is generally agreed that spatial interferometry at optical wavelengths holds a great potential for discoveries in the future. In this respect, an interferometry mode included in the VLT project has to be considered within a development program, including space as well as ground based facilities, as outlined by Table 4.2-1.

Table 4.2-1

Prospective development program in interferometry

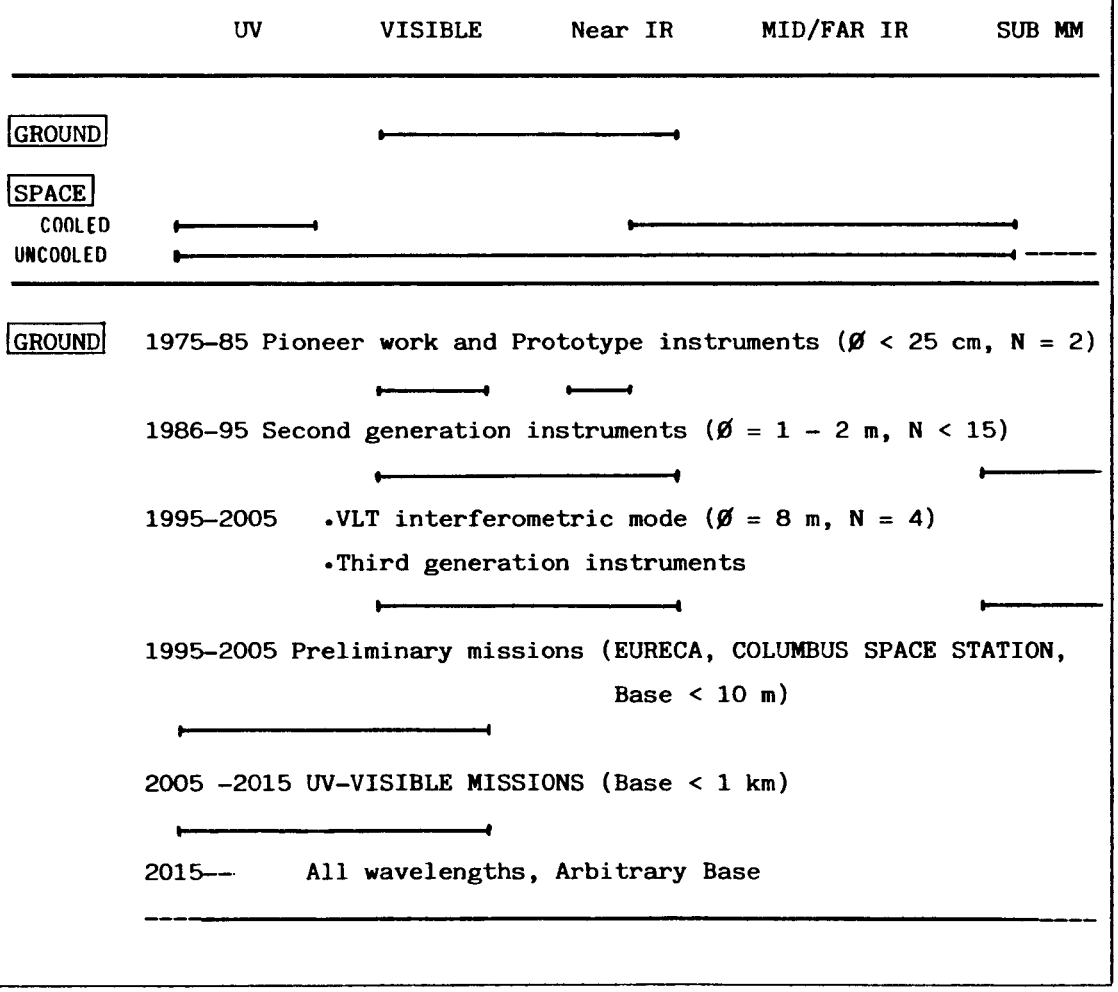

Table 4.2-2

OPTICAL INTERFEROMETRY IN THE WORLD

Existing or Planned instruments

Number of TELESCOPES	DIAMETRE	LOCATION	BASELINE	SPECTRAL RANGE	Date of OPERATION
2	26cm	CERGA	N-S <100m	visible + 2.2 µm	1977
2	150cm	CERGA	N-S <100m	visible + 2-10 µm	1985...
2	100cm	CERGA	100m E-W fixed	heterodyne 10.6 µm	
2	50cm 100cm	Smithsonian Mt. WILSON		visible (astro-métrie) visible	1983 1986
2	10cm 1-2m ?	SYDNEY "		visible visible	1985 project
2	165cm	BERKELEY	fully variable	heterodyne 10.6 µm direct 5-20 µm	1986
6	240cm	ARIZONA	MMT fixed	visible + 10 µm	1984
6	20cm	Univ. ERLANGEN (RFA)	<100m	visible	1986
2	150cm	Univ. GEORGIA		visible (astro-métrie)	project
3	100cm	Univ. HAWAI	N-S+E-W	infrared 2-20 µm	project

SPACE (proposals)					Target dates
2	30cm DUO	Harvard	6m	visible	1995
2	30cm ISIS	Erlangen	4m	visible	1995
15	1m OASIS	RGO/GB	20m	visible/uv	2000 ?
15	1m TRIO	Cerga	1-100km	visible/uv	2000 ?
10	1.8m COSMIC	Smithsonian	20m	visible/uv	2000 ?
2	1m SAMSI	"	∿ km	visible/uv	2000 ?

The prototype instruments have shown the basic feasibility of interferometry in the presence of the atmosphere. The second generation instrument will explore in detail important problems such as phase reconstruction, long integrations, ultimate noise sources; but, more important, it is likely that they will be scientifically very productive. They will also contribute to the training of a new generation of astronomers. Table 4.2-2 gives an overview of existing or planned instruments.

The VLT interferometry mode will only be used for dedicated projects, where a high sensitivity is required (at infrared wavelengths) or where integration time must be reduced to acceptable values (at visible wavelengths, for bright objects $m_V < 10 - 13$). The possibility of sub-aperture combination will also give it a superior image reconstruction capability. The VLT mode will benefit of all the results from the previous step, and explore in detail the possibility of large dishes combination.

It is expected that new scientific results come from the VLT, which none of the other 2nd generation instrument would give.

Space-based interferometry will work with a much higher efficiency. Although active optics technology may allow to build diffraction-limited lightweight monolithic mirrors larger than the size of the Space Telescope, coupling telescopes interferometrically appears to be the best approach to high angular resolution in space. This has raised considerable interest during the last few years as shown by the proceedings of two recent colloquia (Reasenberg 1984, Olthof 1984). The most ambitious projects such as TRIO (ESA) or SAMSI (NASA) envisage optical coupling of independent spacecraft over kilometric baselines but rigid structures such as OASIS (ESA) or COSMIC (NASA) are also considered. Ground-based interferometers will not be able to compete with such instruments. However, because of the difficulties introduced by the use of cryogenic liquids in space and because atmospheric distorsions are much less severe in the infrared than in the visible, infrared interferometry will likely be developed on the ground well before it is used in space.

The angular resolution provided by the Space Telescope will be less good than the one already obtained at optical wavelengths from the ground, but the absence of atmospheric disturbances will allow a better sensitivity.

The results of the ground program will highly benefit to the space missions, in the fields of scientific motivation and training, image reconstruction, image algorithms.

4.3 *Recommendations*

A number of developments are necessary to ensure a proper analysis of the VLT interferometry option. It is therefore recommended that appropriate action be taken either within the VLT project group, or at European level, or at national levels, for these subjects to be investigated.

• Recomm. 1 :

The mechanical stability requirement determines the shortest wavelength at which interferometry will be possible. Specifically, the VLT must have mechanical stability at the combined focus, both for lateral displacements (tracking) and longitudinal displacements (path equality). The required stability probably cannot be achieved without an active system, at least for the longitudinal errors.

It is therefore recommended that

(a) – a specific technical study be made as soon as possible, over a time scale of a year, to estimate the achievable stabilities, that is, the amplitude of fluctuations in the optical path at frequencies from 0.01 Hz to 100 Hz, with respect to ground, for the telescopes as they are now conceived, as well as proposed solutions for improvements;

(b) – a specific optical study be carried out to establish the feasibility and costs of an active system, including sensors and actuators, to correct for the residual path errors.

• Recomm. 2 :

The incorporation of 2 smaller size movable telescopes (2–3 m) in the VLT design is an unescapable conclusion if the interferometry concept is selected.

• Recomm. 3 :

Adaptive optics developments should be vigorously initiated and pursued. Its feasibility on faint visible and infrared objects must be evaluated.

• Recomm. 4 :

Impact of interferometry on site selection should be carefully considered, implying the parameters: seeing, outer scale of turbulence,

infrared quality, seismicity, overall size (N-S + E-W).

• Recomm. 5 :

Image reconstruction algorithms should be developed, with emphasis on the specific condition encountered in optical interferometry (phase gradient measurement). This work could be jointly carried with the European Space Agency, since many aspects of image reconstruction will be similar in ground-based and space-borne interferometry. The experience of radio-astronomers is essential and the two communities should actively collaborate.

• Recomm. 6 :

The feasibility of moving at least one (the last to be built) of the 4 main telescopes of the VLT needs to be studied.

• Recomm. 7 :

Continuation and development of diffraction limited work, at visible and infrared wavelength, on 4 m-class telescopes (for example, high resolution testing station at the 4.2 m Hershell telescope Nasmyth focus, improvement of seeing on the 3.6 m CFHT and 3.6 m ESO).

• Recomm. 8 :

In order to test the full range of problems affecting interferometric use of the VLT (stringent limits on mechanical fluctuations due to tracking and secondary mirror support), techniques for displacing optical telescopes on rails, wind and thermal effects, best methods of beam conbining, delay lines, operational aspects, etc. it would be desirable to operate a prototype two-telescope interferometer carrying mirrors in the 1.5 to 2 m class, on an acceptable mountain site. This interferometer could be made fully operationnal on a short (2-3 years) time scale and capitalize all experience gained with the various existing interferometers (I2T and GI2T at CERGA, interferometer at Erlangen, US instruments and current studies).

4.4 *Frontier of technological research*

The development of interferometry within the VLT project will stimulate the technology in new and interesting areas

- stabilisation at sub-micron accuracy of long optical paths. This will couple with laser research, with gravitational wave detection based on interferometric technics, with future space developments (accurate satellite positioning).
- adaptive optics with large number of elements (> 100), with possible new technics of phase correction (active laser beams, integrated mirrors...).
- monomode optical fibers at visible and infrared wavelengths (the optical fiber coupling option, although very attractive, has not been stressed in this report because of the heavy development work requested before it represents a credible alternative).

All these areas may contribute later to space projects in astronomy as well as in other fields. It is worth noting that european firms and laboratories are already highly qualified in these fields and have the capabilities to foster such developments.

Chapter 5 – Conclusion

Optical interferometry offers to explore a completely new field, by imaging objects with 1 to 10 milliarcsec resolution at visible and infrared wavelengths. It will for the first time bring optical imaging close to VLBI resolution, which reaches 0.3 marcsec in H_2O lines and will attain 0.1 marcsec at millimetric wavelengths.

The analysis carried in this Report as well as the results of existing instruments show that ground-based interferometry is feasible and will be scientifically productive. Full optimization of a ground based interferometer is certainly wavelength-dependent, from the blue part of the visible spectrum to the longest infrared wavelengths, ca. 20 μm.

Broadly speaking, such an optimum interferometer may be an array of six or more movable telescopes, 1.5 to 3 m in size, fully dedicated to interferometry, installed in a site having excellent seeing and infrared characteristics, allowing 200 meters baselines in every direction.

An instrument in space would have superior performances, especially at visible wavelengths. In the infrared, its superiority would only be achieved by a proper cooling of the whole optics. It is not expected that such complex space missions, although highly desirable, could fly before the years 2005–2015.

An interferometric mode for the VLT has been studied in detail in this Report with respect to performances, feasibility and constraints on the project.

The VLT array design, which was not driven by interferometry consideration and should probably not be, is far from the ideal interferometric design, and a complete reconfiguration of the VLT has not been retained here. Nevertheless, even within the present concept, slightly amended, VLT interferometry will bring two specific advantages : high sensitivity in the infrared and short observing time in the visible. Each of these requires specific conditions to be fulfilled: adaptive optics for the former, fast, accurate and many-pixels detectors for the latter.

The concept of fixed telescopes as well as the limited fraction of VLT time for interferometry suggests to implement interferometry in an hybrid configuration, where two smaller (ca. 2 m), movable telescopes will complement the VLT telescopes, providing great flexibility of beam combination, extensive spatial frequency coverage, optimum return for the focal plane

instrumentation investment and continuous interferometric work at the VLT site.

The constraints brought on the VLT design by interferometry are surprisingly limited in number as well as in depth : seeing quality and infrared transmission at the site, adaptive optics at infrared wevelengths are not specific to interferometry. The mechanical stability of telescopes is the most serious requirement; the requested stability, which is indeed wavelength-dependent, is not achievable in a pure passive way; an active system of control will be required, but its construction will be eased if the telescopes design itself accounts for these stability requirements.

The implementation of the interferometric mode on a given site is also creating some constraints : size and direction of the array, position of auxiliary telescopes. Fortunately, trade-offs are easier here, and even a one-hundred by one-hundred meter configuration already brings a factor of 12 in resolution over single telescopes.

It is fair to say that the available expertise on ground based interferometry is positive but yet limited. Speckle interferometry with a single telescope provides today a sound and precisely verified experimental and theoretical basis for the prevision of interferometric sensitivities. Other peculiars of interferometry, such as adaptive optics phase noise or sensitivity to thermal background, will be explored in the next ten years by existing or planned small instruments. It is expected that, over the long lifetime of the VLT, these points will be fully understood and solved.

VLT interferometry has a great discovery potential : the study of star surfaces, with their convection and magnetic fields, the formation of dust and molecules in circumstellar envelopes, the complex dynamics which prevails in the young stars where disks and bipolar flows are formed, the condensation and cooling of fragments of matter in nearby stars eventually forming planetary systems, the structure of galactic nuclei, all these phenomena, and many others, occur on physical sizes which can be reached with the VLT interferometer, at flux levels which fits its sensitivity. Ultimately, optical interferometry will reach, on the ground or in space, the image quality a VLA-type instrument with its 27 antennae. In the meantime, the limited number of VLT telescopes gives to optical interferometry a status comparable to centimetric VLBI or to existing millimetric interferometers and one may only wish to equal their performances by joining the expertise of optical and radio astronomers.

Appendix A1 - ADAPTIVE OPTICS

Phasing at least partially the whole pupil of a VLT simple telescope to compensate for atmospheric phase errors is advantageous for normal imaging as well as for spectroscopy. Yet, it becomes a fundamental requirement for efficient interferometric combination of two or more large telescopes.

Recent progresses both in adaptive optics technology and in the understanding of atmospheric perturbations make this goal realistic on the VLT time scale, especially at infrared wavelengths.

Basically two different correction strategies are possible: zonal or modal correction. If the modal approach is used rather than a zonal decomposition, significant correction is possible even with a limited number of modes, allowing partial or full pupil correction.

An adaptive system contains four basic elements: an optical train and receiver, a phase-error sensor, a servo-control system, and an optical phase shifting element. The distorsion of the received wavefront is usually compensated by reflecting the light beam at a deformable mirror. The surface is adjusted in real-time to compensate the path length aberrations. The information required to deform the mirror is obtained by analyzing the reflected beam with a wavefront sensor. Two methods in wavefront sensing have been developed further for this type of application: the Shack-Hartmann test and the shearing interferometer. With these wavefront measurements a map of wavefront errors determines the signal required to drive the deformable mirror by expanding the spatial $f_n(\vec{r})$ and temporal $a_n(t)$ dependent correction function $C(\vec{r},t)$

$$C(\vec{r},t) = \Sigma\, a_n(t)\, f_n(\vec{r})$$

A typical set of spatial functions are the Zernicke polynomials, which are usually used to describe the common optical aberrations. For atmospheric turbulence compensation they are only optimal for the modes with lower numbers. High order spatial and temporal frequency fluctuations can be more efficiently handled by the Karhunen-Loève functions.

Typical values for the spatial and temporal constraints at different wavelengths are given in Table A1-1.

For 8–10 m telescopes this would lead in the visible to approximately 6000 controlled subapertures working at frequencies up to 1000 Hz. More realistic and technically feasible is the correction at infrared wavelengths. Systems with 150 to 200 subapertures have been developed and tested for military applications (e.g. Itek Corp., AOA, CGE, MBB, etc...)

In order to avoid wavefront sensing at infrared wavelengths, experiments are in progress to use the low spatial frequencies in the visible transfer function for the correction in the infrared. So far this approach looks very promising.

The resulting partially corrected atmospheric transfer function has been computed by Roddier and Roddier (1986) using a standard atmospheric model and assuming sensing at λ_1 = 0.5 μm while observing at λ_2 = 1.25 μm, 2.2 μm, 4.8 μm or 10 μm. The result shown on Fig. A1–1 looks very promising. The main problem is that most IR sources have no visible counterpart. Wavefront sensing will require a near visible star as a reference. Calculations show that corrections degrade rapidly when the angular distance of the reference star increases. Fig. A1–2 shows the corrected transfer function at λ = 2.2 μm for a reference star at θ = 10" and θ = 20". The size of the so called isoplanatic patch over which correction is acceptable increases as $\lambda^{6.5}$ so that there is a reasonable chance to find a reference star close enough when working at λ = 10μm (Fig. A1–3).

Existing technology and developments expected during the next few years make it absolutely likely that the single VLT telescopes will be equipped with adaptive correction devices allowing a full pupil correction at wavelength longer than 4 μm. These systems will give an interferometer the required phase uniformity over the individual pupils. At shorter wavelengths, partial MTF correction will still be obtained. Furthermore, it has to be investigated whether the deformable mirrors can additionally be used for the stabilisation of the interferometric beam combination train (§ 3.4).

It has been recently proposed (Foy and Labeyrie 1985) that the fundamental problem of the availability of a reference star within the isoplanatic angle might be solved by shooting laser pulses through the observing telescope or an auxiliary telescope to a layer in the atmosphere about 80 km high which reemits by scattering or excitation of sodium atoms sufficient light for the telescope to pick it up as a point source, providing a reference point source with seeing information. If this could work in practice (and such laser ranging has been done for other purposes), it would represent a breakthrough in the problem of the isoplanatic angle.

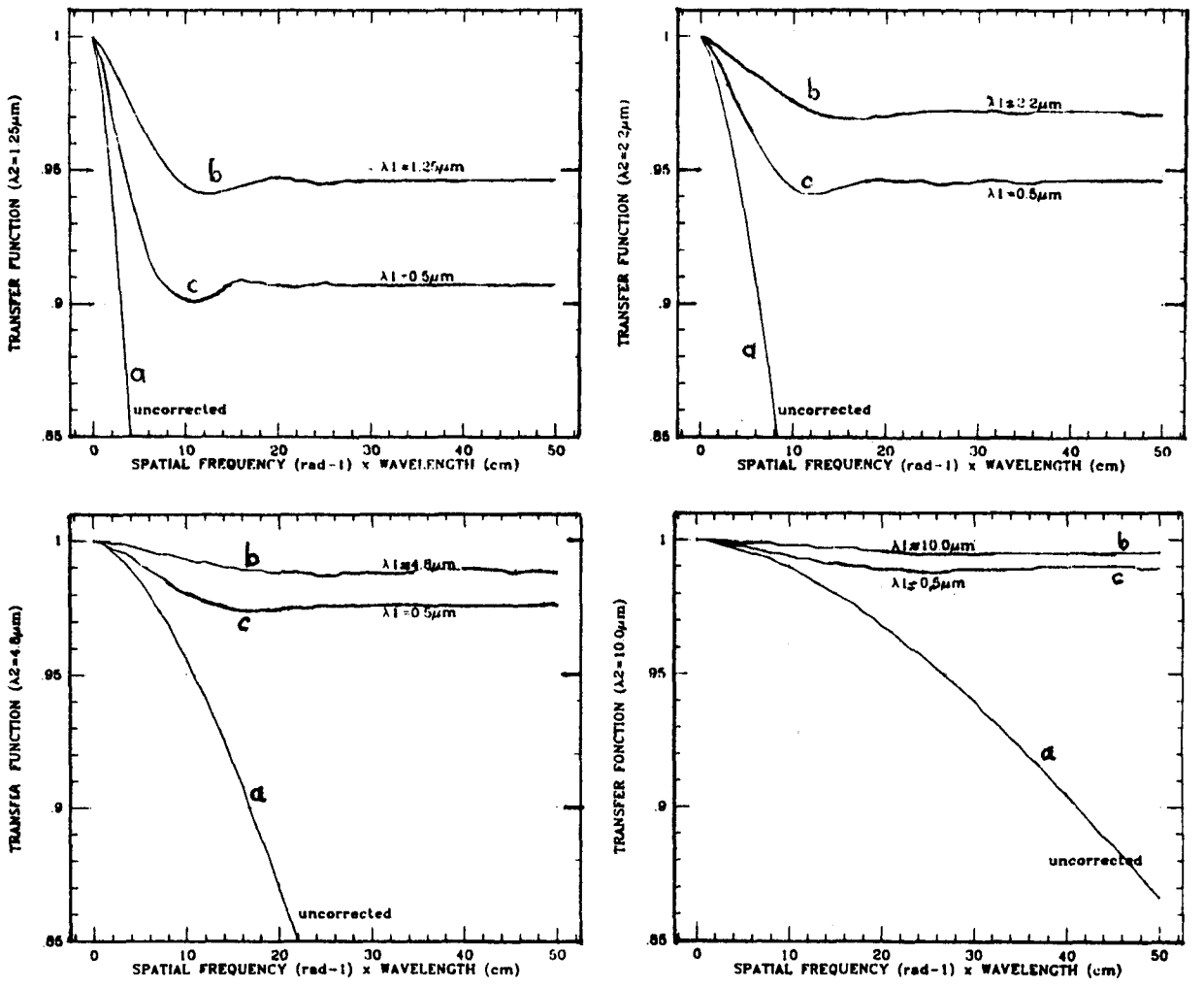

***Figure A1–1** : Modulation transfer function in the infrared at four wavelengths λ_2 (1.25, 2.2, 4.8 and 10 μm).*

a) uncorrected, fully degraded by atmosphere (1 arcsec seeing, zenith observation), b) fully corrected assuming a wavefront sensor at the same wavelength λ_2 ($\lambda_1 = \lambda_2$), c) partially corrected, wavefront sensor at λ_1 = 0.5 μm. Abcissae: multiply by 20 to obtain units of arcsec^{-1} x μm (Roddier and Roddier 1986).

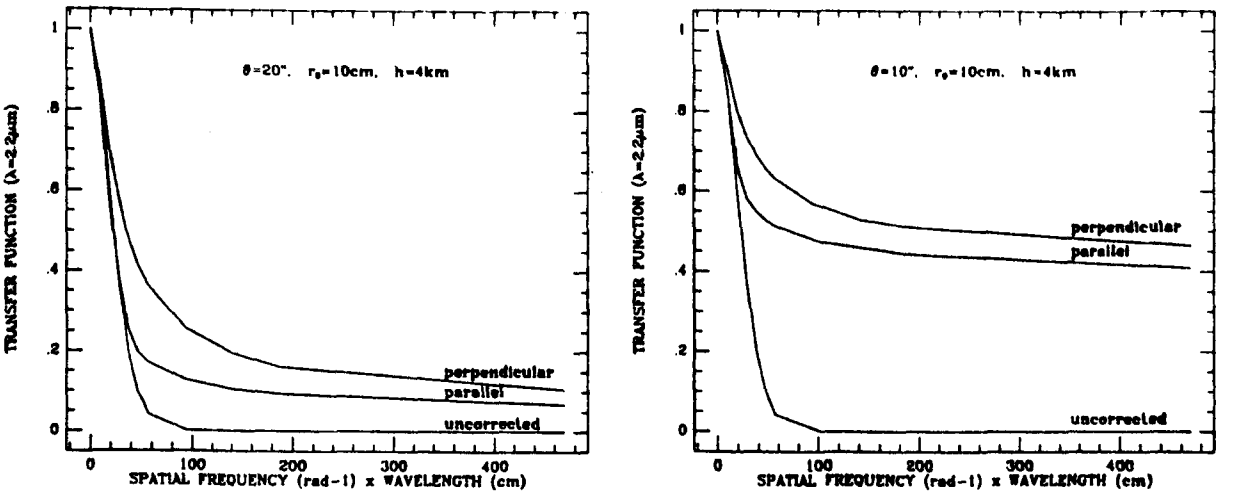

Figure A1–2 *: Corrected MTF at λ = 2.2 μm, using a reference star at θ = 10 and 20" (seeing 1", turbulent layer at h = 4 km). The size of the isoplanatic field is linear with h^{-1} (Roddier and Roddier, 1986). Abcissae as in Fig.A1.1. Note the slight anisotropy of the correction.*

Table A1–1

Fried's seeing parameter : $r_o \propto \lambda^{6/5}$

λ	0.5 μm	2.2 μm	5 μm	10 μm
r_o	10 cm	60 cm	160 cm	360 cm

Number of independent correction : $N \propto (D/r_o)^2 \propto \lambda^{-12/5}$

For D = 4 m

λ	0.5 μm	2.2 μm	5 μm	10 μm
N	1600	45	∿ 3	∿ 1

Maximum optical path correction : $\Delta z \propto \lambda (D/r_o)^{5/6} \propto \lambda^0$

For D = 4 m $\Delta z \approx \pm 7$ μm

Time constant : $\tau \propto r_o \propto \lambda^{6/5}$

λ	0.5 μm	2.2 μm	5 μm	10 μm
τ	6 ms	35 ms	95 ms	220 ms

Isoplanatic patch size : $\theta \propto \lambda^{6/5}$

λ	0.5 μm	2.2 μm	5 μm	10 μm
θ	1.8"	10"	30"	70"

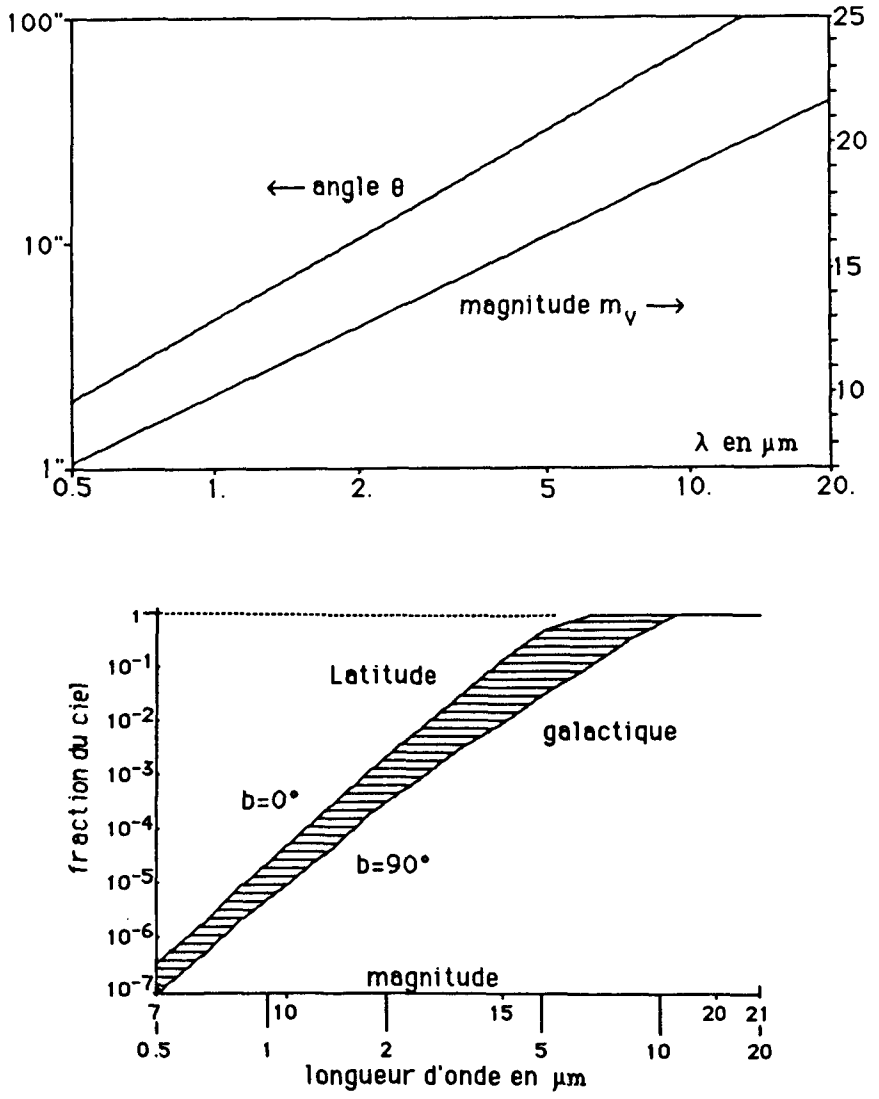

Figure A1–3 *: Offset adaptive optics*

a) Isoplanatic field versus wavelength [$r_0(\lambda) \alpha \lambda^{1.2}$ *dependence*], *on left scale. The curve is normalized for a 2" isoplanatic field at 500 nm. Right scale : visual magnitude* $m_v(\lambda)$ *of a star bright enough to inform a wavefront sensor able to correct the spatial frequencies from 0 to* D/λ. [*Assumptions are* $m_v(500nm) = 7$; *number of photons* $\alpha\ r_0^2(\lambda)$; *exposure time* $\tau_c(\lambda) \alpha\ r_0(\lambda)$. *The number of photons available for the correction varies as* r_0^3, *hence as* $\lambda^{3.6}$].

b) Fractional area of sky covered by the isoplanatic fields $\theta(\lambda)$ *containing at least one star of magnitude* $m_v < m_v(\lambda)$, *from Allen (1973), at galactic latitudes* 0° *and* 90°.

Appendix A2 - (u,v) COVERAGE AND IMAGE RECONSTRUCTION

Five different interferometer configurations were considered. They are shown on Fig. A2-1a to d. The first (QEW) has four fixed telescopes (a) on a line at azimuth 100 deg. The departures from a strictly east-west line leaves some north-south resolution even at the equator. The four telescopes are placed so as to provide the six space harmonics of 25 m up to a 150 m. The second test configuration (QEW+NS) has the fourth telescope moving on a line orthogonal to the line at azimuth 100 deg (b). The other three telescopes are fixed. The simulation has been done with that fourth telescopes successively placed at three positions -50 m, 0 m and +50 m from the position on the basic line defined by the three other telescopes. The third test configuration is a compact arrangement of 4 telescopes (c) with one every 16 m. The fourth test is a fixed Y arrangement (d), with one of the three arms beeing north-south. The fifth test has one fixed telescope at the center of the wye and three movable telescopes, one of each arm of the wye (e). VARY has been tested in to different configurations thus providing twelve space harmonics. All telescopes are 8 m in diameter. They are drawn to scale on Fig. A2-1. In the simulations, the spatial frequency diagrams (u,v diagrams) presented in Fig. A2-2 have been convolved with the spatial transfer function of a single 8 m aperture. This assumes that the whole of this aperture has been properly phased by means of either active optics (infrared case) or some kind of speckle interferometry (visible case).

The model sources shown on Fig. A2-3 have four components of different intensities and sizes. Observations have been simulated with the interferometers described above. (u,v) diagrams and point spread functions have been computed (Figs. A2-2a to A2-2e) for each array and for two declinations, -15 and -65 deg. The site was assumed at a latitude of -25 deg. The sources were assumed at the field center. The point spread functions have been used to restore the images by means of the CLEAN algorithm which is a way to recover the missing space harmonics by interpolation in visibility space. This process does not extrapolate in visibility space that is to say it does not provide improved resolution relative to the actual observations. Figs. A2-4a to A2-4e show the obtained raw maps at declinations -65 deg and -15 deg for the test arrays and two different amounts of random phase errors, 0 deg rms in the

upper frames of Figs. 4 and 60 deg rms in the lower frames of Figs. 4. The axes are labelled in arc sec at 1 mm wavelength which is equivalent to milliarsec at 1 micron wavelength.

Because it is likely that only phase gradients will be measured, phase offsets (in addition to random phase errors) shoud have been assumed between the various (u,v) track in a case like QEW or COMPACT where (u,v) tracks never cross one another. However, in the case of QEWS + NS some (u,v) tracks are crossing one another. It can therefore be assumed that this kind of partial redundancy will allow the construction of a consistent set of phases from the observations all over the (u,v) plane within arbitrary phases which does not prevent image reconstruction. The two arbitrary phases just prevent absolute positionning of the source. Figs. A2-5a to A2-5e show the restored images after processing by the CLEAN algorithm.

The conclusions are the following. At low declination, the restoration is acceptable only when a N-S coverage is provided (QEWNS, FIXY or VARY). In particular, this more than compensates for non-zero random phase errors.

Figure A2.1 :

The five configurations used to test the VLT-PSF in the interferometric mode. The four telescopes (8m) are on scale with the selected baselines.

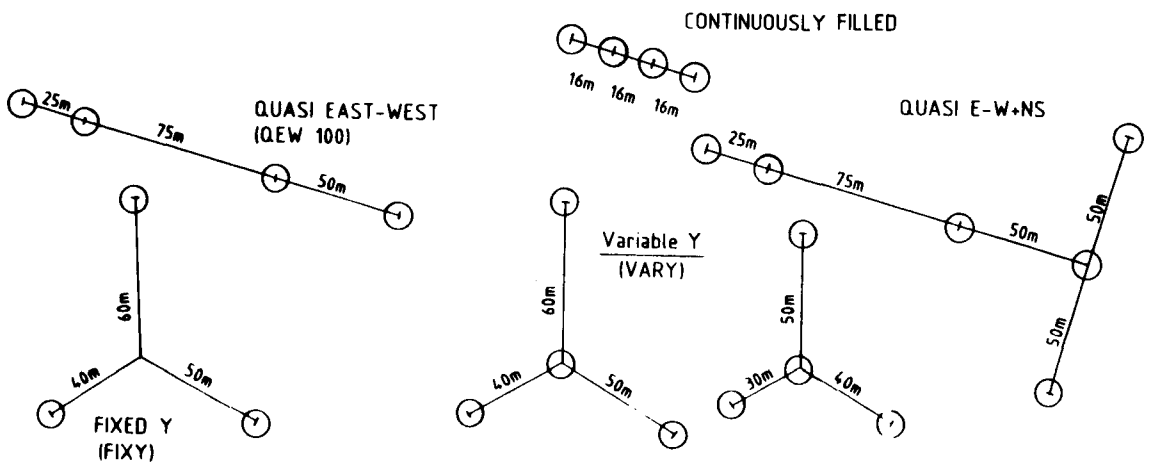

FIGURE A2.2 (a to e)

Spatial frequency coverage (u,v) and point spread functions for the five studied interferometers. Full contours are 0.1, 0.2, 0.3, 0.5 of maximum. Dashed contours are -0.1, -0.2 and -0.3 of maximum. Axes labelling is in milliarcsec at 1 μm wavelength.

Figure A2.2a

QEW - Frequency coverage and Point Spread Function

(δ = -15° and -65°)

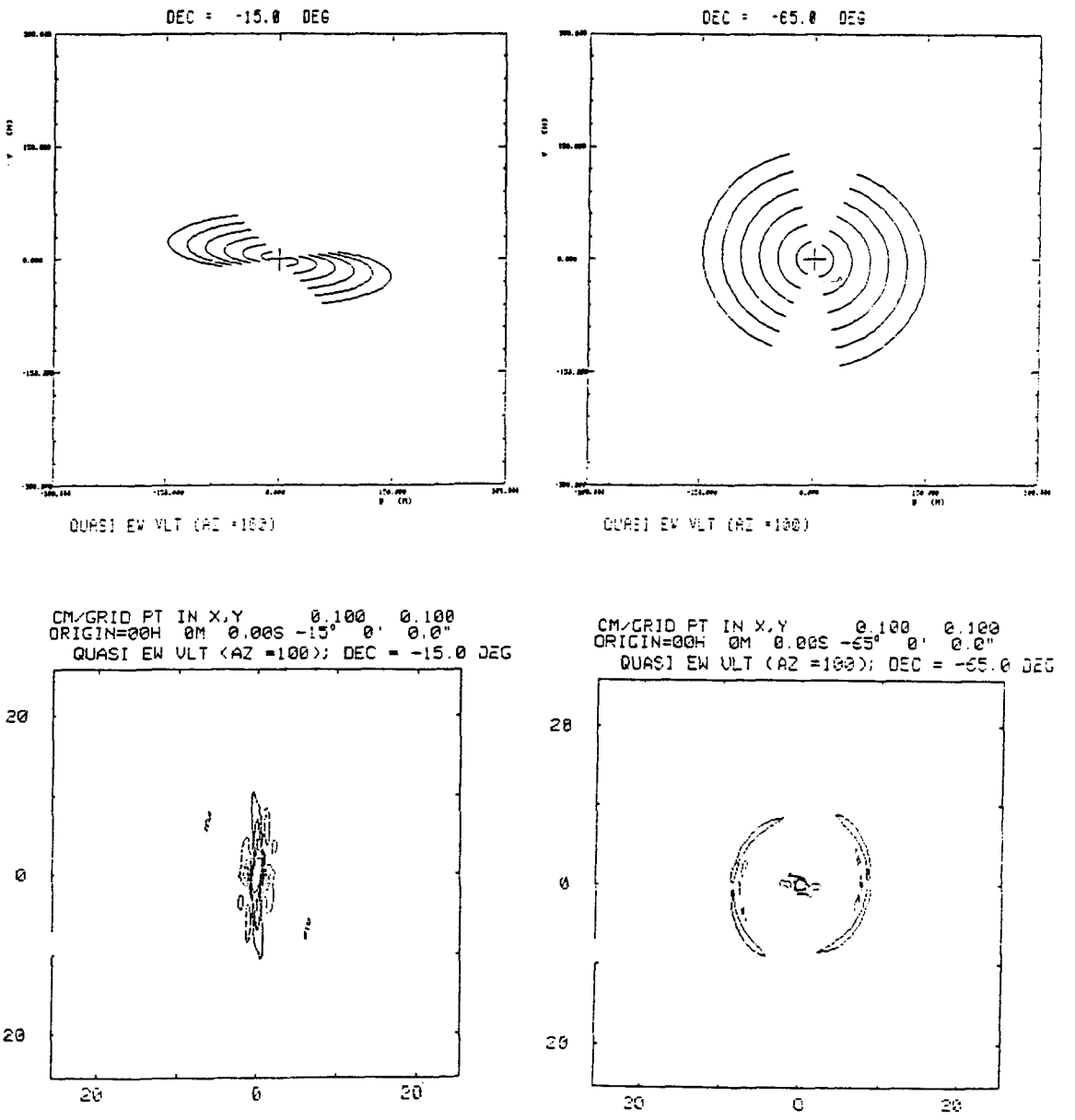

Figure A2.2b

QEW+NS - Frequency coverage and Point Spread Function

(δ = -15° and -65°)

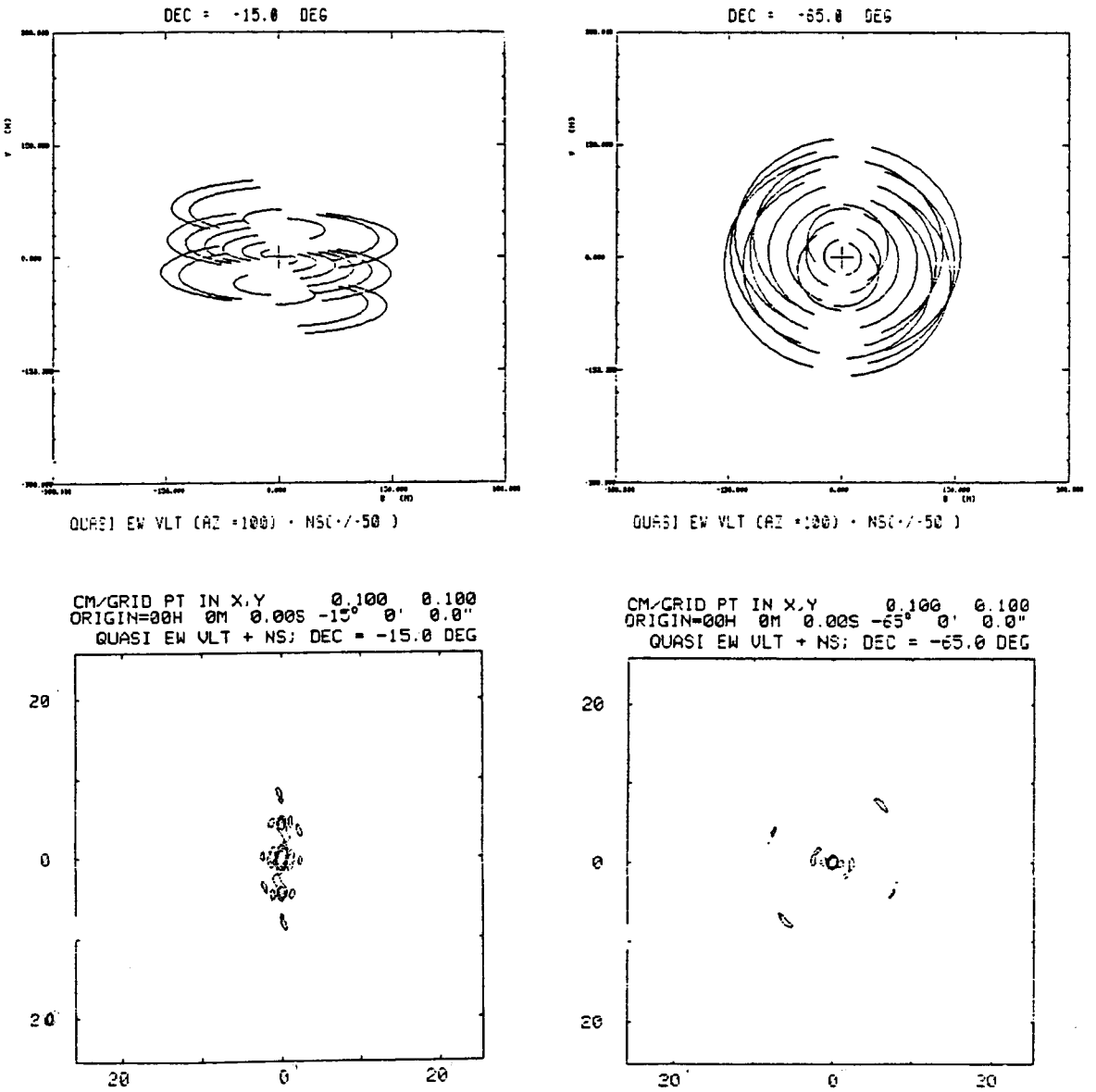

MILLI ARC SEC AT λ = 1 μm

Figure A2.2c

Compact continuously filled - Frequency coverage and Point Spread Function

($\delta = -15^{\circ}$ and -65°)

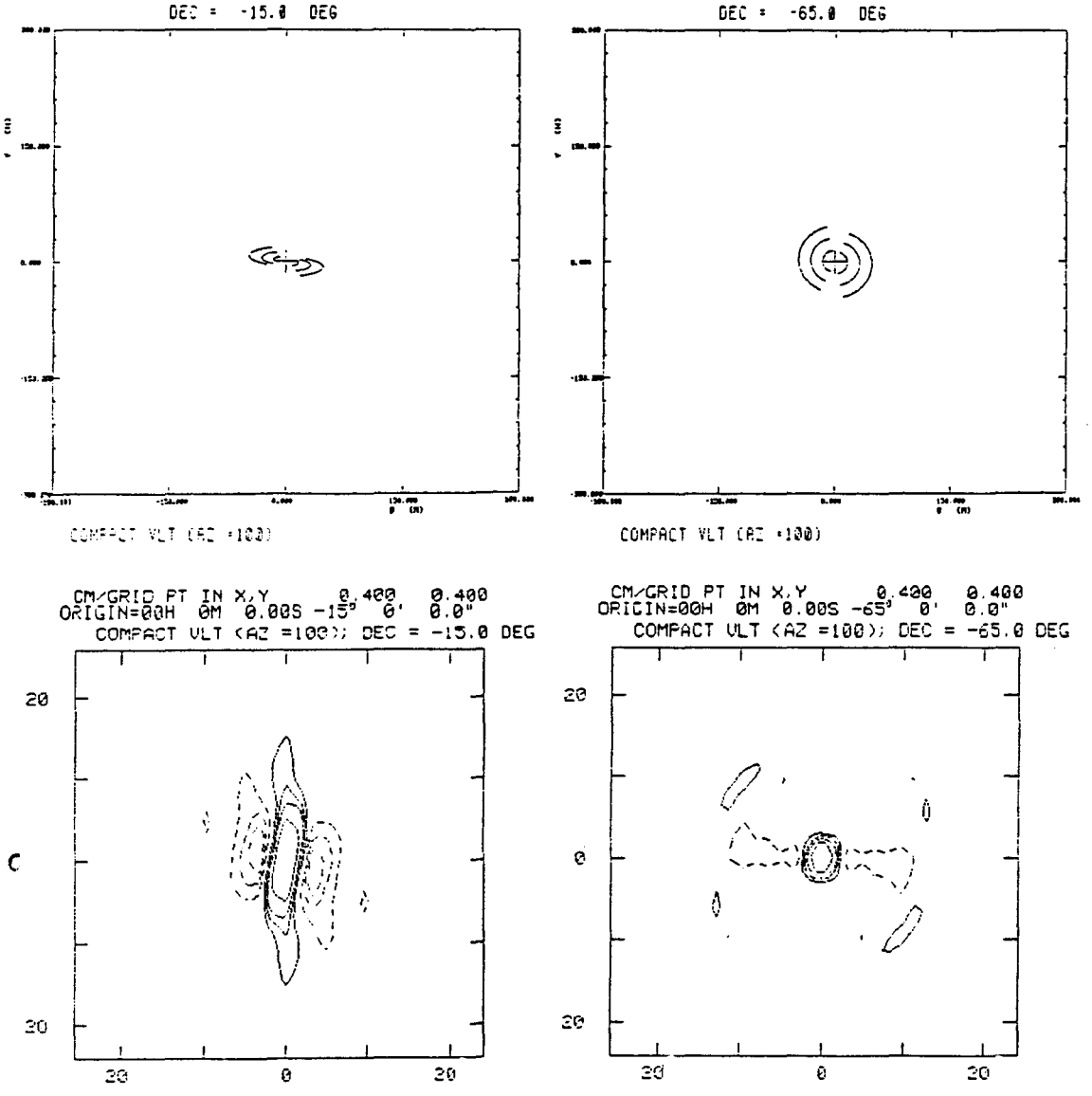

Figure A2.2d

Fixed Y - Frequency coverage and Point Spread Function

(δ = -15° and -65°)

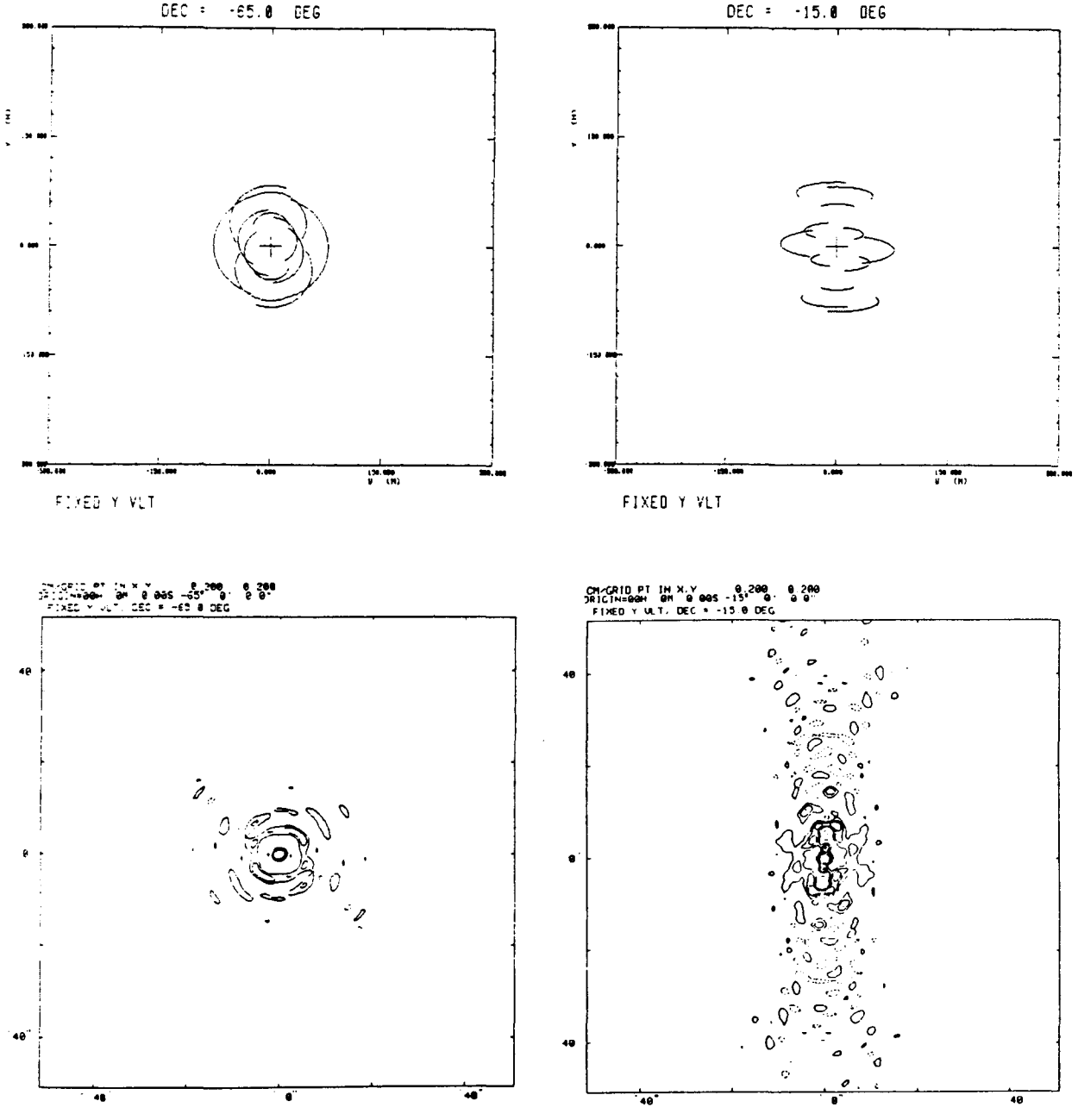

MILLI ARC SEC AT λ = 1 μm

Figure A2.2e

VARY - Frequency coverage and Point Spread Function

(δ = -15° and -65°)

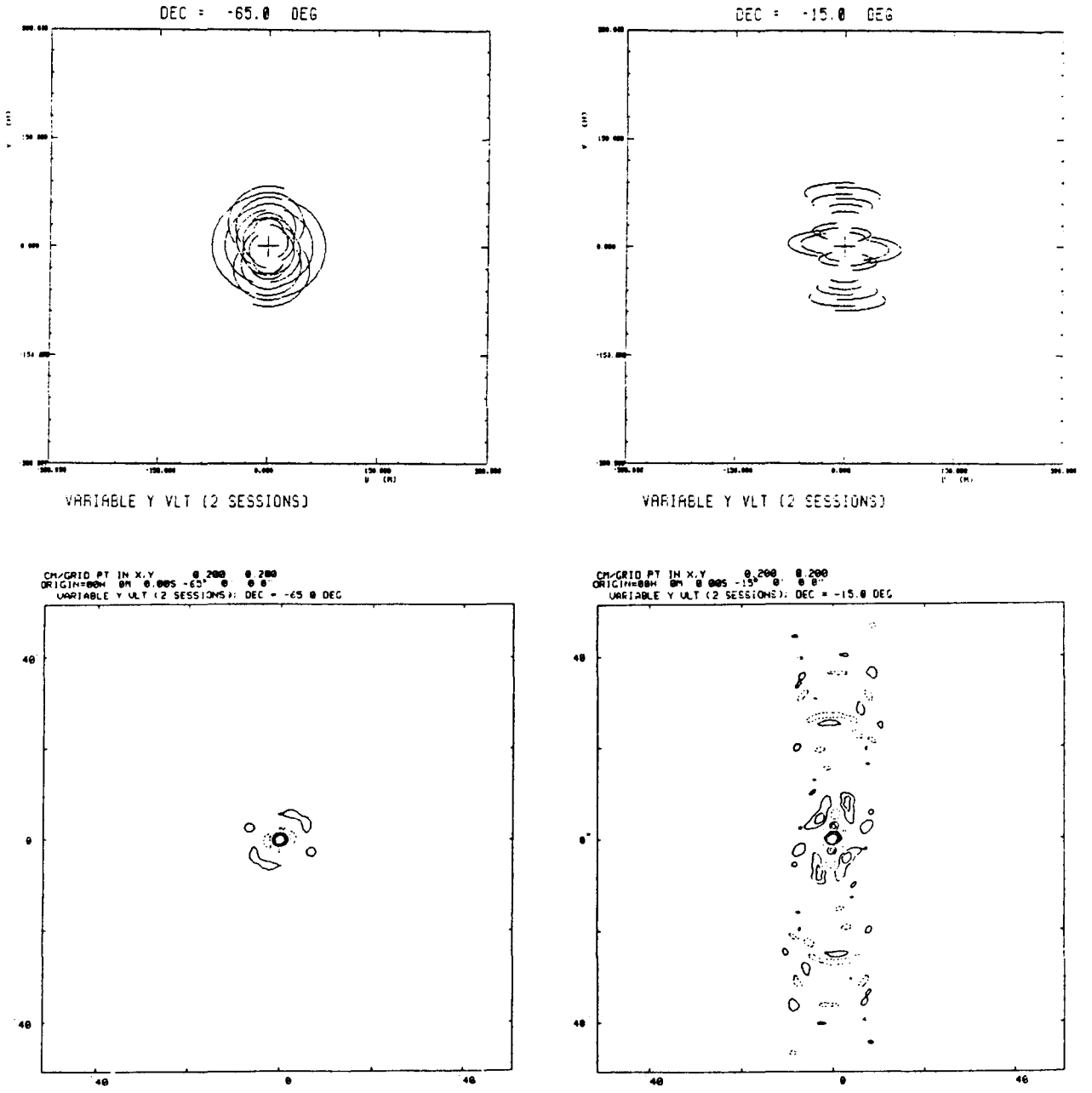

MILLI ARC SEC AT λ = 1 μM

MODEL 1

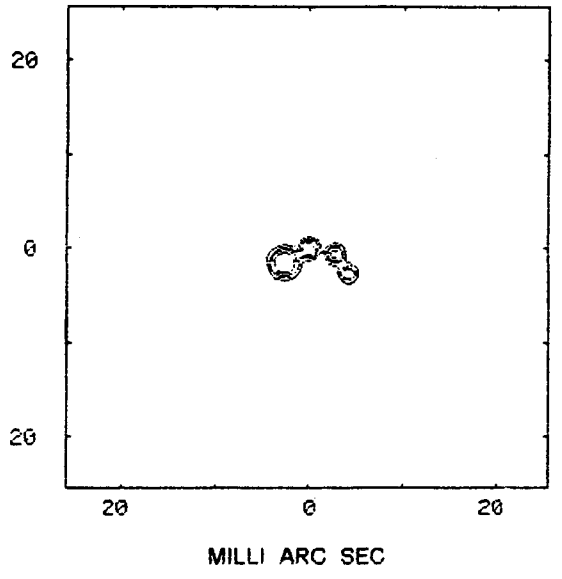

Figure A2.3 *: The model source used for image simulation.*

MODEL 1 was used in cases a), b), d), e), while MODEL 2 was used in the less resolving case c).

Source sizes are in milliarcsec for λ = 1 μm operation of the interferometer. Intensity levels are over a dynamic range of 10. (0.1, 0.2, 0.3, 0.5 and 1.0).

MODEL 2

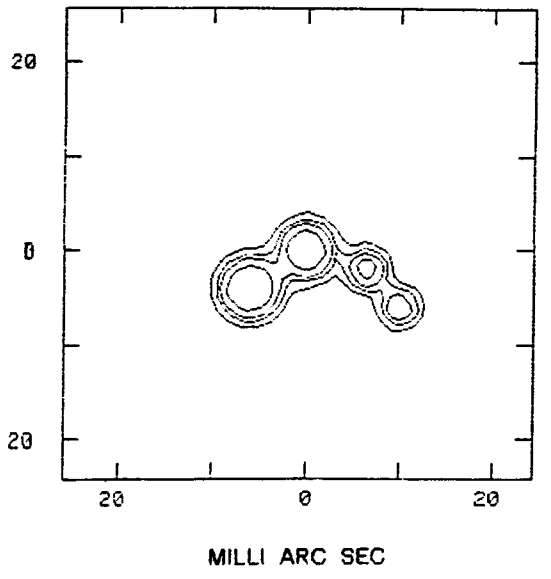

FIGURE A2-4 (a to e)

Raw maps of the sources of Fig. 3 seen with the five interferometers (a to e) and for two declinations (−15 and −65 deg). The upper frames have no random phase errors, the lower frames have 60 deg rms phase errors. The contours are the same as in Fig. 2. Axes labelling is identical to the source maps of Fig. 3. Observations are assumed at λ = 1 μm. At longer wavelengths, PSF will degrade accordingly.

Figure A2.4a

QEW - Image Restoration of the model source (Raw maps)

Upper : 0° phase error - Lower : 60° rms phase error.

(δ = −15° and −65°)

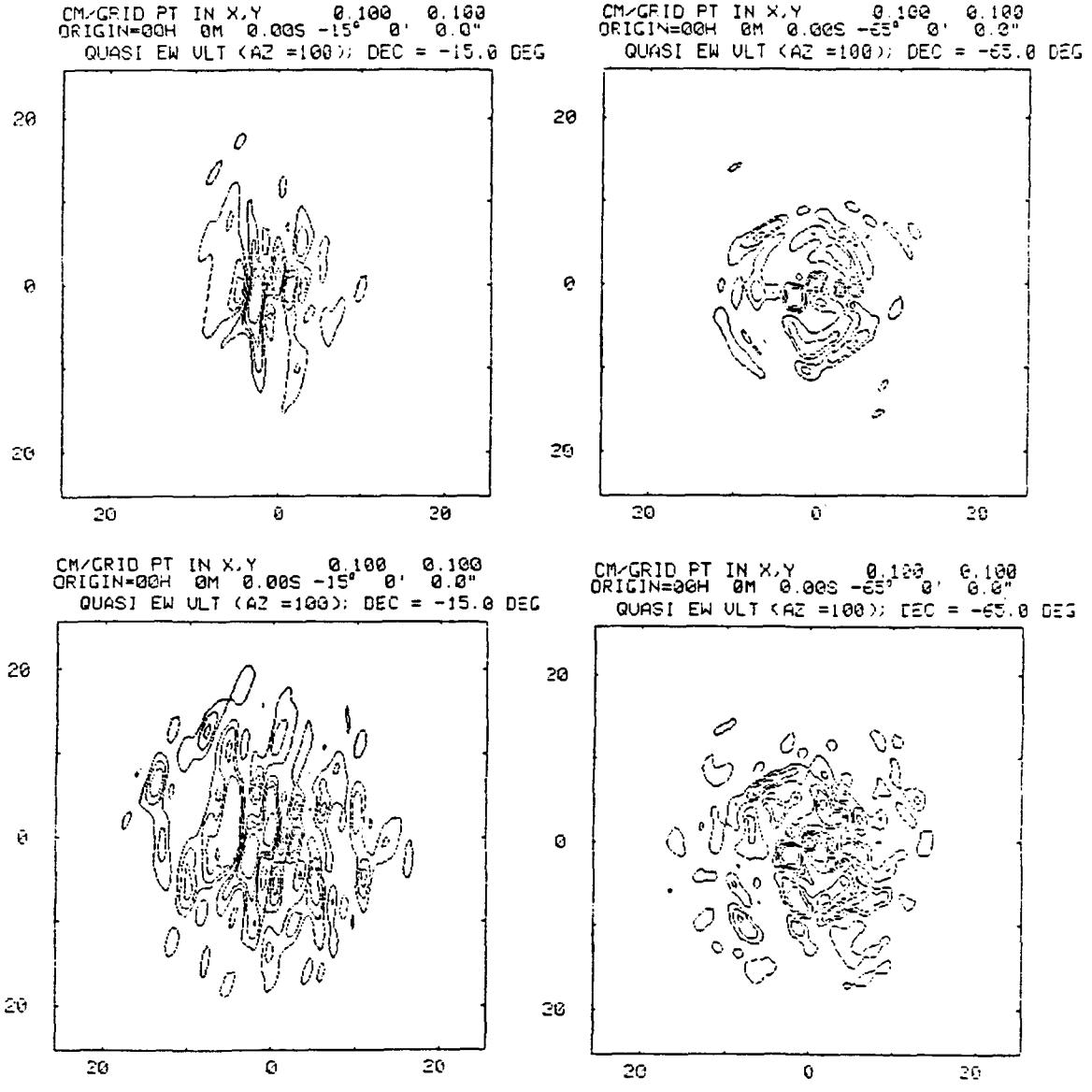

Figure A2.4b

QEW+NS - Image Restoration of the model source (Raw maps)

Upper : 0° phase error - Lower : 60° phase error.

(δ = -15° and -65°)

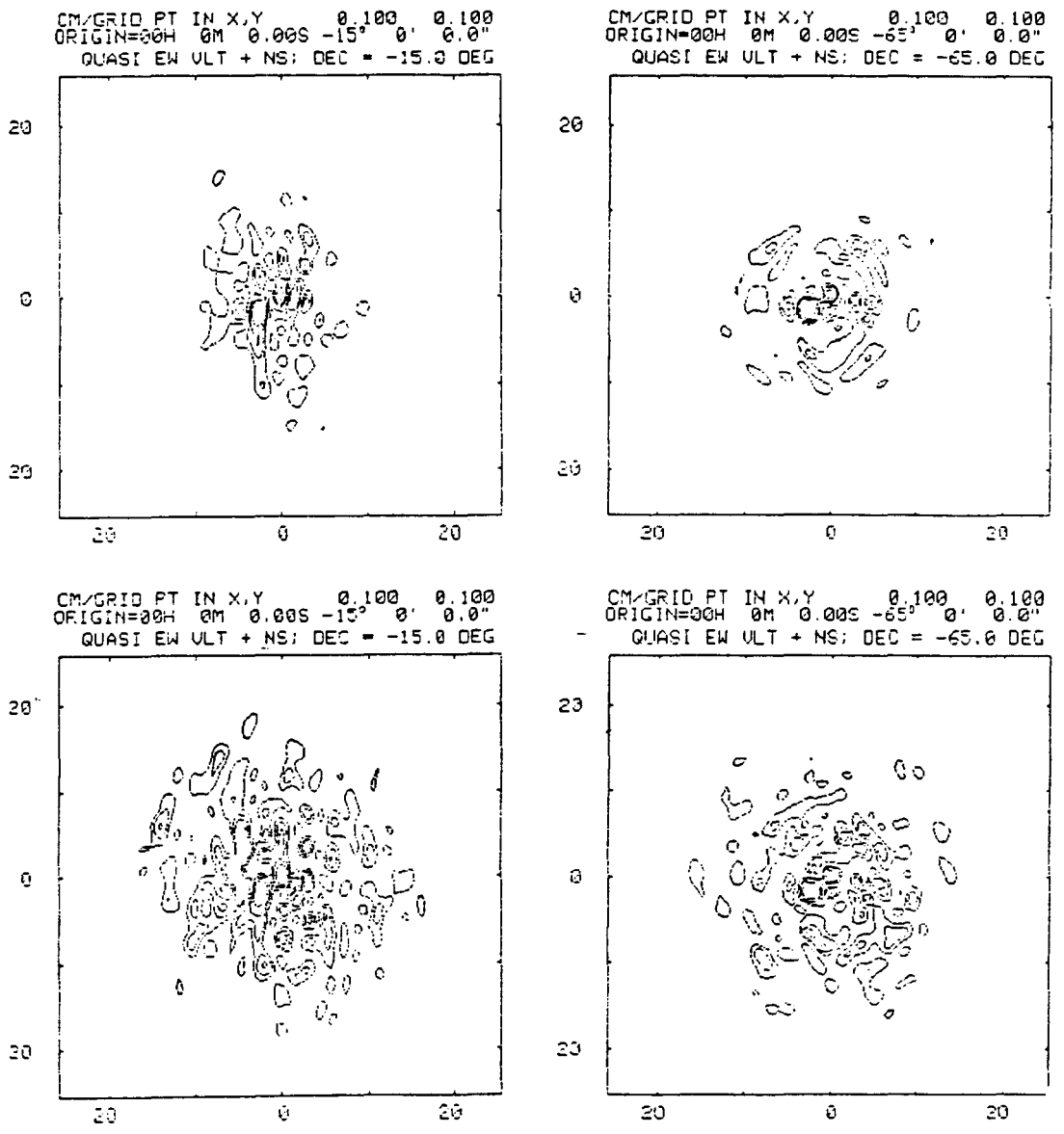

Figure A2.4c

Compact - Image restoration of the model source (Raw maps)

Upper : 0° phase error - Lower : 60°rms phase error

(δ = −15° and −65°)

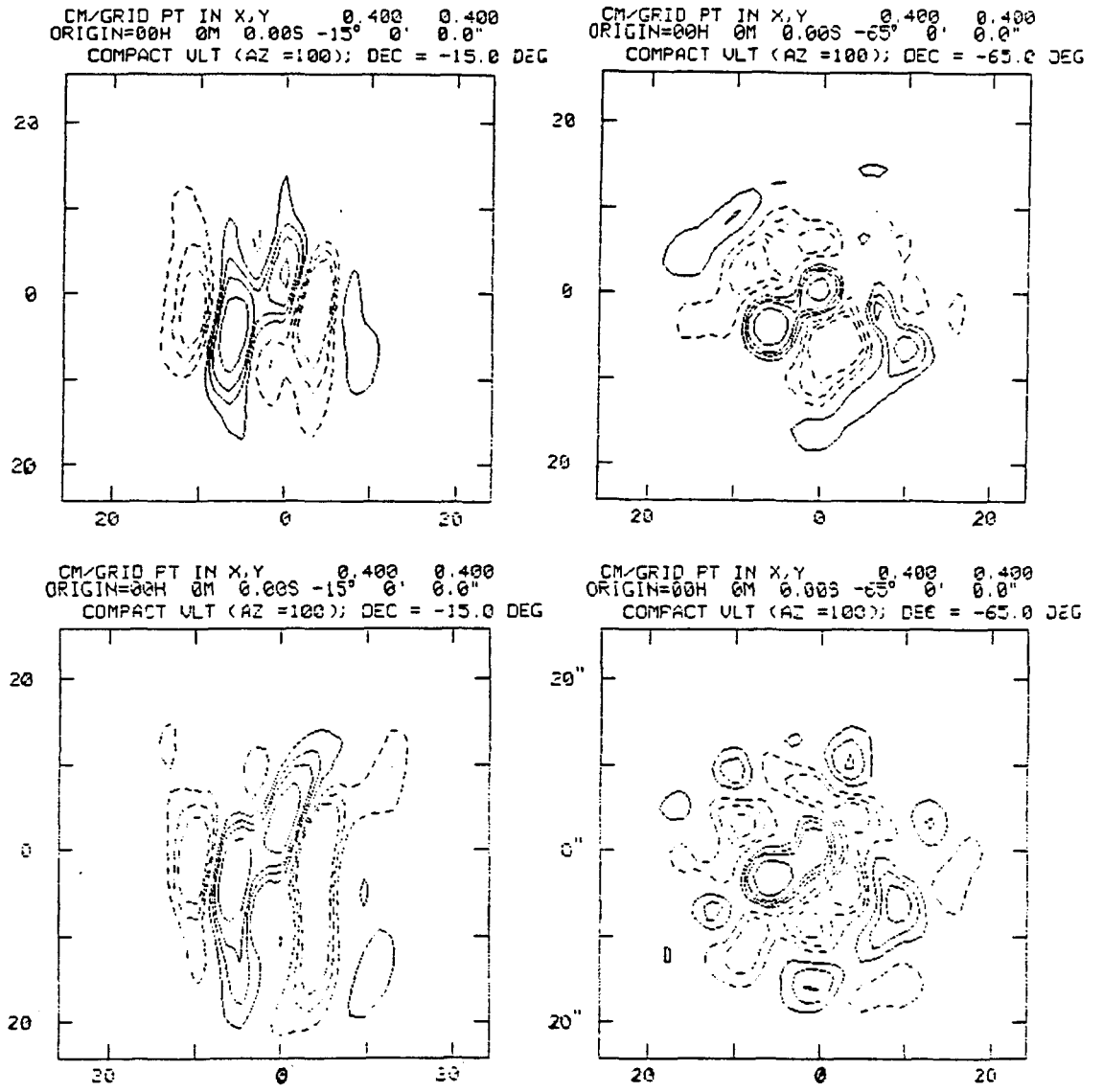

Figure A2.4d

Fixed Y - Image restoration of the model source (Raw maps)

Upper : 0° phase error - Lower : 60°rms phase error

(δ = −15° and −60°)

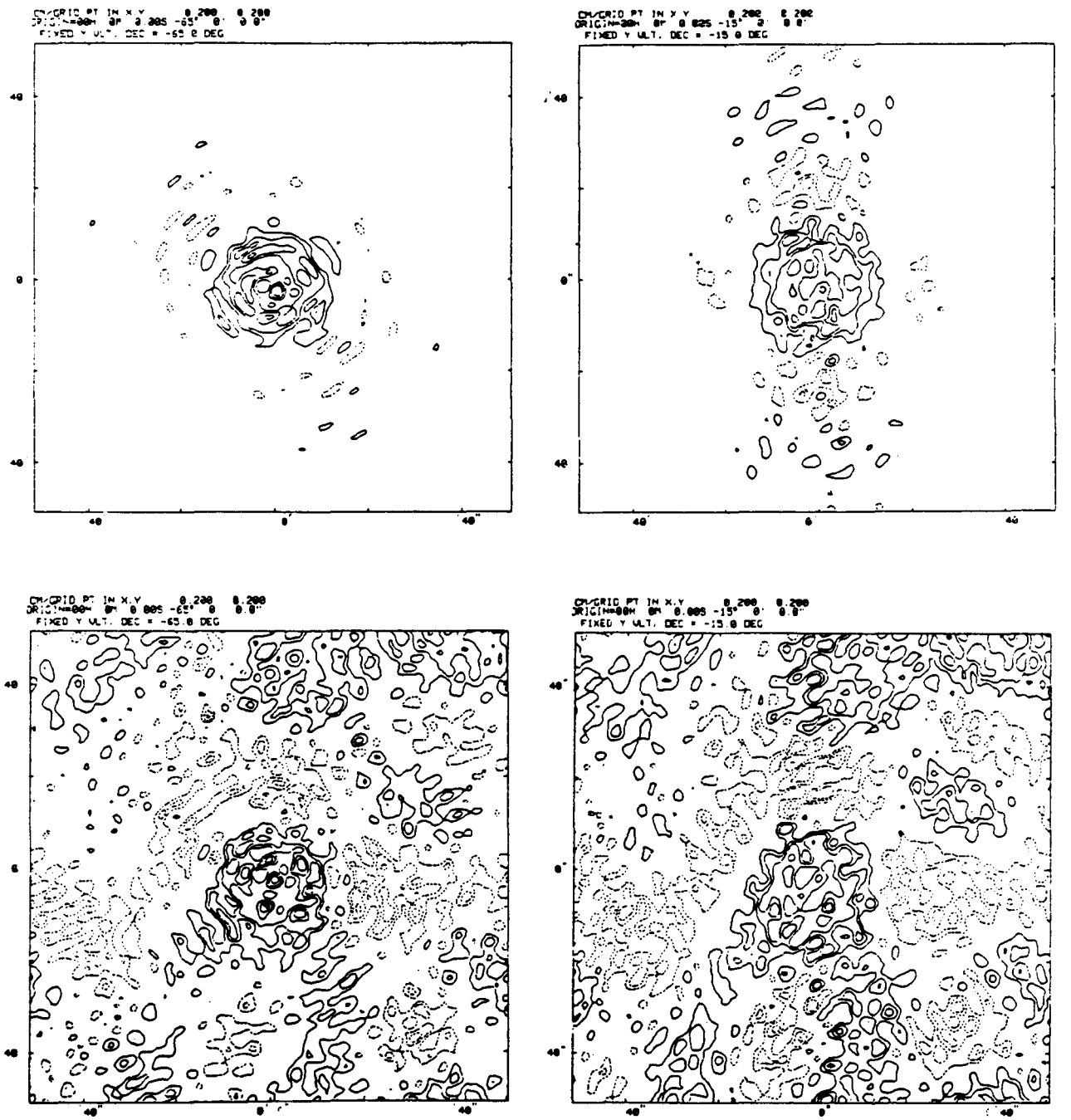

MILLI ARC SEC

Figure A2.4e

VARY - Image restoration of the model source (Raw maps)

Upper : 0° phase error - Lower : 60°rms phase error

(δ = −15° and −60°)

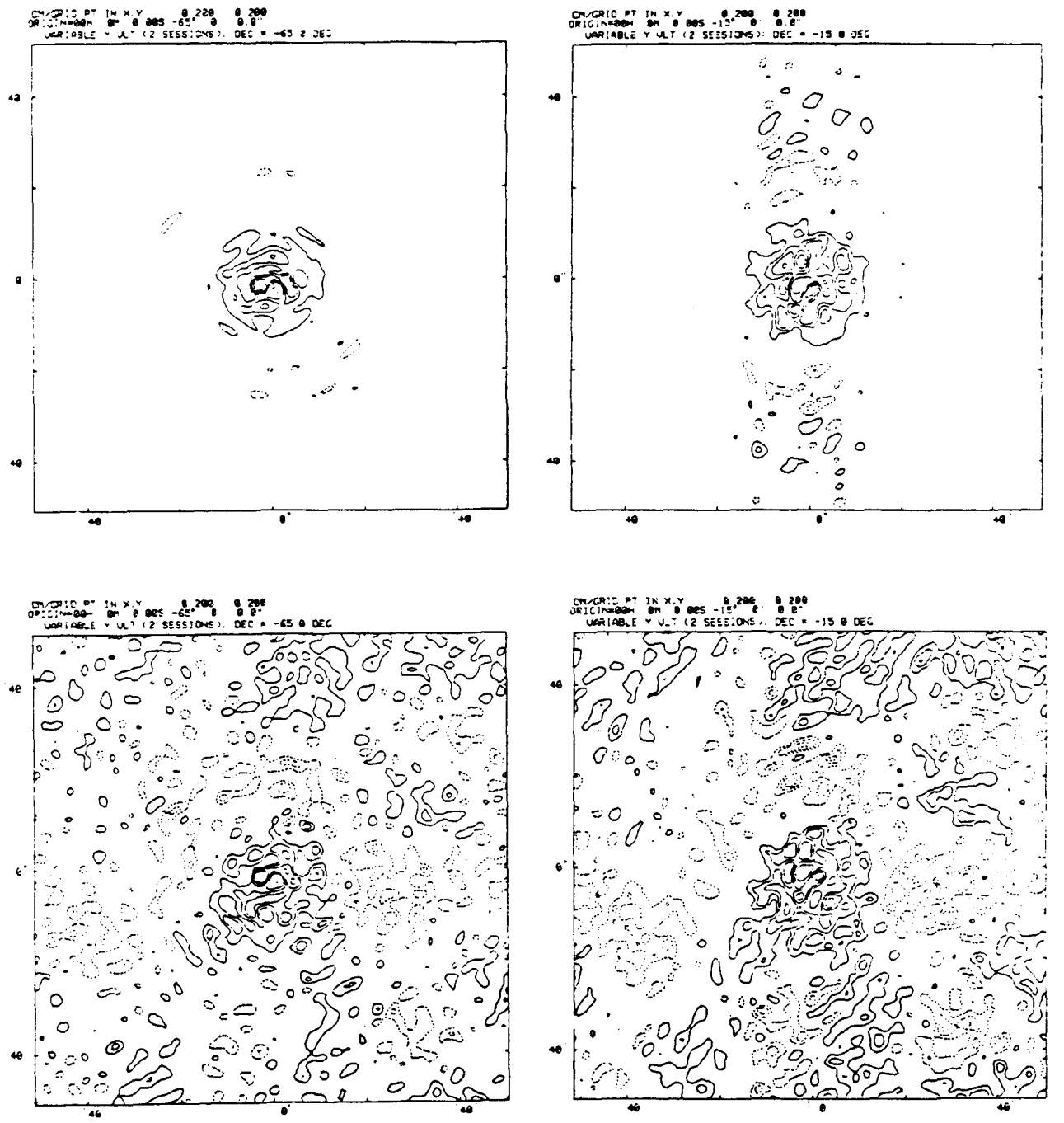

FIGURE A2.5 (a to e)

Restorations of the source observations by means of the CLEAN algorithm for the five interferometers (a to e) and the two declinations studied. The ordering of frames is identical to Fig. 4. The contours are the same as in Fig. 3. Axes labelling is identical to the source maps of Fig. 3. Observations are assumed at λ = 1 μm. At longer wavelengths, PSF will degrade accordingly.

Figure A2.5a

QEW - Image Restoration of the model source (cleaned map)

Upper : 0° phase error - Lower : 60° rms phase error

(δ = −15° and −60°)

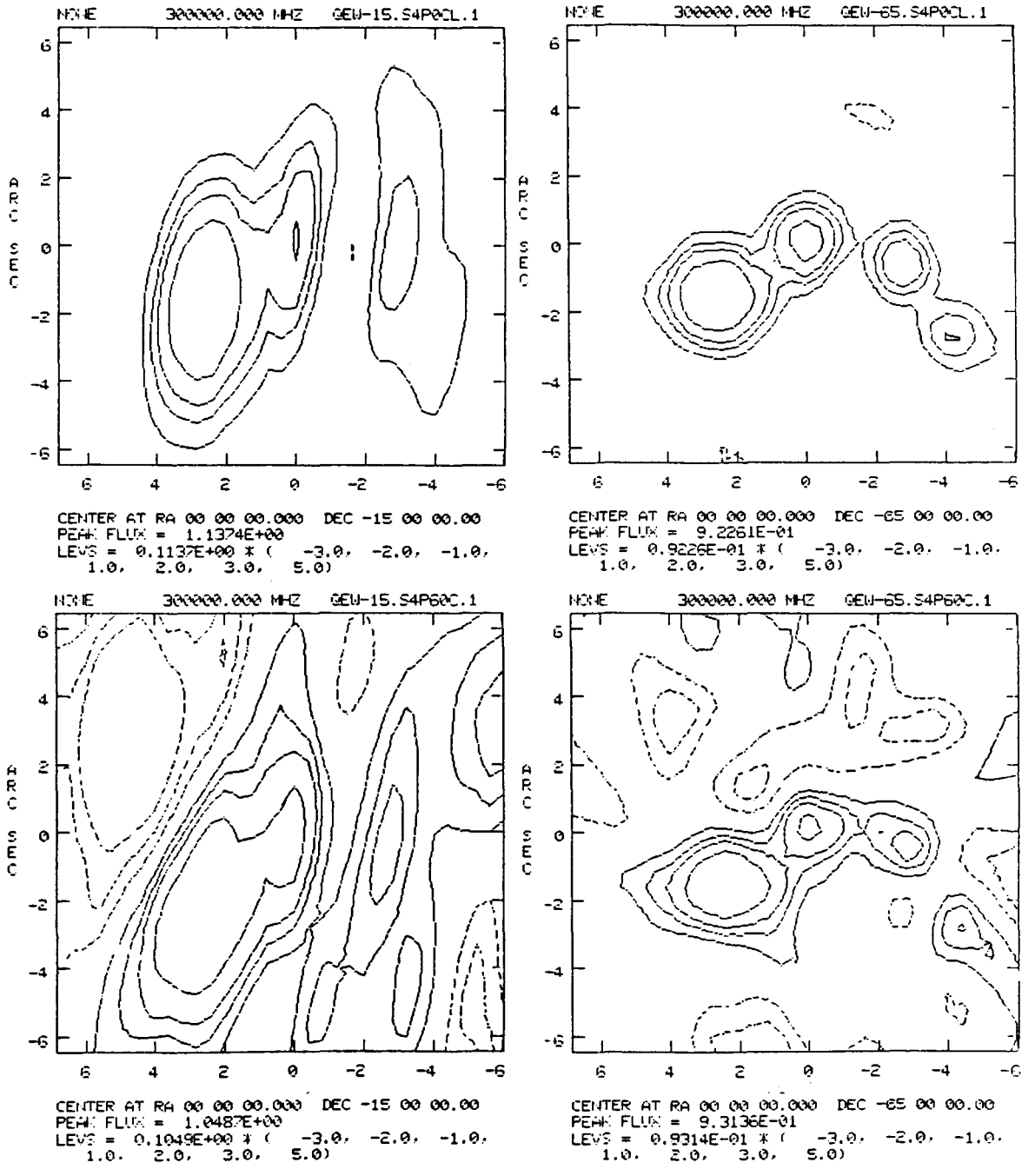

Figure A2.5b

QEW+NS - Image Restoration of the model source (cleaned map)

Upper : 0° phase error - Lower : 60° rms phase error

(δ = −15° and −65°)

0°

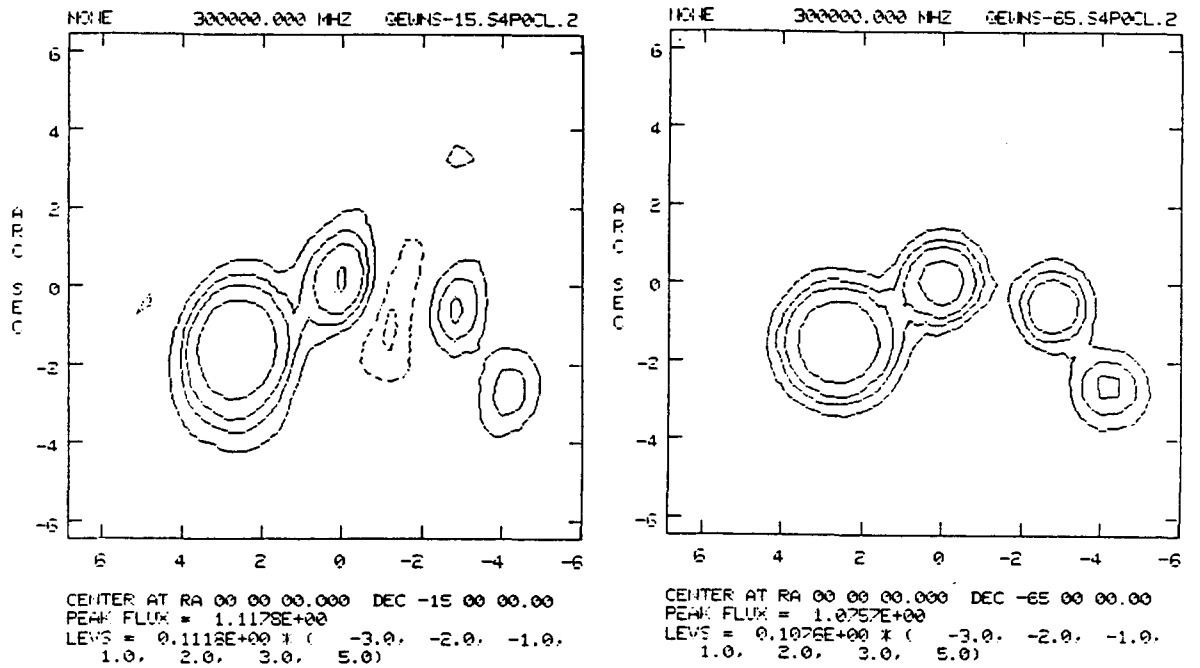

60°

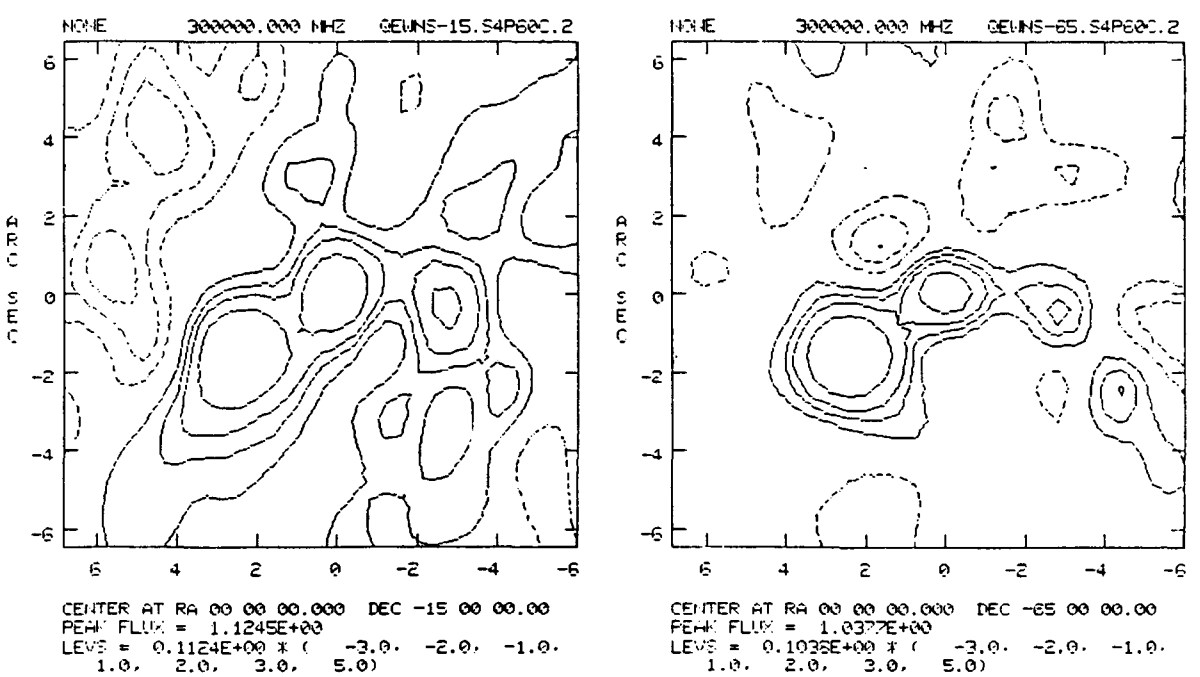

Figure A2.5c

Compact - Image Restoration of the model source (cleaned maps)

Upper : 0° phase error - Lower : 60° rms phase error

(δ = −15° and −60°)

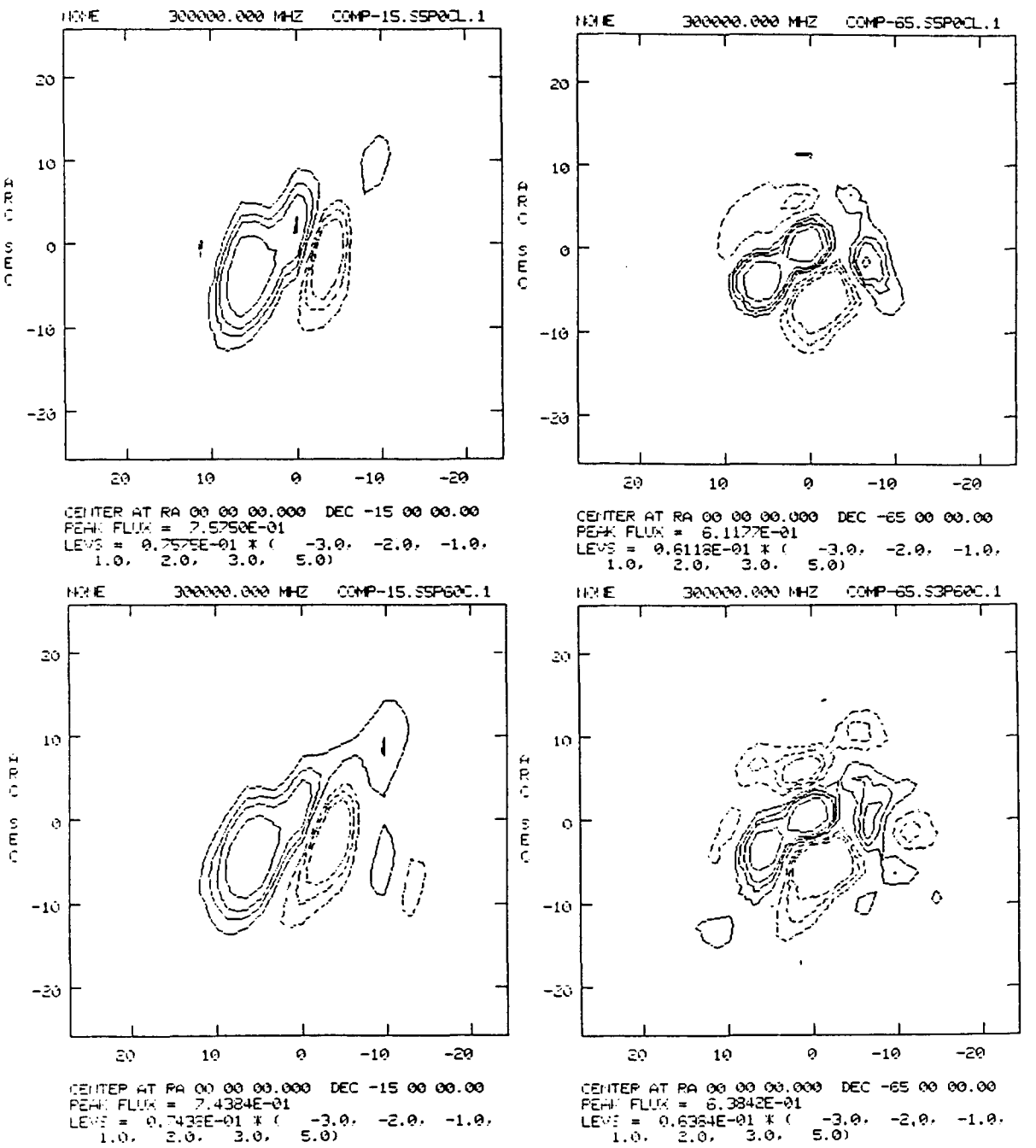

Figure A2.6d

FIXED Y - Image Restoration of the model source (cleaned maps)

Upper : 0° phase error - Lower : 60° rms phase error

(δ = −15° and −60°)

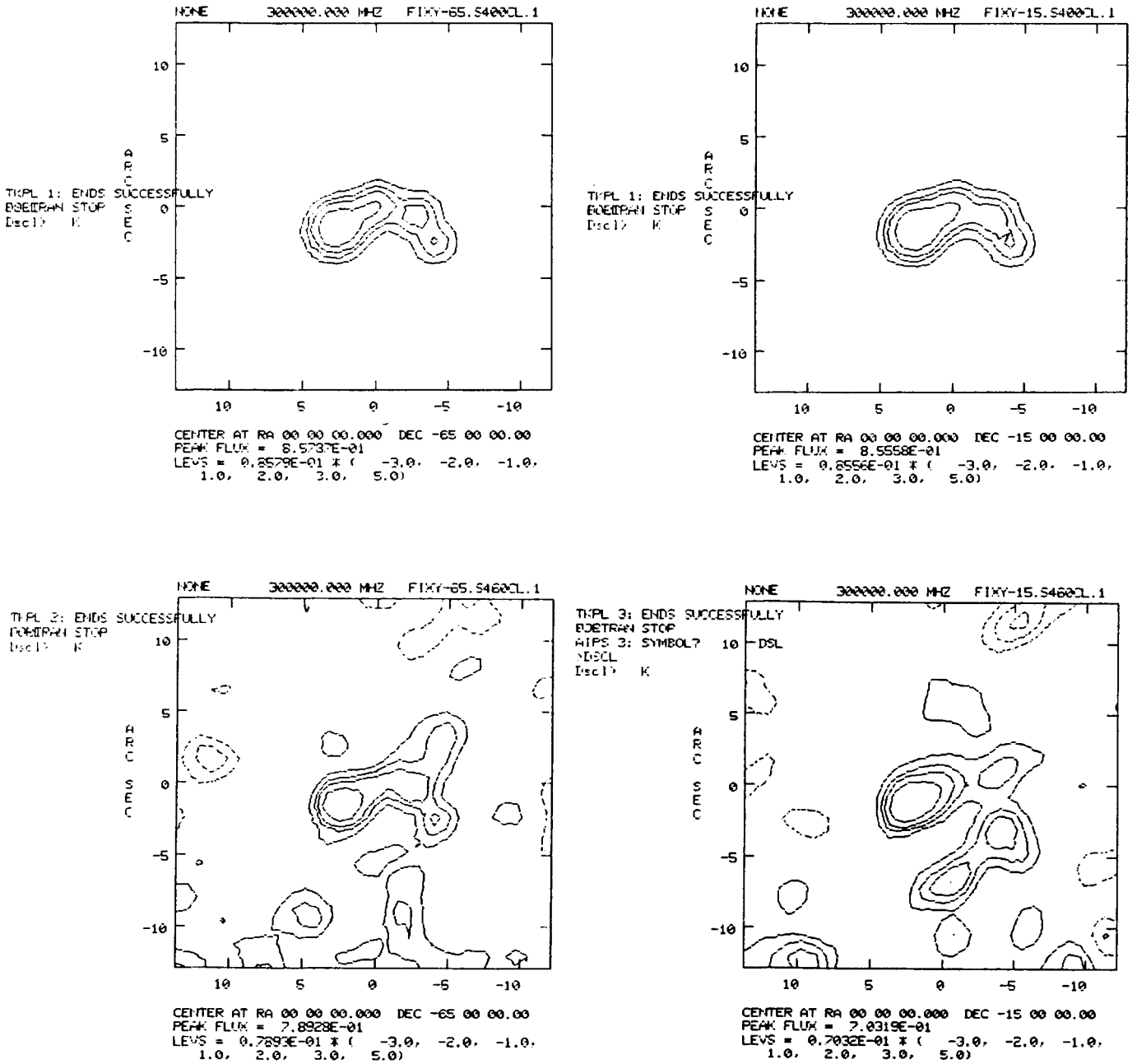

Figure A2.6e

VARY - Image Restoration of the model source (cleaned maps)

Upper : 0° phase error - Lower : 60° rms phase error

(δ = −15° and −60°)

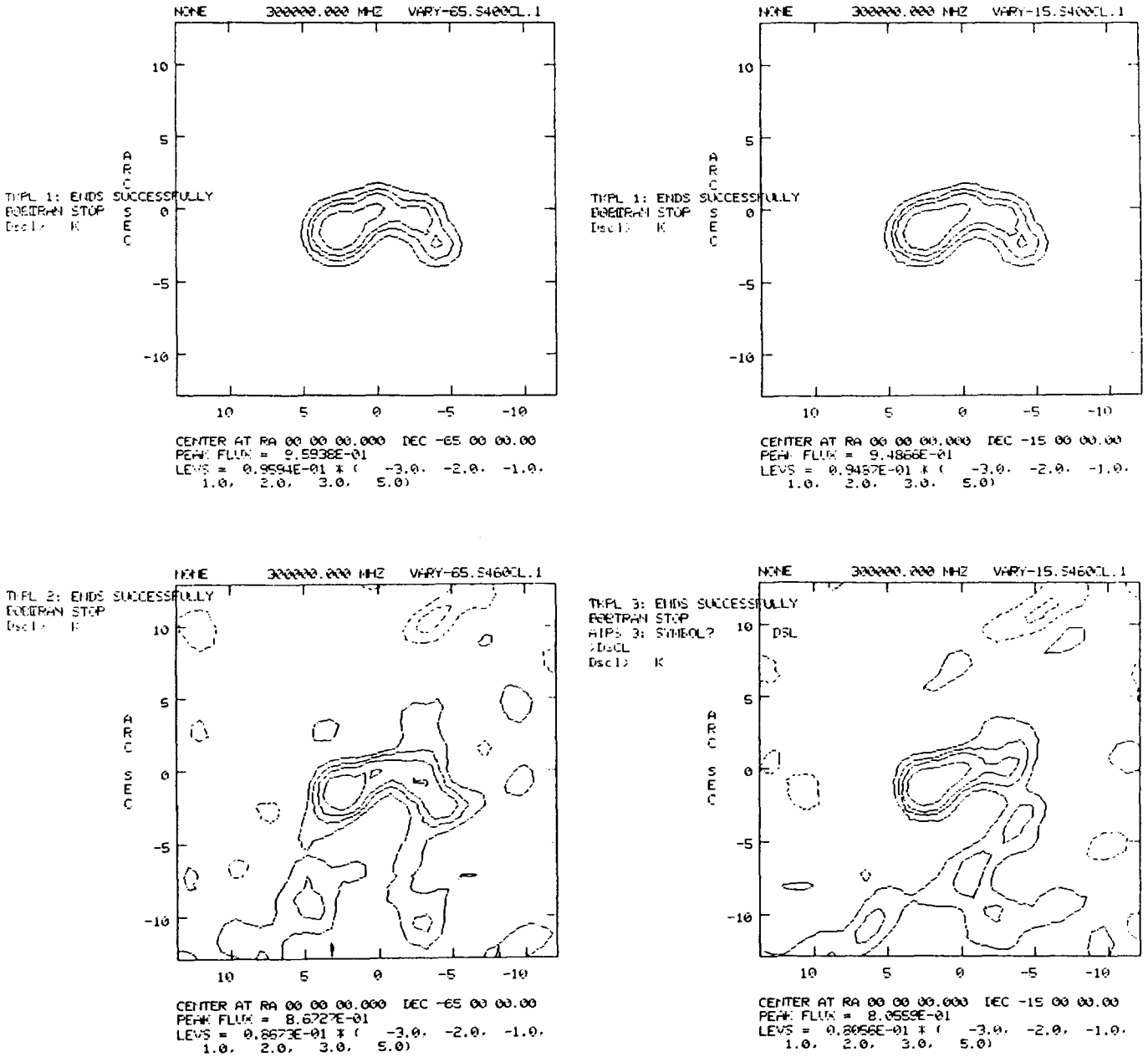

Appendix A3 - SENSITIVITY AT INFRARED WAVELENGTHS

This Appendix presents Signal-to-noise derivation for two beam interferometry as a function of wavelength, telescope size and atmospheric condition.

A3.1. *Introduction*

Beside the quality of the detectors, the beam etendue, the special bandwidth necessary to guarantee coherence of the wavefront over the telescope diameter or separation, the life time during which the atmosphere is frozen i.e. during which we can consider the interference to remain stable, the number of speckles all together determine an ultimate sensitivity, which is strongly wavelength-dependent. At the shortest wavelengths detector noise dominates, while background photon noise from thermal atmospheric emission takes over as wavelength increases.

We discuss here in some detail the effect of these parameters. Basic formulae are taken from a survey paper of Roddier and Léna 1984, which analyses the most critical aspects.

A3.2 *Basic aspects*

We consider here a two beam interferometer (the case of simultaneous interference of more than two telescopes does not modify the general approach). The beams from the two telescopes pointing the same object are recombined, giving an interference pattern. Its visibility is measured in amplitude, and possibly in phase, for later image reconstruction. We shall limit the discussion to amplitude measurements. This visibility measurement is dramatically dependent on the atmosphere which disturbs the wavefronts. As a result the recombined aperture image shows a large number of random positioned fringe fields, varying in time. The seeing cell size can be described with the Fried parameter $r_0(\lambda)$, depending on wavelength. An interference pattern in the recombined pupil shows a number of flat fields, of a size $r_0(\lambda)$,

each one with its own interference phase, all varying continuously with time in position and phase. In the visible $r_0(v) = 0.1$ m corresponds to a seeing of 1".

Interference of two wavefronts spatially separated requires temporal coherence, i.e. limited spectral bandwidth, which depends on their separation. The maximum acceptable bandwidth is of $\delta\sigma_L$ cm^{-1} for a separation of L m. If the object (or a nearby reference source) is bright enough to track the atmospheric phase fluctuation over L, the width can be enlarged to a value $\delta\sigma_D$ depending only on telescope diameter D. Finally, if adaptive optics is used, the width is only limited by the atmospheric windows and becomes independent of D.

The interference pattern can be considered as stable during the life time of a speckle. Its value is related to the wind velocity dispersion for which we assume an average value of 5 m/s.

These various factors can be formulated as follows using the Fried parameter in the visible $r_0(v)$ (in m), the telescope diameter D (in m) and the wavenumber σ (in cm^{-1}) as independent parameter :

$$r_0(\sigma) = 1.45\ 10^5\ r_0(v)\ \sigma^{-6/5}$$

$$N_s(\sigma) = 1.10\ 10^{-10} \left[\frac{D}{r_0(v)}\right]^2 \sigma^{12/5}$$

$$\delta\sigma_D = 1.04\ 10^4 \left[\frac{r_0(v)}{D}\right]^{5/6} \quad \text{and}$$

$$\delta\sigma_L = 1.04\ 10^4 \left[\frac{r_0(v)}{L}\right]^{5/6} \quad \text{if } L \leq L_o, \text{ outer scale of turbulence}$$

$$\tau = 0.36\ \frac{r_o(\sigma)}{\delta v} = 1.04\ 10^4 r_o(v)\ \sigma^{-6/5} \quad \text{for } \delta v = 5 \text{ m/sec}$$

To calculate the sensitivity, we make the following assumptions :
- observation of a single object in the field, of intensity F_0 (W/m^2-cm^{-1} or Jy), either unresolved (V=1) or partially resolved (V < 1).
- limited beam etendue and possible use of array detectors (N pixels), each one being diffraction-limited (throughput λ^2). The total etendue is therefore $A\Omega = N_S\lambda^2$, with N_S the number of speckles, calculated for a seeing of 1".

Arrays format N is fixed for a particular bandpass to $N \geq N_S$, i.e. N is wavelength dependent. Such considerations do not apply for $\delta\sigma$ or τ, as both can be varied depending on L or $r_o(v)$.

With these assumptions :

$A\Omega = 4.40\ 10^{-12}\ D^2\ \sigma^{2/5}\ m^2sr.$

$\Omega = 5.60\ 10^{-12}\ \sigma^{2/5}\ sr.$

sized to the wavelength of operation by a FOV stop or by omitting "not used" pixels. The final value of the signal-to-noise ratio in a visibility measurement depends on the photometric $(S/N)_{ph}$ and the contrast $(S/N)_C$ of the interference pattern.

$$(S/N) = (S/N)_{ph} \times (S/N)_C$$

The value of $(S/N)_{ph}$ depends on the intrinsic detector noise and of the background noise. The value $(S/N)_C$ depends on the detection technique :

i) if the image is quasi-diffraction limited (long wavelengths or adaptive optics), one single interference pattern is present over the pupil and $(S/N)_C = 1$. The bandwidth is $\delta\sigma_D$ (or even $\delta\sigma_p$).

ii) if the image contains N_S speckles, an array with N_S pixels is required. For objects bright enough to give a signal-to-noise larger than unity over a single exposure, over each pixel, the array signals can be added up coherently (in phase), while the noise adds up incoherently. This gives $(S/N)_C = N_S/\sqrt{N}$. The band with $\delta\sigma_D$ is applicable and integration over long time becomes possible, not increasing the limiting flux, but increasing the accuracy of the estimate of the visibility V.

Finally, for very weak objects, the array signals can only be added up incoherently, just like the noise of the pixels... Therefore $(S/N)_C = \sqrt{N_S/N}$, whereas a filter of bandwidth $\delta\sigma_L$ must be used.

A3.3. *The detailed Signal-to-Noise estimates*

The whole discussion presented here covers the various observing configuration, depending on the detector format (single pixel or array), on the thermal background and on the possibility of time integration.

In what follows, the following assumptions are made :

t = 1 Transmission of the optical system

η = 1 Quantum efficiency of detector

ϵ = 1 Emissivity of the atmosphere

r = 1 Geometrical coverage of the pixels in the arrays.

The first two factors interact with the S/N as $(t\eta)$ or $(t\eta)^{1/2}$ in the detector noise (3.3.1) and background noise (3.3.2) regions respectively.
The third factor varies with wavelength and is connected to the temperature of the atmosphere which is arbitrarily chosen as 280 K. Hence a worst case has been selected here.

3.3.1. S/N with noise limitation from the thermal background

As the thermal background increases with wavelength the inherent photon noise E_{ph} determined by the mean square deviation in the rate of arrival of the photons at the detector may exceed the intrinsic detector or amplifier noise E_n. We derive :

$$E_{ph} = hc\sigma \sqrt{N_{ph}^2} \approx hc\sigma \sqrt{N_{ph}} \quad WHz^{-0.5}$$

with N_{ph} the number of arriving photons, h = 6.62 10^{-34} J-s and c = 3 10^{10} cm s^{-1}.
Because $N_{ph} hc\, \sigma = E_a\, A\, \Omega\, \delta\sigma\, \tau$ we find :

$$E_{ph} = \sqrt{E_a\, A\, \Omega\, \delta\sigma\, \tau\, hc\, \sigma} \quad E_a \text{ in } W/m^2 srcm^{-1}$$

and with a signal $F_o\, A\, \delta\sigma\, \tau$ we obtain :

$$(S/N)_{ph} = \frac{F_o}{\sqrt{E_a}} \sqrt{\frac{A\, \delta\sigma\, \tau}{\Omega\, hc\sigma}}$$

In all cases we assume that E_a in $W/m^2 srcm^{-1}$ is generated by a blackbody of 280 K, which is certainly a worst case.

If we adopt an array read-out noise of 500 e^-rms, a value quite conservative for array performances, we find thermal noise to be dominant at $\lambda \geq 5\ \mu m$.

a) Diffraction-limited image (adaptive optics)

In this case $(S/N)_c = 1$ and for an exposure time T and visibility V = 1,

$$(S/N) = (S/N)_{ph} = \frac{F_o}{\sqrt{E_a}} \sqrt{\frac{A\delta\sigma}{\Omega\, hc\sigma}} \sqrt{T}$$

$A\Omega = \lambda^2$, $\delta\sigma = \delta\sigma_D$

$$(S/N) = \frac{F_o}{\sqrt{E_a}}\ 1.83\ 10^{+17}\ D^{19/12}\ r_{o_v}^{17/12}\ \sigma^{-1/10}\ \sqrt{T}\ \ F_o\left[W/m^2 cm^{-1}\right]$$

The result is strongly diameter dependent and seeing dependent.
With D = 8 m, $r_o(v) = 0.1$ m, T = 1 s, we calculate for (S/N) = 1

λ	$E_a^{280}(W/m^2 srcm^{-1})$	$F_o(Jy)$
3.5	$1.17\ 10^{-4}$	$4.22\ 10^{-4}$
5	$3.26\ 10^{-3}$	$2.15\ 10^{-3}$
10	$7.02\ 10^{-2}$	$9.31\ 10^{-3}$
20	$1.24\ 10^{-1}$	$1.15\ 10^{-2}$

For sources brighter than F_o, the atmospheric phase excursion can be tracked and long exposures times can be adopted, improving (S/N) on the visibility.

For these results to be valid, we must assume that the adaptive optics does not introduce phase noise on the visibility, a point which remains to be studied in detail.

The effect of adaptive optics on background thermal noise has been studied by Roddier (1986), and its effect has been shown to exist but to be acceptable and not to modify the above values of E_n.

b) Array of detectors, coherent addition of signals

We assume the flux to be distributed over $N \geq N_S$ pixels. For a detection during the exposure time τ, the object must be

$$N_S \left[\frac{T}{\tau}\right]^{1/2}$$

brighter than in the case a) above.

$$N_S \left[\frac{T}{\tau}\right]^{1/2} = 1.08\ 10^{-12}\ D^2\ r_o(v)^{-5/2}\ \sigma^3\ T^{1/2}$$

For D = 8 m, $r_o(v)$ = 0.1 m, T = 1 s this factor is:

λ	N_S	$N_S \tau^{-1/2}$
3.5	137	510
5	58	175
10	11	21.8
20	2	2.7

This limiting brightness, which allows coherent addition of pixels, depends therefore as $D^{-19/12}\ D^2$, i.e. $D^{5/12}$. A gain in diameter gives a degradation of limiting brightness, but a gain in visibility accuracy.

The signal-to-noise ratio, after coherent addition, is :

$$(S/N) = (S/N)_{ph}\ (S/N)_C = (S/N)_{ph}\ N_S/\sqrt{N}$$

and becomes $\sqrt{N_S}$ times the (S/N) per pixel if one takes $N \sim N_S$.

c) Array of detectors, incoherent addition of signals

In this case, signals as well as noise from individual pixels will add up incoherently and $(S/N)_C = \sqrt{N_S/N}$. The instantaneous (τ) (S/N) is given by

$$(S/N) = \frac{F_o}{\sqrt{E_a}}\ \frac{A\ \delta\ \sigma\ \tau}{N_S\ \sqrt{A\Omega\ hc\ \sigma\ \delta\ \sigma\ \tau}}\ \sqrt{\frac{N_S}{N}}$$

The bandwidth $\delta\sigma_L$ must be selected, since the phases can not be determined. $A\Omega = \lambda^2$ is still valid for each pixel. Taking $N = N_S$ the instantaneous (S/N) becomes

$$(S/N)_\tau = \frac{F_o}{\sqrt{E_a}}\ 1.67\ 10^{27}\ \sigma^{-25/10}\ r_o(v)^{35/12}\ L^{5/12}$$

it is now diameter independent !

Long time integration must be quadratic, since the phase of the interference over each pixel is not determined and varies randomly. Hence :

$$(S/N)_T = \left[\frac{S}{N}\right]_\tau \cdot \left[\frac{T}{\tau}\right]^{1/4}$$

For $r_o(v) = 0.1$ m and $L = 20$ m, we obtain $(S/N)_\tau = 1$

λ	E_a^{280} (W/m^{2}srcm^{-1})	F_o(Jy)
3.5	$1.17\ 10^{-4}$	0.12
5	$3.26\ 10^{-3}$	0.27
10	$7.02\ 10^{-2}$	0.22
20	$1.24\ 10^{-1}$	$4.9\ 10^{-2}$

In order to obtain a sensitivity comparable to case a), integration times of 10^8 seconds would be requested, an unrealistic case.

3.3.2. S/N limited by detector noise

We assume a detector noise purely due to read-out, with n = 500 electrons. Per exposure τ, we obtain

$$(S/N)_{ph} = \frac{F_o\ A\ \delta\sigma\ \tau}{n\ hc\sigma}$$

a) Diffraction limited image (adaptive optics)

$(S/N)_C = 1$. We adopt $\delta\sigma_D$: hence

$$(S/N) = \frac{F_o}{n}\ 4.28\ 10^{30}\ D^{7/12}\ r_o(v)^{-11/6}\ \sigma^{-11/5}$$

or with time integration T

$$(S/N) = \frac{F_o}{n}\ 4.20\ 10^{28}\ D^{7/12}\ r_o(v)^{4/3}\ \sigma^{-8/5}\ \sqrt{T}$$

For D = 8 m, $r_o(v)$ = 0.1 m, we obtain with S/N = 1, T = 1 s

λ	F_o (Jy)
2.2	$1.8\ 10^{-4}$
3.5	$0.9\ 10^{-4}$

This case is quite unlikely, because of the difficulty of adaptive optics at wavelengths shorter than 3 μm.

b) Array of detector, coherent addition of signals

The flux is distributed over N_S pixels, and S/N per pixel must be larger than unity during the exposure τ to do coherent addition.

The increase factor above case a) is $N_S(T/\tau)^{1/2}$, i.e. as σ^{-3}.

λ	$N_S\left[\frac{T}{\tau}\right]^{1/2}$
2.2	2050

The limiting brightness, to allow coherent addition of pixels, varies as $D^{-7/12}\ D^2$, i.e. $D^{17/12}$. A gain in diameter means a loss in limiting brightness ! this being due to the very large number of speckles in the image.

c) Array of detectors, incoherent addition of signals

This case may be eliminated, since the large number N_S will completely ruin the S/N ratio.

3.3.3. Infrared interferometry in space

For interferometry in space, we assume no wavefront distorsion, no turbulence, an effective background temperature of 100 K. We derive in the detector-noise case

$$(S/N) = (S/N)_{ph} = \frac{F_o\ A\ \delta\ \sigma}{E_n}\ \sqrt{T}$$

where T is the interference stability time. In the background case, we have

$$(S/N) = (S/N)_{ph} = \frac{F_o\ A\ \delta\sigma\ \sqrt{T}}{\sqrt{E_a\ hc\ \sigma\ A\ \Omega}}$$

Taking $A\ \Omega = \lambda^2$, $\delta\sigma = 0.1\ \sigma$ we find

Detector noise case :

$$(S/N) = \frac{F_o}{E_n}\ .\ 7{,}8\ 10^{-2}\ D^2\ \sigma\ T^{1/2}$$

Background noise case :

$$(S/N) = \frac{F_o}{\sqrt{E_a}}\ 1.77\ 10^{12}\ D^2\ \sigma\ T^{1/2}$$

With these expressions we calculate the sensitivity F_o for S/N = 1, D = 1 m

λ	E_n W-Hz$^{-0.5}$	E_a	F_o(Jy)
1.0	$1.6\ 10^{-17}$	-	
2.0	$3.2\ 10^{-17}$	-	$2.74\ 10^{-4}$
5.0	$8\ \ 10^{-17}$	$2.97\ 10^{-11}$	$1.7\ \ 10^{-3}$
10	$1.6\ 10^{-16}$	$6.66\ 10^{-6}$	$6.8\ \ 10^{-3}$
20	-	$1.12\ 10^{-3}$	0.13

Only at 20 μm the background at the detector exceeds the pure detector noise and a somewhat lower emission or effective temperature of the background would enhance the sensitivity.

A3.4. *Results and conclusion*

The results of the previous discussion are summarized on Fig. A3–1, in the range 1 to 20 μm.

• *If full phasing of pupils by adaptive optics is not feasible, the use of detector* arrays is mandatory to analyse the interference pattern. The interferometer is then inherently limited to objects brighter than a certain threshold value $F_{oT}(\lambda, D)$ [Curves b] and a certain loss is obtained when increasing the diameter, a factor $(D_2/D_1)^{-5/12}$, i.e. a factor of 2 going from 1.5 to 8 m. *On the other hand, a diameter increase improves the S/N ratio as* $D^{7/12}$, *or* reduces the requested observing time for a given S/N on the visibility as $D^{7/6}$.

• When full phasing of pupils is achieved, a sensitivity $F_A(\lambda, D)$ is achieved [Curves a]. It varies as $D^{-17/12}$, i.e. a large gain is obtained with telescope diameter. *An 8 m ground based telescope becomes comparable to a 1 m,* cooled at 100 K, in space.

• Long time (>1s) integration of signals

– does not modify the threshold $F_{oT}(\lambda, D)$, but brings an improvement in visibility accuracy, *i.e. dynamic range, for objects brighter than the threshold.*

– improves the sensitivity $F_A(\lambda, D)$ when an independent phase tracking can be obtained (e.g. using a brighter source in the FOV). Sensitivity will then improve as $\sqrt{T}$.

Figure A3.1.

Sensitivity of an infrared interferometer

Curves a: $F_{o_A}(\lambda, D)$. Limiting flux, with fully phased pupils.

Curves b: $F_{o_T}(\lambda, D)$. Threshold flux, array detector of N_S elements.

Curves c: $F_{o_S}(\lambda)$. Sensitivity of a space interferometer, D = 1 m.

Conditions are :

(a) and (b) : $t = \eta = \epsilon = 1$, T_a = 280 K, n = 500 e^-rms, $r_o(v)$ = 10 cm,

(c) $t = \eta = \epsilon = 1$, detector noise given in A3.3.3, $\delta\sigma = 0.1\ \sigma$, T_s = 100 K

(a), (b) and (c) : T = 1 s

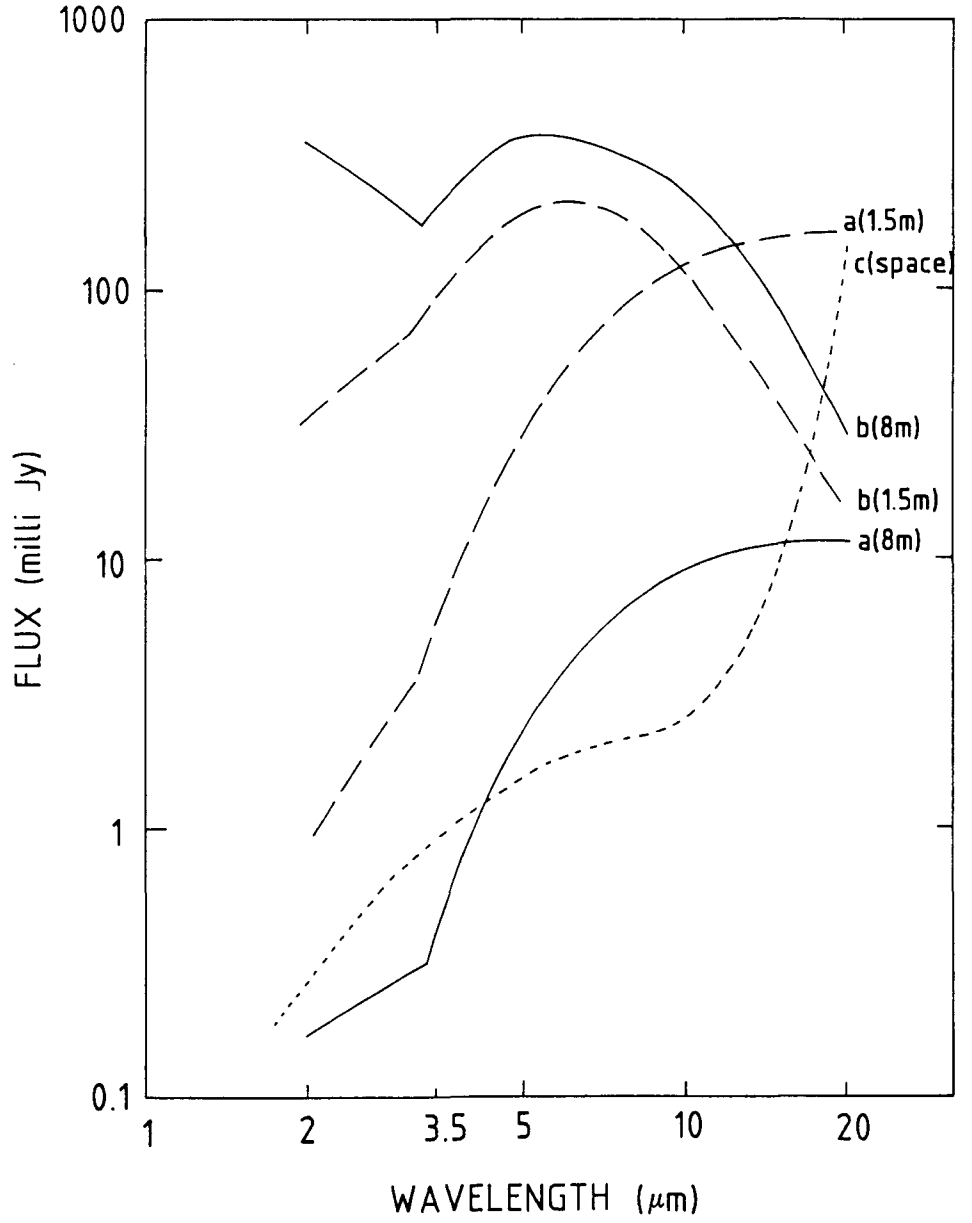

Appendix A4 – MOVABLE TELESCOPES

We discuss here the two possible configurations to move large telescopes.

A4.1 *Point to point translation of the telescopes*

In this configuration the telescopes are supposed to be translated on a certain number of hard standing points situated on a flat site. The number and the layout of these points must be defined in order to achieve the best (u,v) plane coverage. The optical beams from the telescopes are supposed to be combined in a central station and optical delay lines must be provided for the continuous optical path equalisation.

The solution proposed for this approach is derived from a system which is used for the transport and precise positionning of large mechanical pieces to be machined by large CNC (Computer Numerical Control) machine tools. The system is composed of a platform floating on an air film which is towed in place by means of an external power drive: when in place the platform is precisely positioned by means of pins and precision pads that define respectively the lateral and the vertical position. The position accuracy is of the order of 10 micron.

For the translation of a telescope its base would be connected to a platform of sufficient dimension and stiffness, depending on the weight of the telescope a certain number of air cushions must be mounted under the platform. As an example, for a telescope of 300 tons one can estimate a platform of 50 tons: for a total weight of 350 tons it would be necessary, for instance, 16 aero caster load modules K48NHD working at ~ 3/4 full load. The air flow would be ~ 264 L/sec at 2.2 bar. The total lifting area would be 16.5 square meters.

For every point where the telescope is supposed to be moved, an hard standing area with reference points and pads must be provided with the addition of a clamping mechanism to increase the stiffness of the fixation of the telescope to the ground. The hard standing area must be interconnected by cemented roads with suitable load capability and surface smoothers.

A4.2 Continuous movement of the telescope

In this configuration the telescopes are supposed to be moved along straight radial with respect to the central station. The movement of the telescope is made following a predetermined law in such a way to have a continuous optical path equalisation. Due to the stringent requirements on the phase stability of the optical wavefront it is expected that an active phase control will be necessary to take care of small fluctuations of the movement.

The solution proposed for this configuration is also derived with reference to large CNC machine tools. For machining large mechanical pieces [e.g. 500 tons] these machines have a rototraversing table which moves in linear hydrostatic bearings. The movement is provided by backlash-free, high efficiency and stifness hydrostatic worm and rack which in principle do not have limitations on the length of the movement. The movement is very smooth and the positional accuracy is ~ 0.01 mm. The maximum speed of translation is ~ 6 meter per minute. Large horizontal milling and boring machines that have a linear movement of 30 to 40 m. have been already built.

In the case of VLT project the base of the telescope would be fixed to the hydrostatic saddle which will move on a linear hydrostatic bearing of a bed having the desired length. The point of major concern related to the hydrostatic solution is the need for a suitable tight protective cover of the bed top against dust, rain, snow, etc. An investigation is in progress to find a suitable solution to this problem. It is obvious that, as in the case of the point to point configuration, the solution with hydrostatic bed required a flat site. Despite some complexity with the realisation of the hydrostatic rail, this solution presents the best combination of rigidity-frictionless required for the interferometry with movable telescopes.

The investigation made shows that, from the pure mechanical point of view, these could be possible solutions to the problem of moving telescopes that should be analysed in detail by a feasibility study.

The cost-effectiveness of these features remains to be evaluated in the context of the overall VLT project.

The platform concept

To allow all of the desirable telescope–array configurations of interest for interferometry, but also for non–interferometric observing, a smooth platform on which telescopes can be displaced randomly would be ideal. It would also make delay lines unnecessary for interferometry since telescope motions during observation could be programmed to follow the elliptical tracks ensuring equal optical paths. No such possibility was exploited for large radio arrays since smooth platforms spanning many kilometers raise unsolved problems.

The scale of 100–300 m considered for the VLT is compatible with a square or circular platform. Air pads such as described previously can carry the telescopes on smooth concrete. Among the unsolved problems however are:
a - the moderate accuracy of motion achieved on air pads of this type;
b - traction mechanisms for bidirectional motion.

Concerning the traction problem, bidirectional configurations of linear motors could be investigated. As shown in Figure 3.2.1, an array of magnets immersed in the concrete platform can provide a checker–board pattern of magnetic fields. Driving forces can be achieved by electric coils located on the telescope support.

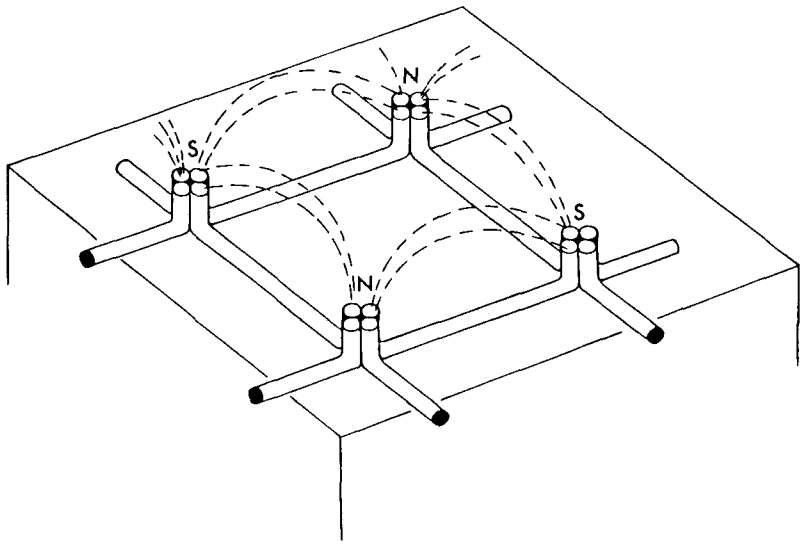

Figure A4–1 *: Immersed electric coils for a continuous 2–D motion over a platform.*

A more conventional approach would use crossed railway tracks (Labeyrie et al. 1984). It however appears less flexible for continuous motion in two dimensions.

Appendix A5 - BEAM COMBINATION

The VLT linear array concept allows a versatile use of the unit telescopes. The individual telescopes could be used either independently or in various combination schemes. The major beam combination modes are (see Fig. A5–1) :

- Incoherent beam combination (Combined Coude Focus)
- Coherent beam combination (Interferometry)

The incoherent combination with a combined Coude focus offers the light collecting power of a 16 m equivalent single dish telescope. The coherent combination path opens long baseline interferometry with a resolution span of approx. 0.5 marcsec in the blue to approx. 30 marcsec at 20 μm wavelength in case a 150 m baseline is selected.

The optical design of the beam combination pathes is mainly determined by the desired field of view of the combined image and the distance between the single telescopes. Both should be as large as possible, a large field of view and a long baseline for high resolution imaging in the coherent combination mode. However, the field of view and the baseline influence directly the dimension and the number of the optical elements in the combination path and therefore the cost of the systems. A lot of technical aspects are valid for the incoherent as well as for the coherent combination system, although, the interferometric combination has much higher technical requirements, mainly with respect to stability. It seems to be appropriate to start the interferometric combination in the IR range and then gradually extend it towards the visible. The optical efficiency of the combined beam modes depends strongly on the availability of high reflectivity coatings. Recent developments indicate progress for high efficiency coatings for IR wavelengths. In any case it is of ultimate importance to keep the mirrors absolutely clean. Additionally the beam path has to be protected against air turbulences, which are mainly critical in the horizontal beam sections.

It is foreseen to equip the beam combination path with an active stabilisation and alignment system. The mirror cells will be supported by 3 motor driven actuators to allow translation and tilt. Though all mirrors will be remotely adjustable, only one will remain adjustable after the initial alignment is performed. Therefore the sole purpose of the remote adjustement is to facilitate this initial tuning of the optical system. For the mirrors being not subjected to

gravity variations, it is hoped that the optical train will need any permanent adjustement. Nevertheless a laser beam may be very useful for checking the alignment and if necessary could provide a continuous stabilisation. For the initial alignment and the later stabilisation it might be advantageous to have the laser source or its image in the center of the secondary mirror, i.e. inside the central obstruction of the telescope. Therefore, all the other mirrors in the beam path should have no center hole.

The present concept with telescopes in alt–az mount has an image and pupil rotation as a consequence. This drawback can be overcome by the use of an image de–rotator or instrumentation mounted on a synchroneously rotating stage. The first solution requires transmissive elements or a large number of reflecting surfaces. Therefore the second solution seems to be the preferable one.

A preliminary conceptual design of the coherent beam combination system shows, that a field of 15 arcsec seems to be possible (see Fig. A5–2). With the independently mounted telescopes the entrance pupils are not coplanar as the telescope points off the zenith angle. In order to guarantee phasing of the separate beams, the Lagrange invariants for the individual telescopes in the array must be equal and additionally the overall Lagrange invariant of the array be conserved. This requires optical path length and pupil corrections. Further investigations have to show the tolerances allowed for the pupil corrections in case of 8 m apertures.

By setting the VLT to the interferometric mode the beams from two telescopes can be combined with an equal path length in the interferometric laboratory. There are at least two options for the path length correction :
(1) use of a trombone as an optical delay line in the combining beams of the individual telescopes and a stationary combining system or,
(2) use of a moving combining system to ensure equal path length.
The optical elements which have to be translated could be mounted on tables supported with air bearings or magnetic bearings to ensure a smooth motion with low pitch and yaw errors, and high vertical and horizontal straightness. Linear brushless DC motors which are available in the necessary length would meet the specifications for a homogeneous slip stick free motion.

Pointing off the zenith angle with two telescopes results in a pupil foreshortening which decreases the synthetic pupil diameter. To maintain the geometrical scaling of the lateral pupil geometry the pupil separation at the combining optics has to compensated.

The longitudinal pupil position must be compensated due to the change of the relative location of the optical elements in the system. With variable optics the images of the pupils can be continuously transformed to the same plane in the combining optics. A spherical continuously deformable mirror with a focal range from −17 m to infinity could be applied.

The interferometric operation mode may imply even stronger the need for a beam protection under vacuum operation than the incoherent beam combination mode. To avoid vacuum tubes with variable length, the most reasonable solution seems to be to have the optical delay lines or the whole combining system inside the vavuum chamber. Unfortunately this will exclude the use of air bearings for the mobile parts. Comparable systems have been built for large laser interferometers and Fourier transform spectrographs.

The operation of the VLT in the interferometric mode requires a continuous optical path correction. To achieve the necessary stability the coherent beam combination path has to be actively stabilized. Techniques developed for laser beam stabilization systems could be applied. A practical implementation could employ three separate servo control systems : a baseline control to maintain the approximate equality for the mean optical path length in the two arms of the interferometer, while tracking of the star. The adaptive optics to compensate wavefront distortions due to atmospheric turbulences. And a path length compensation system using a fringe tracker which corrects the optical path length due to large scale effects of the atmosphere and mechanical system instabilities in real time to maintain the phase of the fringes within a fraction of half of a wavelength. Instead of fringe tracking it is also possible to stabilize the path length with a laser ranging system, which has the advantage not suffering under intensity problems. The operation and performance of the interferometer depends on the ability of measuring the fringe contrast in spite of the changes in fringe phase and the presence of contrast degradation effects caused by the atmospheric and the instrumental perturbations (cf. Appendix 3).

In the original linear array concept of the VLT as described in April 84, it was proposed to achieve the coherent combination in a laboratory separated from the normal Coude laboratory for mainly two reasons :

i) Rapid switch–over from normal operation to the interferometric mode;

ii) Possibility to use mobile 2 m class auxillary telescopes with the same set–up. This combination provides several important advantages such as a full time use of the interferometer with an optimum telescope size and

complementarily a continuous coverage of the spatial frequency plane.

The construction of these two auxillary telescopes has not been considered so far in the budget, but are seen by the VLT study group as a necessary complement, should interferometry be retained as a fundamental option.

Figure A5.1 *: Schematic view of the incoherent and coherent beam combination modes of the non-redundant array. Incoherent combination is shown for the telescopes B and D, coherent combination for A and C. The optical elements are not in scale.*

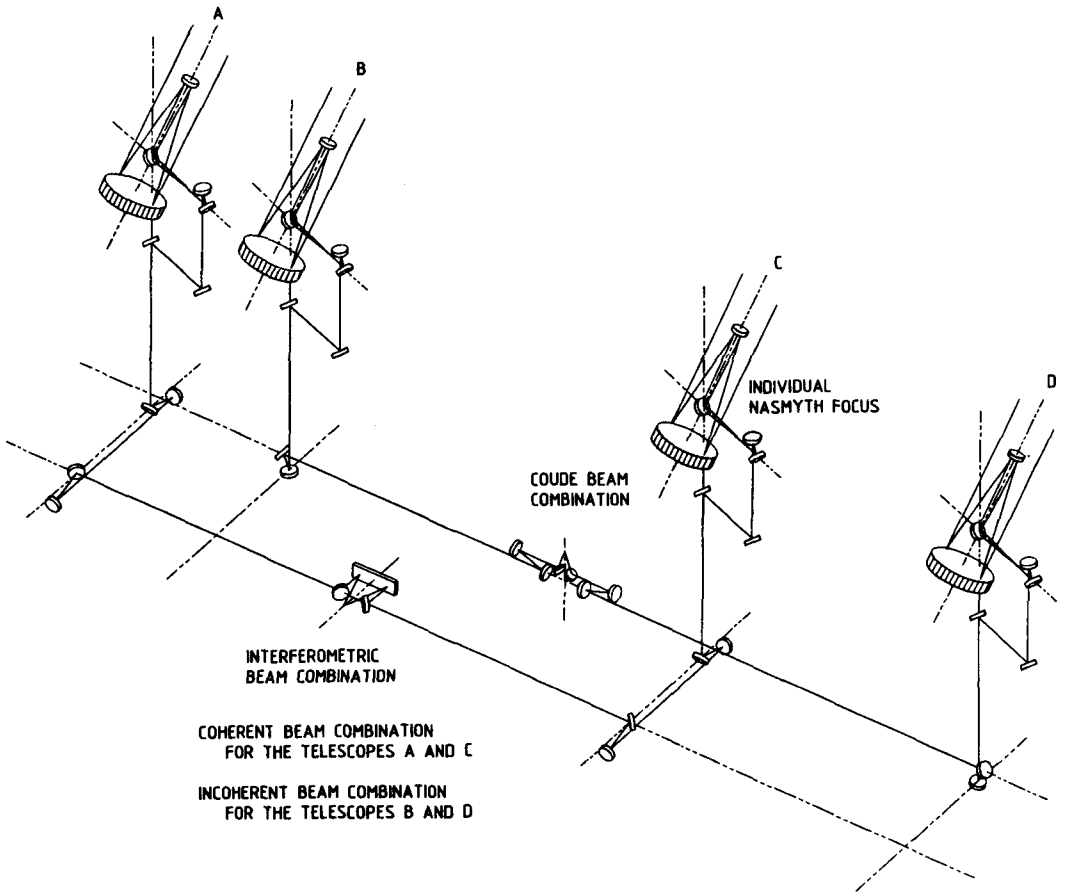

Figure A5.2. *: Schematic view on the interferometric beam combination path. A key element in this design is the variable pupil relay mirror with a focal length range from 17 m to infinity. For the combination of the light from two telescopes a F/6.2 telescope with 600 mm diameter moving on an air cushion table is foreseen.*

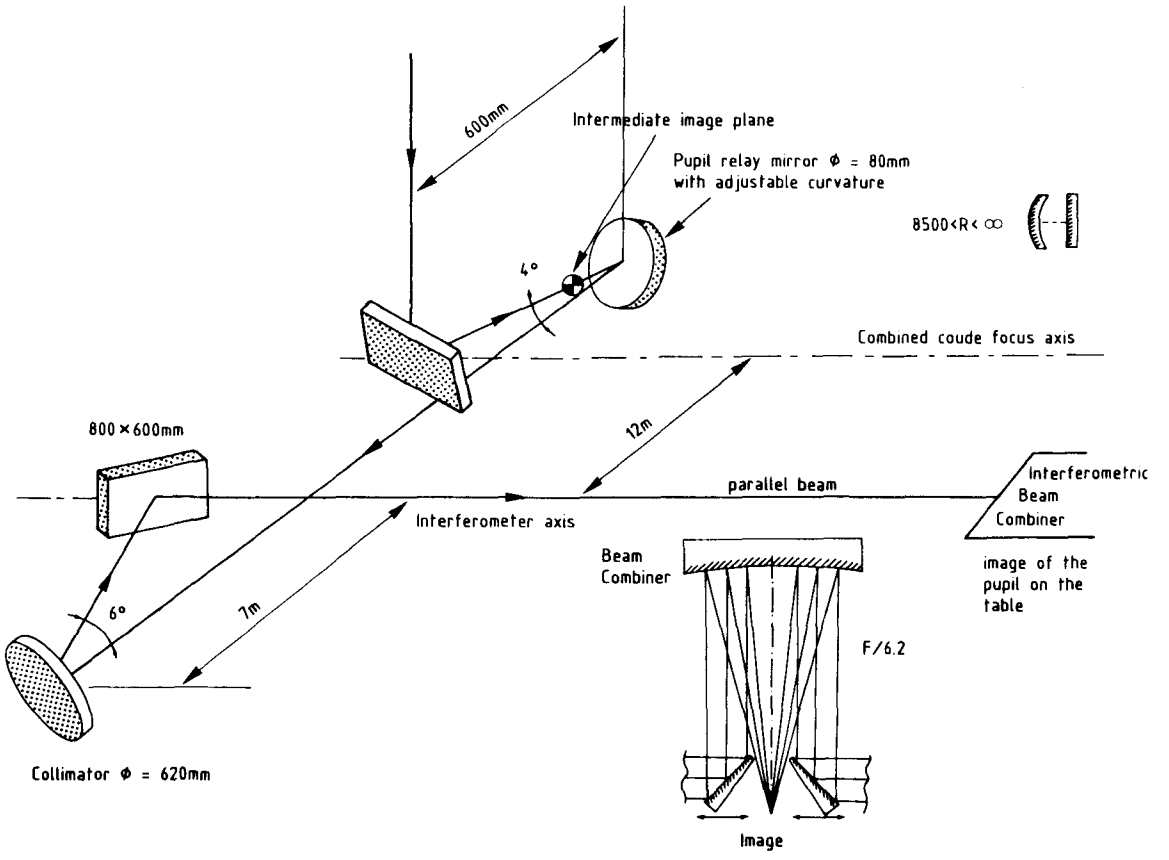

Appendix 6 - DIFFRACTION LIMITED IMAGING WITH A SINGLE TELESCOPE

Diffraction limited imaging with a single 8–10 m telescope provides 10 to 20 times less angular resolution, but is nevertheless a very appealing goal, which has little consequences on cost and on management of a VLT.

A6.1 *Speckle interferometry at visible wavelengths*

The 8m–telescopes of the VLT will be extremely attractive for high–resolution speckle work since they can yield an angular resolution of about 0.01" in the visible. The limiting magnitude will be very seeing–dependent. In nights of very good seeing the limiting magnitude will be about 20^m. Objects of 17th magnitude were already observed at 1" seeing, with about 30 min. observing time and with relatively simple speckle cameras.

Various speckle methods are available. The list below describes some of these methods and the information which can be reconstructed by these methods:

Labeyrie's speckle interferometry (Labeyrie 1970):
diffraction–limited autocorrelations,
Knox–Thompson method (Knox and Thompson 1974):
diffraction–limited images,
Speckle masking (Weigelt and Wirnitzer 1983):
diffraction–limited images
Speckle spectroscopy (Stork and Weigelt 1984):
diffraction–limited objective prism spectra
Differential speckle interferometry (Beckers 1982).

Speckle observations with high signal–to–noise ratio will be possible at 20th magnitude if
- a site is selected which has 0.5" seeing or better in many nights (flexible scheduling) and slow seeing variations (jet stream turbulence avoided).
- dome seeing is avoided completely
- the mirror quality is very good (better than 0.2")

- observations are performed in many spectral channels simultaneously (e.g. by dichroic beam splitters)
- one telescope is used for the object and a second telescope is used to measure the speckle transfer function.

A6.2 *Pupil-plane interferometry*

Pupil-plane interferometry has been suggested as a substitute for speckle interferometry as early as 1972 (Breckinridge 1972; Kenknight 1972). Since there is no attenuation of the amplitude of the object Fourier components in the pupil plane, this technique avoids calibration errors inherent to speckle methods. Moreover averages can be taken over a smaller number of frames since turbulence does not contribute to the variance of the amplitude estimate. For faint objects both methods are photon-noise limited and the S/N ratios have been shown to be ultimately the same (Dainty and Greenaway 1979). For bright objects the S/N ratio per frame saturates to unity in a speckle experiment whereas it keeps increasing as the square root of the number of photons in a pupil plane experiment (Goodman and Belsher 1977). In this case pupil-plane interferometry can be far superior to speckle interferometry.

Pupil plane interferometry would be very effective in the IR, since most IR observations are limited by speckle noise and calibration errors (Chelli and Mariotti 1986). A Fourier Transform Spectrometer can be modified to do pupil-plane interferometry (Mariotti and Ridgway 1986), yielding both angular and spectral information at the same time.

Stellar diameter measurements have been demonstrated by Currie et al. (1974) using a wavefront folding interferometer (Koster prism). Roddier and Roddier (1983) obtain two-dimensional visibility maps using a rotation shearing interferometer. By processing only 71 frames they have been able to map the visibility function of Alpha Orionis with a S/N ratio superior to that of speckle measurements using several thousand frames, showing evidence for a dust envelope close to the stellar disk (Roddier and Roddier 1983). An image of this envelope has been reconstructed from these data (Roddier and Roddier 1985; Roddier et al. 1984). New data obtained with the same interferometer show evidence for two faint stellar companions to Alpha Orionis (Karovska 1984; Roddier et al. 1985). These results clearly demonstrate the efficiency of pupil-plane interferometry.

Whereas the transfer function for speckle interferometry is the autocorrelation of the pupil transmission function, the transfer function for pupil plane interferometry depends upon the wavefront shear used. Because of the circular symmetry of telescope pupils, rotational shears are the most convenient since they make use of all available photons. In this case the transfer function has the same shape as the pupil transmission function. Using a 180 degree rotational shear with a full aperture allows to observe simultaneously every spatial frequency up to the telescope frequency cut-off. Because most telescopes have a centrally obscured pupil, additional observations are necessary to recover the low spatial frequency information. An important requirement for this type of observations is that the telescope should have the smallest possible central obstruction.

As for speckle interferometry, this techniques requires that every effort should be made to minimize refractive index inhomogeneities along the optical path inside the dome. Experience indicated that any source of heat close to the beam (generally electronics at prime focus and warm wires along spider arms) have a detrimental effect.

A6.3 *Speckle interferometry at infrared wavelengths*

Until now high resolution IR imaging has been restricted to one-dimensional (1-D) speckle interferometry because IR arrays have not been implemented in adequate systems. However this is to be done in the very near future and should be a qualitative improvement (access to regularly sampled 2-D visibilities and therefore easy-to-reconstruct images) but not a significative one in terms of S/N per single resolution element.

Practice has led to the following technical requirements in addition to usual IR constraints:

- excellent tracking do not truncate the image wings despite a field of a few arcsec; good and fast blind pointing for source switching;

- telescope mean MTF i) very stationary ii) very good as aberrations severely degrade the visibility S/N; this point makes active optics quite promising if it can keep the mean MTF still stationary;

- temperature gradients cancelled or inversed; apart from bad seeing, the possibility of image degradation by these gradients is the major because it is not stationary, not linear and usually not under control.

The resolution (in the Rayleigh's sense) of an 8m dish being 54 marcsec at K, 93 marcsec at L and 118 marcsec at M, the effective resolution, based on simple model fitting, can reach 20, 31 and 39 marcsec respectively at K, L and M.

For a 1-D system, the sensitivity is not improved by sizing the collector dish up, on the contrary 0.4 mag is lost when the detector is background-limited. However comparing 4 m and 8 m dishes at same resolution shows a gain of 0.2 mag (at M) to 1.0 mag (at M). For a 2-D system (CID receptor) a gain of 0.75 mag (prop. to D) is obtained. Theoretical magnitudes, attained within 1 mag by present systems, are 7.7 at K, 5.8 at L depending on limitation type, 4.5 at M with a seeing of 1.3 arcsec at V (and 1 h integration, 200 ms exposure time, S/N of 10, emissivity of 0.15).

Their r_0-dependence (proportionnal to r_0^2 at 1-D, to r_0 at 2-D) recalls that the seeing quality has also a huge quantitative impact.

Present techniques (with a computer of $\geq$ 0.1 Mflops) would already allow to implement:

- autoguiding with the source signal itself;
- on-line best image sorting and phase computation by Knox and Thompson algorithms;
- on-line preliminary image restoration.

A speckle IR system should make use of these potential facilities at the only price of software work.

The technique itself is still evolving towards more efficient although more complicated configurations which will be fully operational at the time of VLT's first light, like IR shearing interferometer and differential speckle interferometer. These "second generation" instruments bring improvements of limiting magnitudes and spatial resolution in their own working domain.

REFERENCES

For clarity, we have separated the references in two parts :
a) references which are specific to interferometry and interferometric methods.
b) general astrophysical references, mostly called in § 1.3.

a) *References on Interferometry*

- Assus, P. et al. *L'interféromètre infrarouge du CERGA*, J. Optics (Paris), 10, 1979.

- Baldwin, J.E., Haniff, C.A., Mackay, C.D., Warner, P.J., *High resolution optical imaging : application of closure phase*, 1986, Nature, in press.

- Barletti, R. et al. *Mean vertical profile of atmospheric turbulence relevant for atmospheric seeing*, 1976, JOSA, 66, 1380.

- Beckers, J., *Differential speckle interferometry*, Optica Acta, 29, 361, 1982.

- Beckers, J.M., Hege, E.K., *The use of the MMT for interferometric imaging*, in Very Large Telescopes, their Instrumentation and Programs, Proc. IAU Coll. No 79, 1984, Garching bei Munchen, eds M.H. Ulrich and K. Kjar, ESO, 279–293.

- Beckers, J.M., *Comments on interferometric arrays*, NOAO/ADP R&D Note No 84–3, 1984.

- Beckwith, S., Zuckerman, B., Strutskie, M.F., Dyck, H.M., *Discovery of solar–system size halos around young stars*, Ap.J., 287, 793, 1984.

- Breckinridge, J.B., *Coherence interferometer and astronomical application*, Appl. Opt. 11, 2996–2998, 1972.

- Chelli, A., Perrier, C., Biraud, Y., *One dimensional high resolution image reconstruction on Eta Carinae at 4.6 μm*, Astron. Astrophys., 117, 199, 1983.

- Chelli, A., *Infrared speckle methods*, in Very Large Telescopes, their Instrumentation and programs, IAU Coll. No79, 1984.

- Chelli, A., Perrier, C., Léna, P., *The sub-arc second structure of IRc2 at 5 microns*, Ap. J., 280, 163, 1984.

- Chelli, A., Mariotti, J.M., *Visibility and phase analysis for image and pupil plane interferometry at optical wavelength*, Astron. Astrophys., 157, 372, 1986.

- Citterio, O., *Consideration on the microseismicity, in connection with the use of the VLT in the interferometric mode*, Note for VLT interferometry group, 1984.

- Citterio, O., *Consideration on the movability of the Telescopes for the VLT interferometry configuration*, Note for VLT interferometry group, 1985.

- Cornwell, T.J., Wilkinson, P.N., *Self Calibration*, in "Measurement and Processing for Indirect Imaging", IAU/URSI Symposium. Ed. J.A.-Roberts, Sydney, 1983, Cambridge Univ. Press.

- Currie, D.G., Knapp, S.L., Liewer, K.M., *Four stellar diameter measurements by a new technique, amplitude interferometry*, Astrophys. J., 187, 131-134, 1974.

- Currie, D.G., *The development, fabrication and Astronomical application of a wide-band long baseline optical amplitude interferometer*, University of Maryland, Tech. Report 77-075, 1977.

- Currie, D.G., *On astronomical applications of the Very Long Baseline amplitude interferometer*, in High angular resolution stellar interferometry, Proc. IAU Coll. No 50, 1979, Univ. of Maryland, eds J. Davis and W.J. Tango, Chatterton Astron. Dept., Sydney.

- Dainty, J.C., 1975, *Topics in applied physics*, Vol. 9, (Springer).

- Dainty, J.C., Greenaway, *The signal-to-noise ratio in speckle interferometry*, IAU Colloquium No 50, Davis and Tango edt., Univ. Sydney, 23 1-18, 1979.

- Davis, J., *An 11 metre Michelson stellar interferometer*, New Zeeland Journal of Science, 22, 451-455, 1979.

- Davis, J., *Long baseline interferometry and binary stars*, in Current Techniques in Double and Multiple Star Research, Proc. IAU Coll. No 62, 1981, Flagstaff (Arizona), eds R.S. Harrington and O.G. Franz, Lowell Observatory Bull. No 167, Vol. IX No 1, 191-201.

- Di Benedetto, G.P., Conti, G., *Stellar diameter measurements by two-aperture interferometry in the infrared*, Astrophys. J., 268, 309-318, 1983.

- Di Benedetto, G.P., *Long baseline Michelson stellar interferometry in the near infrared*, Astron. Astrophys., 148, 169, 1985.

- Dyck, H.M., Beckwith, S., Zuckerman, B., *Speckle interferometry of IRC+10216 in the vibration-rotation lines of CO*, Astrophys. J., 271, 179, 1983.

- Dyck, H.M., Zuckerman, B., Leinert, C., Beckwith, S., *Near infrared speckle interferometry of evolved stars and bipolar nebulae*, Astrophys. J., 287, 801, 1984.

- Dyck, H.M., Berg, E., Harris, D., *A study of microseismic and man-made vibrations on Mauna Kea*, P.A.S.P., Submitted, 1986.

- Enard, D., *Off-axis phase variation with various interferometer configuration*, Note VLT, 1984.

- Faucherre, M., Bonneau, D., Koechlin, L., Vakili, F., Astron. Astrophys., 120, 263, 1983.

- Foy, R., Labeyrie, A., *Feasibility of adaptive telescope with laser probe*, Astron. Astrophys., 1985, submitted.

- Franza, F., Wilson, R.N., *States of the ESO new technology telescope project*, SPIE, 332, 90, 1982.

- Goodman, J.W., Belsher, J.F., *Photon limitations in imaging and image restoration*, Report TR-77-175, 1977, ARPA Order No 2646, Rome Air Development Center, Griffin AFB, N.Y. 13441.

- Greenaway, A.H., *The signal-to-noise ratio in long-baseline stellar interferometry*, Optica Acta, 26, 1147-1171, 1979.

- Greenaway, A.H., *The interferometric observing efficiency of arrays of large aperture telescopes*, Optics Commun, 29, 279, 1979.

- Hanbury-Brown, R., Davis, J., Allen, L.R., *The angular diameters of 32 stars*, Mon. Not. R. Astr. Soc., 167, 121-136, 1974.

- Hardy, J.W., *Active optics in astronomy*, 1981, Proc. ESO Conferences on scientific importance of high angular resolution at IR and optical wavelengths, 25.

- Hegben, J.C., Hege, E.K., Beckers, J.M., *Use of the coherent MMT for diffraction limited imaging*, S.P.I.E., 628, Tucson, 1986.

- Hege, E.K., Beckers, J.M., Strittmatter, P.A., and McCarthy, D.W., *Multiple mirror telescope as a phased array telescope*, Appl. Optics, 24, 2565, 1985.

- Hofman, K.H., Weigelt, G., *Speckle masking observation of the central object in the giant H II region NGC 3603*, Astron. Astrophys., submitted, 1986.

- Karovska, M., *Les observations à haute résolution de la supergéante Bételgeuse*, Thèse de spécialité, Université de Nice, 1984.

- Karovska, M., Nisenson, P., Noyes, R., Roddier, F., *On the α Orionis triple system*, Ap. J., submitted, 1986.

- Kenknight, C.E., *Autocorrelation methods to obtain diffraction limited resolution with large telescope*, Astrophys. J., 176, L43–L45, 1972.

- Knox, K.T., Thompsom, B.J., *Recovery of images from atmospherically degraded short exposures images*, Astrophys. J. Lett., 193, L45, 1974.

- Koechlin, L., Bonneau, D., Vakili, F., *Détection d'un effet de phase à l'interféromètre du CERGA: application au mouvement orbital de Capella*, Astron. Astrophys., 80, L13, 1979.

- Koechlin, L., Rabbia, Y., *Mesures de diamètres à l'interféromètre optique du CERGA: dévelopements et résultats récents*, Astron. Astrophys. (in press), 1985.

- Labeyrie, A., *Attainment of diffraction limited resolution in large telescopes by Fourier Analysis speckle patterns in star images*, Astron. Astrophys. 6, 85, 1970.

- Labeyrie, A., *Interference fringes obtained on Vega With two optical telescopes*, Astrophys. J., 196, L71–L75, 1975.

- Labeyrie, A., Kibblewhite, J., de Graauw, T., Noordam, J., Weigelt, G., Roussel, H., 1982, in Conf. Proc. "Very Long Baseline Inteferometry Techniques", Toulouse, 1982.

- Labeyrie, A., et al., *Progress of the Large Interferometer at CERGA*, in Very Large Telescopes, their Instrumentation and Programs, Proc. IAU Coll. No 79, 1984, Garching bei Munchen, eds M.H. Ulrich and K. Kjar, ESO, 267–278.

- Labeyrie, A., 1985, *Passive and active control of vibrations*, Note for VLT Interferometry group, 1985.

- Lannes, A., in Topical Meeting on Signal Recovery - Optical Society of America, Honolulu, 1986.

- Léna, P., in Infrared Astronomy, Eds Setti G., Fazio, G. - Reidel 1977.

- Léna, P., *High angular resolution in the infrared: prospects for space observation*, in "Kilometric Arrays in Space", ESA-SP 226, 1985.

- Léna, P., Merkle, F., Schmieder, F.X., *Large field adaptive optics*, 1986, to be submitted.

- Lohmann, A.W., Weigelt, G., Wirnitzer, B., *Speckle masking in astronomy: triple correlation theory and application*, Appl. Opt. 22, 4028, 1983.

- Loos, G.C., Hogge, C.B., *Turbulence in the upper atmosphere and isoplanetism*, Appl. Opt. 18, 2654–2661, 1979.

- Mac Carthy, D., Low, F.J., *Detection of a close companion to VB8*, Ap. J., 290, L9, 1985.

- Mariotti, J.M., Chelli, A., Foy, R., Léna, P., Sibille, F., Tchountonov, G., *Infrared speckle imaging*, Astron. Astrophys. 120, 237, 1983.

- Mariotti, J.M., and Di Benedetto, G.P., *Path length stability of synthetic aperture telescopes*, in IAU Coll. 79, 1984.

- Mariotti, J.M., Ridgway, S., 1986, Private Comm.

- Michelson, A.A., Pease, F.G., *Measurements of the diameter of Alpha Orionis with the interferometer*, Astrophys. J., 53, 249-259, 1921.

- Olthof, edit. *Workshop on kilometric optical arrays in space*, Cargese, ESA, 1984.

- Oppenheim, A.V., Lin, J.S., 1981, Proc. IEEE, 69, 529-541.

- Reasenberg, R.D., edit. *Workshop on optical interferometry in space*, Baltimore, Bull. Am. Astronom. Soc., 16, 747-837, 1984.

- Roddier, F., 1975, *Imaging in Astronomy*, OSA/SPIE Conference, Boston.

- Roddier, F., *Special requirements for high angular resolution interferometry*, ESO Workshop on Site Testing for Future Large Telescopes, La Silla, 4-8 Oct. 1983, (A. Ardeberg, L. Woltjer, edit.), 193-201.

- Roddier, F., *Testing seeing quality*, Workshop for Future Large Telescope, Cargese (May 1983), Conf. Proc. (ESO), 255-261.

- Roddier, C., Roddier, F., *High angular resolution observations of Alpha Orionis with a rotation shearing interferometer*, Astrophys. J., 270, L23-L26, 1983.

- Roddier, F., *How to achieve diffraction limited resolution with large space telescopes*, Adv. Space Res., 2, 3, 1983.

- Roddier, F., Roddier, C., Karovska, M., *High angular resolution interferometric observations of Betelgeuse in the visible*, UCLA Workshop on Mass Loss from Red Giants, M. Morris and B. Zuckerman edit., Reidel, 1984.

- Roddier, F., Léna, P., *Long-baseline Michelson interferometry with large ground-based telescopes operating at optical wavelengths*
I. *General formalism. Interferometry at visible wavelengths*, J. Optics (Paris), 15, 171-182, 1984.
II. *Interferometry at infrared wavelengths*, Ibid., 15, 363, 1984.

- Roddier, F., 1985, NOAO R. & D. Note Number 85-4.

- Roddier, F., Roddier, C., *An image reconstruction of Alpha Orionis with a rotation shearing interferometer*, Astrophysical J., 295, L21, 1985

- Roddier, F., O.S.A. Topical meeting on Quantum Limited imaging, Honolulu, 1986.

- Roddier, F., Roddier, C., *Modeling atmospheric effects in adaptive optics systems for astronomical telescopes*, in SPIE 628, Tucson, 1986.

- Roddier, F., Eisenhardt, P., *IR Background speckle noise induced by adaptive optics in astronomical telescopes*, in S.P.I.E. 628, Tucson, 1986.

- Schwartz, P., Simon, T., Zuckerman, B., Howell, R., Ap. J., 280, L23, 1984.

- Shao, M., Staelin, D.H., *Long baseline optical interferometer for Astrometry*, J. Opt. Soc. Am., 67, 81-86, 1977.

- Shao, M., Staelin, D.H., *First fringe measurements with a phase-tracking stellar interferometer*, Applied Optics, 19, 1519-1522, 1980.

- Stork, W., Weigelt, G., 1984, *Speckle spectroscopy*, in Conf. Proc. International Commission of Optics 13, Sapporo, 1984, p. 642.

- Sutton, E., Storey, J., Betz, A., Townes, C., Spears, D., Ap. J., 217, L97, 1977.

- Tango, W.J., Twiss, R.Q., *Michelson stellar interferometry*, Progress in Optics, E. Wolf edit. (North-Holland), 17, 239-277, 1980.

- Tarenghi, M., Ziebell, M., *ESO automatic prime focus camera and the problem of remote control*, 1982, SPIE Vol. 331, 404.

- Terlevich, Melnick, 1985, M.N.R.A.S., 213, 841.

- Thom, C., Granes, P., Vakili, F., 1986, *Optical interferometric measurements of γ Cassiopeiae envelope in the Hα line*, Nature, submitted.

- Townes, C.H., *Spatial interferometry in the mid-infrared region*, J. Astrophys. Astr., 5, 111-130, 1984.

- Venkatakrishnan, P., Chatterjee, S., *On the saturation of the refractive index structure function*, M.N.R.A.S., submitted, 1986.

- Waller, W., *Field of view constraints on actively controlled long-baseline stellar interferometry*, J. Opt. Soc. Am., 70, 1096, 1980.

- Walter, M., Weigelt, G., 1985, *Roll deconvolution of ST data*, Advances in Space Research, in press.

- Weigelt, G., Wirnitzer, *Optics Lett.*, 8, 389, 1983.

- Wilson, R.N., 1982, Opt. Acta, 29, 985.

- Wilson, R.N., *The NTT (New Technology Telescope) predecessor of the VLT*, 1983, Procedings ESO Workshop on VLT Cargèse, 173.

- Woolf, N., *High resolution imaging from the ground*, Ann. Rev. Astron. Astrophys., 20, 367, 1982.

- Woolf, N., *Adaptive optics*, 1984, Proc. IAU No 79, Garching, 221.

b) General astrophysical references

- Abt, H., in Protostars and Planets, Vol. II, Tucson, 1985.

- Anandarao, B., Vaidya, D., Astr. Ap., 161, L9, 1986.

- Aumann et al., Ap.J., 278, L23, 1984.

- Aumann, A., P.A.S.P., 97, 885, 1985.

- Baier, G., Ladebeck, R., Weigelt, G., Astron. Astrophys., 151, 61, 1985.

- Beckwith, S., Zuckerman, B., Skrutskie, M., Dyck, H., Ap.J., 287, 793, 1984.

- Blazit, A., Bonneau, D., Koechlin, L., Labeyrie, A., Ap.J., 214, L79, 1977.

- Bloemhof, E., Danchi, W., Townes, C., Ap.J., 299, 138, 1985.

- Bonneau, D., Foy, R., XIX IAU General Assembly, Commision 29, working group "Peculiar Red Giants".

- Chelli, A., Perrier, C., Léna, P., Ap.J., 280, 163, 1984.

- Cox, A.N., Ann. Rev. Astron. Astrophys., 18, 15, 1980.

- De Robertis, M.M., Osterbrock, D.E., Ap.J., 301, 98, 1986.

- Devereux, N.A., Becklin, E.E., Scoville, N., Ap.J., 1986, in press.

- Dyck, M., Simon, T., Zuckerman, B., Ap.J., 255, L103, 1982.

- Dyck, M., Zuckerman, B., Leinert, C., Beckwith, S., Ap.J., 287, 801, 1984.

- Dyck, M., Kibblewhite, E., P.A.S.P., 98, 260, 1986.

- Dyer, C.C., Ap.J., 287, 26, 1984.

- Encrenaz, T., Proceedings of ESO Conf. "Scientific Importance of High Angular Resolution at Infrared and Optical Wavelengths", Garching RFA, 307, 1981.

- Faucherre, M. et al., Astron. Astrophys., 120, 263, 1983.

- Ferland, G.J., Osterbrock, D.E., Ap.J., 300, 658, 1986.

- Foy, R., Bull. Information CDS, 20, 42, 1981.

- Foy, R., Chelli, A., Sibille, F., Léna, P., Astron. Astrophys., 79, L5, 1979.

- Harrison, B., Pedlar, A., Unger, S.W., Burgess, P., Graham, D.A., Preuss, M.N.R.A.S., 218, 775, 1986.

- Heckman, T.M., Miley, G.K., Green, R.F., Ap.J., 281, 525.

- Hinkle, K., Barnes, T., Ap.J., 227, 923, 1979.

- Hinkle, K., Hall, D., Ridgway, S., Ap.J., 252, 687, 1982.

- Holzer, T., McGregor, K., Mass Loss from Red Giants, Astroph. Sp. Sc. Library, 117, 229.

- Kielkopf, J., Brashear, R., Lattis, J., 1985, Ap.J., 299, 865.

- Labeyrie, A., Koechlin, L., Bonneau, D., Blazit, A., Foy, R., 1977, Ap.J., 218, 175.

- Lacey, C.G., Ostriker, J.P., Ap.J., 299, 633.

- Léna, P., in Workshop on ESO's Very Large Telescope, Cargèse, 1983.

- Masegosa, J., Moles, M., Penston, M.V., M.N.R.A.S., 218, 541, 1986.

- Meaburn, J., Heloden, J.C., Morgan, B.L., Vine, H., M.N.R.A.S., 200, 1p., 1982.

- Meaburn, J., Morgan, B.L., Vine, H., Pedlar, A., Spencer, R., Nature, 296, 331.

- McCarthy, D.W., Low, F.J., Kleinmann, S.G., Gillett, F.C., Ap.J., 257, L75, 1982.

- McCarthy, D., Probst, R., Low, F., Ap.J., 290, L9, 1985.

- Moran, J. et al., Ap.J., 271, L31., 1983.

- Nisenson, P;, Stachnik, R., Karovska, M., Noyes, R., Ap.J., 297, L17, 1985.

- Perrier, C., Chelli, A., referred to in Chelli, 1985, IAU Colloquium No. 79.

- Perrier, C., Mariotti, J.M., Ap.J., submitted, 1986.

- Peterson, B.M., IAU Circ. 4036, 1985.

- Poeckert, R., 1982, in "Be stars", IAU Symposium 98, eds M. Jaschek and H.G. Groth, p.453.

- Rees, M., in Scientific Importance of High Angular Resolution, Garching, 1981.

- Roddier, F., Roddier, C., Ap.J., 285, L21, 1984.

- Rodriguez, L., Canto, J., Torreles, J., Ap.J., 301, L25, 1986.

- Sahai, R., Wannier, P., Ap.J., 299, 424, 1986.

- Schwarzschild, M., Ap.J., 195, 137, 1975.

- Snell, R., Bally, J., Strom, S., Strom, K., Ap.J., 290, 587, 1985.

- Thompson, R.J., 1976, Ph.D. Thesis, Univ. Sydney.

- Tyson, J.A., Ap.J., 272, L41, 1983.

- Ulrich, M.H., in Scientific Importance of High Angular Resolution, Garching, 1981.

- Whittle, M., M.N.R.A.S., 213, 1, 1985.

- Wilson, L.A., Hill, S.J., Ap.J., 228, 854, 1979.

- Zinneker, Perrier, C., Astron. Astrophys. 1986, submitted.